A STRUCTURAL ANALYSIS OF THE GRENVILLE FRONT ZONE, NORTHEAST GAGNON TERRANE, LABRADOR

DENNIS LEWIS BROWN

NOTICE

The quality of this microform is heavily dependent upon the quality of the original thesis submitted for microfilming. Every effort has been made to ensure the highest quality of reproduction possible.

If pages are missing, contact the university which granted the degree.

Some pages may have indistinct print especially if the original pages were typed with a poor typewriter ribbon or if the university sent us an inferior photocopy.

Reproduction in full or in part of this microform is governed by the Canadian Copyright Act, R.S.C. 1970, c. C-30, and subsequent amendments.

AVIS

La qualité de cette microforme dépend grandement de la qualité de la thèse soumise au microfilmage. Nous avons tout fait pour assurer une qualité supérieure de reproduction.

S'il manque des pages, veuillez communiquer avec l'université qui a conféré le grade.

La qualité d'impression de certaines pages peut laisser à désirer, surtout si les pages originales ont été dactylographiées à l'aide d'un ruban usé ou si l'université nous a fait parvenir une photocopie de qualité inférieure.

La reproduction, même partielle, de cette microforme est soumise à la Loi canadienne sur le droit d'auteur, SRC 1970, c. C-30, et ses amendements subséquents.

A STRUCTURAL ANALYSIS OF THE GRENVILLE FRONT ZONE, NORTHEAST GAGNON TERRANE, LABRADOR

BY

© DENNIS LEWIS BROWN

A thesis submitted to the School of Graduate Studies in partial fulfilment of the requirements for the degree of Master of Science

Department of Earth Science
Memorial University of Newfoundland

December 1990

St. John's Newfoundland

ISBN 0-315-65348-5

ABSTRACT

The study area, located in western Labrador near the projected intersection of the front zones of the Grenville and Hudsonian orogens, occupies part of Gagnon terrane in the Parautochthonous Belt of the Grenville Province. Rocks in the area consist principally of supracrustal units of the Early Proterozoic Knob Lake Group, and a newly recognized, tectonically overlying unit, the Equus Lake formation, both of which are intruded by Middle Proterozoic gabbros of the Shabogamo Intrusive Suite.

The structural elements in the rock units record evidence of a polyorogenic history that is attributed to NW-trending structures of the ca. 1800 Ma Hudsonian orogeny that were overprinted by NE-trending structures of the ca. 1000 Ma Grenvillian orogeny.

Grenvillian deformation and metamorphism resulted in the formation of a relatively deep level, north-verging foreland fold and thrust belt. Four structural domains have been defined based on variations in morphology and orientation of structural elements, and internal domain geometry. Each domain is interpreted to be a structurally distinct thrust bound unit or group of units that has

undergone a unique deformational history. The map pattern indicates a complex stacking order of the domains, and of thrust slices within domains, that involved development of northwest- to north-directed fold nappes followed by out-of-sequence thrusting.

Metamorphic grade varies from lower to upper greenschist facies. Plagioclase-amphibole geothermometry shows qualitatively that there is an increase in Grenvillian metamorphic grade from northwest to southeast across the area. Quantitative garnet-biotite geothermometry indicates that the Grenvillian metamorphic grade attained temperatures of 450 °C in the southern part of the area. Inversion of temperature with structural height in the thrust stack is a well known feature from higher level thrust stacks and implies thrusting post-dated the metamorphic peak.

Documentation of the northern margin of Gagnon terrane as a NW-directed metamorphic fold and thrust belt corroborates similiar interpretations from elsewhere along the Grenville Front, and is in accord with the models of the Grenville Province as a collisional orogen.

ACKNOWLEDGEMENTS

The author wishes to thank Drs. T. Rivers and T. Calon for their supervision and support throughout this project. Energy Mines and Resources, Newfoundland Department of Mines, and the Northern Sciences Training Program provided financial and logistical support for the field work. I would like to thank the staff at the Department of Earth Sciences for their help and friendliness. I would also like to thank my fellow students for the many great conversations. My family, whose continued support and love are greatfully acknowledged, especially my father, who became ill and died while I was in the field working on this project. Rod Churchill provided capable field assistance. Finally, I would like to extend special thanks to Mary Scott whose support both in and out of the field were invaluable.

CONTENTS

TABLES

FIGURES

thrusts and folds.

CHAPTER 1

Introduction

1.1 Grenville Province

The Grenville Province is a one billion year old orogenic belt, the youngest in the Canadian Shield, extending from southeastern Labrador westward through Quebec into southeastern Ontario and New York state. The overall structural grain of the Grenville Province, particularly its front zone, is oriented northeast-southwest, truncating the fabric of older orogens to the northwest. Wynne-Edwards (1972) was the first to recognize that the Grenville Province is composed largely of older, tectonically reworked rocks, including those of the Penokean, Superior, Churchill, Nain, and Makkovik orogens. The recently recognized Labrador orogen (Nunn et al., 1985) is also found within the Grenville Province. A minor proportion of the Grenville Province consists of Lower Proterozoic to Neohelikian rocks that were undeformed prior to the Grenvillian orogenic events (Rivers and Chown, 1986).

Although the Grenville Province was recognized as a distinct structural province as early as 1948, its origin is still controversial. Discussion centers largely around

the nature of the Grenvillian orogeny, and a number of diverse tectonic models have been proposed to explain the tectonic evolution of the orogen (eg. Dewey and Burke, 1973; Wynne-Edwards, 1976; Baer, 1974, 1981; Windley, 1986, 1989; Culotta et al., 1990). Notable constraints on the models so far presented are the almost complete lack of Grenvillian calc-alkaline plutons of batholithic proportions and of ophiolitic material that could be related to subduction and associated arc magmatism, and subsequent closure of an ocean basin. However, Grenvillian plutons have been known for some time to occur in Ontario (Silver and Lumbers, 1965) and have recently been found in southeastern Labrador (Gower et al., 1987). As well, Brown et al. (1975) described an island arc complex in southeastern Ontario that likely resulted from subduction and plate collision. Furthermore, Culotta et al. (1990) have identified a major west-dipping seismic reflector that they interpreted as an intra-Grenville Province suture zone.

It is known that the Grenville Province consists of autochthonous, parautochthonous, and allocthonous belts, parallel to the strike of the orogen, all separated by ductile faults (Rivers et al., 1989). There also exists a well-recognized fold and thrust belt locally along the Grenville Front (eg. Rivers, 1983a; van Gool et al.,

1988), a feature common to many collisional orogens. To summarize, the present level of understanding of the tectonic history of the Grenville Province is consistent with collision between two continental masses that resulted in northwest-directed translation of material over the Archean craton. However, details of the nature of the deformation and metamorphism related to the collisional orogeny are far from complete.

1.2 Tectonic Subdivision of the Grenville Province

Wynne-Edwards (1972) provided the first comprehensive study of the Grenville Province as a whole. He subdivided the Grenville Province into seven segments largely on the basis of structural and metamorphic style, and geophysical signature. These subdivisions separate areas of major lithological difference, but cut geological boundaries to outline areas of different structural and metamorphic style. Recent mapping of the Grenville Province on a number of scales, using the techniques of modern structural geology, metamorphic petrology, and geochronology, has rendered the subdivisions of Wynne-Edwards largely inadequate. A new subdivision of the Grenville Orogen was proposed by Rivers et al. (1989) that is more in keeping with

orogenic models developed for Paleozoic and younger orogens. This model is followed in this study.

The subdivision of Rivers et al. (1989) consists of a Parautochthonous Belt, an Allochthonous Polycylic Belt, and an Allochthonous Monocylic Belt, all parallel to the strike of the orogen, and set apart by three first-order tectonic boundaries, the Grenville Front, the Allochthon Boundary Thrust, and the Monocyclic Belt Boundary Zone, respectively. On the basis of local geology, these belts can be further divided into terranes (eg. Gower and Owen, 1984; Rivers and Nunn, 1985; Rivers and Chown, 1986; Davidson, 1986; Rivers et al., 1989; Indares and Martignole, 1989). These subdivisions are outlined below.

By definition the Grenville Front marks the northwestern limit of Grenvillian deformation and metamorphism (Gower et al., 1980) and separates the tectonic foreland from the Grenville Province. The Grenville Front is a contractional fault system along much of its length and is locally the locus of major uplift (Rivers, 1983a; Owen et al., 1986; Davidson, 1986; Indares and Martignole, 1989). Recent deep seismic studies in Ontario and Ohio have shown that the Grenville Front in these places extends into the lower crust (Green et al., 1988; Culotta et al., 1990).

The Parautochthonous Belt to the south of the Grenville Front is up to 150 km wide, and contains mainly rocks of older orogenic belts that were variably deformed during the Grenvillian orogeny, but which can still be correlated with rocks in the foreland to the north. Locally, there are also supracrustal rocks that were undeformed prior to the Grenvillian orogeny (e.g. Knob Lake Group, southwestern Labrador). The Parautochthonous Belt is characterized along much of its length by northwest directed folding and thrusting (Rivers, 1983a; Davidson, 1986; van Gool et al., 1987, 1988; Brown et al., in press), and an increase in Grenvillian metamorphic grade southeastward away from the Grenville Front (Rivers, 1983b; Owen et al., 1986; Indares and Martignole, 1989).

The southern boundary of the Parautochthonous Belt, the Allochthon Boundary Thrust is a shallow southeast-dipping to subhorizontal mylonite zone that forms the boundary between the Parautochthonous Belt and the allochthons to the southeast.

The Allochthouous Polycyclic Belt is composed of a number of terranes of pre-Grenvillian, upper amphibolite to granulite facies orthogneisses and younger intrusions of granite and gabbro, and anorthosite, all of which were

variably reworked during the Grenvillian orogeny. The Monocyclic Belt Boundary Zone is the southern boundary of the Allochthonous Polycyclic Belt, locally obscured by intrusions, where it is in tectonic contact with the overlying Allochthonous Monocyclic Belt.

The Allochthonous Monocyclic Belt consists of greenschist to upper amphibolite facies supracrustal rocks that were not significantly tectonized prior to the Grenvillian orogeny.

The morphology of the Grenville Province, as defined by the internal structure of these imbricated belts, along with their disposition within the province, is common to collision orogens.

1.3 Tectonic Setting, Southwestern Labrador

The Grenville Province in southwestern Labrador consists of the Allochthonous Polycyclic and the Parautochthonous belts. Two terranes make up the Parautochthonous Belt in southwestern Labrador, Gagnon terrane, adjacent to the Grenville Front (Rivers et al., 1989), and the structurally overlying Molson Lake terrane (Connelly et al., 1989) to the southeast (Figure 1.1).

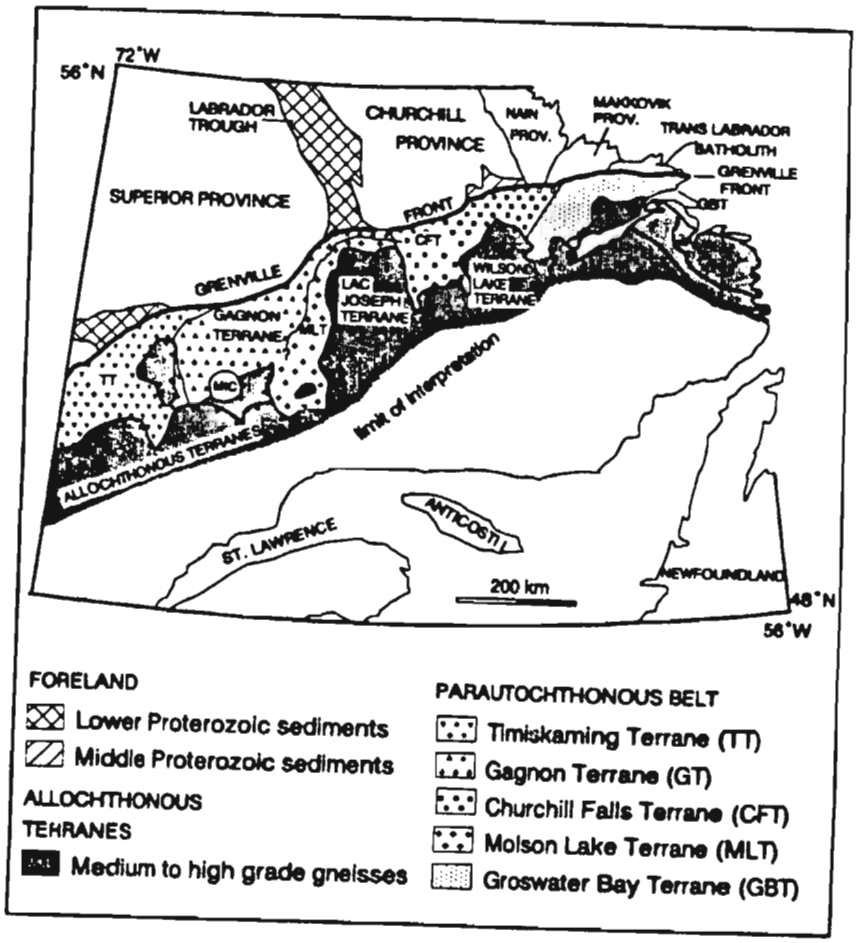

Figure 1.1. Geological map of the Grenville Province in southern Labrador showing the distribution of the various tectonic elements.

Gagnon terrane consists principally of reworked Archean basement rocks of the Ashuanipi Metamorphic Complex that have been variably retrogressed during the Grenvillian orogeny, and greenschist to amphibolite facies metasedimentary rocks of the Lower Proterozoic Knob Lake Group and the Middle Proterozoic Shabogamo gabbro, the latter two of which were undeformed prior to the Grenvillian orogeny.

The structural style of Gagnon terrane in the Labrador City area, where it has been studied in detail, is dominated by northwest-verging, tight to isoclinal, typically coaxial F_1 and F_2 folds and southeast-dipping plastic shear zones (Rivers, 1983a; van Gool et al., 1988; Brown et al., in press.). In this area, kinematic indicators show that movement along shear zones occurred by northwest-directed thrusting that telescoped both basement and cover rocks (Rivers, 1983; van Gool et al., 1988). As well, out-of-sequence thrusting has been demonstrated locally (van Gool et al., 1988; Brown et al., in press). Late, regional-scale northwest-trending F3 folds overprint earlier structures. van Gool et al. (1988) also documented a 200m-wide late extensional fault zone (the Bruce Lake shear zone) parallel to the Grenville Front.

Grenvillian metamorphic grade in this part of Gagnon terrane increases southeastward away from the Grenville Front, from greenschist to upper amphibolite facies. Middle amphibolite facies pelitic assemblages record pressures of 600 to 800 MPa, indicating depth of burial of 20 to 30 km (Rivers, 1983b).

The geometry, ductile nature, and metamorphic grade of the northwestern Gagnon terrane suggest that it forms part of a deeply exhumed, metamorphic foreland fold and thrust belt with substantial basement involvement and with a structural style that is similar to that of better known fold and thrust belts developed at shallower crustal levels (Rivers, 1983a; van Gool et al., 1987, 1988; Brown et al. in press)

The structurally overlying Molson Lake terrane is composed principally of foliated granitoid rocks of unknown age, and coronitic gabbro that is correlated with the Proterozoic Shabogamo gabbro in the Gagnon terrane (Connelly et al., 1989). The structural style of the Molson Lake terrane is poorly defined, but it appears to be significantly different from that of Gagnon terrane (van Gool pers. comm.).

The Allochthonous Polycyclic Belt in southwestern

Labrador is represented by the Lac Joseph terrane (Rivers et al., 1989), which is composed of polycyclic, upper amphibolite to granulite facies paragneisses, intruded by granitoid rocks and gabbros. The paragneisses, granitoid rocks, and gabbros have yielded U-Pb zircon ages between 1600 and 1690 Ma (Rivers and Nunn, 1985; Thomas et al., 1985, 1986; J. Connelly, pers. comm., 1990), suggesting that the U-Pb zircon system was not significantly reset by the Grenvillian tectono-thermal events. Paleo-pressures recorded by mineral assemblages in Gagnon terrane suggest that Lac Joseph terrane was part of a significant tectonic load on the Parautochthonous Belt, and likely acted as the dominant thrust sheet (cf. Boyer and Elliot, 1982) in the Grenville thrust system in southwestern Labrador.

1.4 Thrust Tectonics in the Grenville Province

There have been significant advances made in the last twenty years in understanding the kinematic, mechanical, and geometric principles of non-metamorphic thrust belts, mostly of Phanerozoic age (eg. Dalhstrom, 1969; Chapple, 1978; Boyer and Elliot, 1982; Davis et al., 1983; Dahlen et al., 1984; De Paor, 1988; Mitra and Nanson, 1989). These principles have recently been

applied with some success to older and deeper metamorphic thrust belts (King, 1986; van Gool et al., 1987, 1988; Lucas, 1989; Brown et al., in press).

Rivers (1983a) was the first to recognize the existence of a foreland-style fold and thrust belt in Gagnon terrane. He suggested that previously undeformed lower Proterozoic platformal rocks were folded and thrust towards the northwest during the Grenvillian orogeny. More recent studies by van Gool et al. (1987, 1988) and Brown (1988) have confirmed these interpretations and added to them.

Since it is now recognized that the northwest margin of Gagnon terrane forms a foreland fold and thrust belt, albeit of deeper level and more bulk plastic structural style than most fold-thrust belts described to date, it is reasonable that the geometric principles applied to higher-level fold and thrust belts should also be applied to this part of Gagnon terrane. This allows comparisons to be made between shallow- and deep-level terranes, and may permit extrapolations of higher level crustal structural style to depth.

1.5 Purpose and Scope

The purpose of this study is to document the structural style and the metamorphic imprint of a lesser known portion of Gagnon terrane to further elucidate the tectonic framework of the Grenville fold and thrust belt in southwestern Labrador. Detailed structural maps and cross-sections of the area have been constructed to examine the tectonic evolution of this part of the Gagnon terrane using the principles applied to high level thrust belts referred to above. Macroscopic, and mesoscopic structural data are used to examine the relationships between folding and thrusting within and between individual thrust sheets. Finally, petrologic investigation of mineral assemblages, and quantitative analysis of the compositions of coexisting minerals are used to estimate variations in metamorphic grade across the area, and to determine the relationships between deformation and metamorphism. These will then be used to relate the tectonic evolution of this part of Gagnon terrane to the tectonic framework of the Grenville Province in southwestern Labrador.

1.6 Setting of the Study Area

The study area is situated within Gagnon terrane, approximately 120 kilometers northeast of Labrador City (Figure 1.2). Rocks in the area consist of Lower Proterozoic metasediments of the Knob Lake Group and Middle Proterozoic gabbro of the Shabogamo Intrusive Suite (Rivers, 1982). No Archean basement rocks occur in the study area, in contrast to the area near Labrador City. Rivers (1982, 1983a) suggested that cover rocks in this area were weakly deformed prior to the Grenvillian orogeny, during the ca. 1800 Ma. Hudsonian Orogeny. During the Grenvillian Orogeny rocks in the area were refolded and thrust northwestward over the Churchill Province craton, reworking earlier Hudsonian structures (Rivers, 1982). Regional Grenvillian metamorphic grade in the area is low, reaching middle to upper greenschist facies near the southeastern margin of the Gagnon terrane, although locally higher grade hornfelsic zones occur in metamorphic aureoles adjacent to large gabbroic intrusions. Due to poor exposure, the location of the Grenville Front is poorly defined, but is inferred by Rivers (1982) to lie to the immediate north of the map area (Figure 1.2).

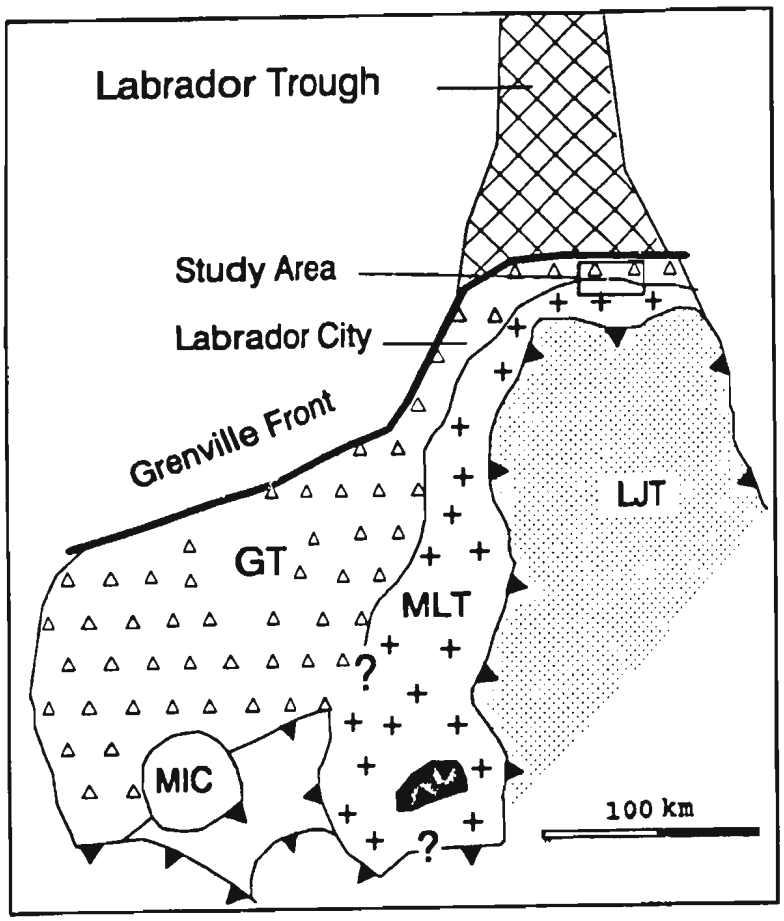

Figure 1.2. Geological map of southwestern Labrador showing the location of the study area in relation to the various tectonic elements. All acronyms are the same as in Figure 1.1.

CHAPTER 2

Lithostratigraphy

2.1 Introduction

Rocks in the Tiphane Lake area consist predominantly of a Early Proterozoic miogeoclinal sedimentary cover sequence, part of the Knob Lake Group, that forms the southern continuation of the Labrador Trough into the Grenville Province (Wardle and Bailey, 1981). The stratigraphic sequence of the Knob Lake Group established by Wardle and Bailey is based on mapping in well-preserved sequences within the Labrador Trough, where stratigraphic continuity can be demonstrated. This sequence was modified slightly by Rivers (1983a) to incorporate units and lithofacies restricted to the Grenville Province.

The Knob Lake Group was unconformably deposited on a subsiding continental margin (Wardle and Bailey, 1981) on the edge of the Superior Craton (Figure 2.1). Cratonic Archean crystalline rocks of the Ashuanipi Metamorphic Complex form the basement upon which these sediments were deposited (Wardle and Bailey, 1981). The stratigraphy

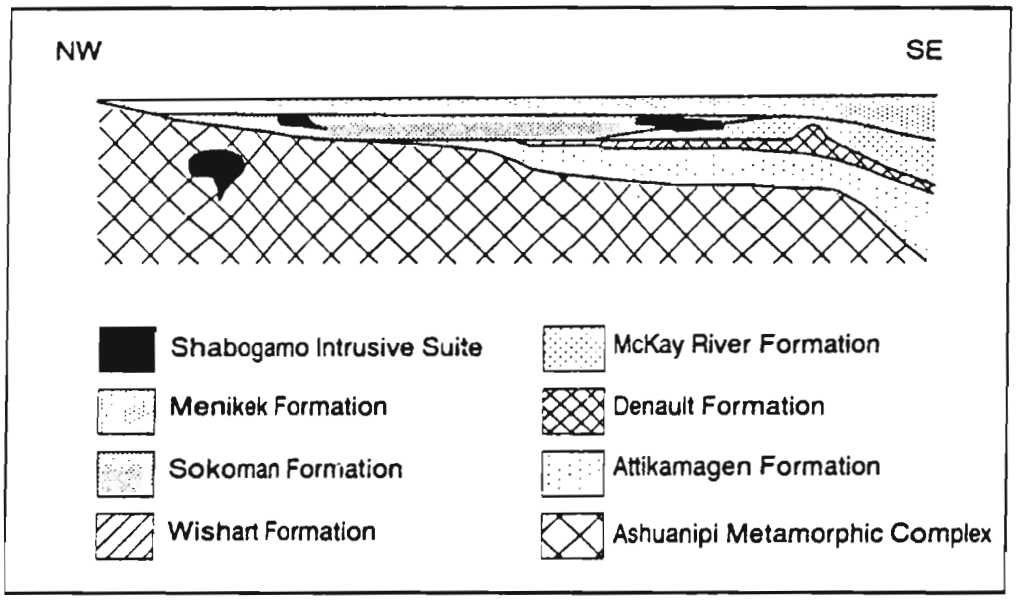

Figure 2.1. Schematic stratigraphic reconstruction of the Proterozoic shelf for the Grenville Province in southwestern Labrador. (modified after Rivers, 1983a).

from the Labrador Trough is also continuous for hundreds of kilometers within the Grenville Province, and is assumed to continue through the present study area (Rivers, 1982), thus providing regional stratigraphic way-up criteria throughout Gagnon terrane. Volcanic and volcaniclastic rocks are laterally discontinuous, but occupy known stratigraphic positions within the Knob Lake Group. Within the study area, however, the stratigraphic relationships are not always obvious because of folding and imbrication by faulting, but the overall stratigraphic framework has been assumed to be the same and less disrupted portions of the stratigraphic sequence can be used to work out local structural detail (see attached map). In this chapter a brief description of rock types in the field area is given, and the reader is referred to the relevant portions of Chapters 3 and 4 for details of the mineral assemblages.

2.2 Stratigraphy

No rocks of the Ashuanipi Metamorphic Complex outcrop in the Tiphane Lake area, and the main rock types are those of the Knob Lake Group and the Shabogamo Intrusive Suite (Rivers, 1982). There is also an isolated occurrence of a newly recognized unit that contains

clasts of all Knob Lake Group rocks present in the area, and is intruded by the Shabogamo gabbro. This unit is interpreted to be part of a molasse sequence that formed after the 1800 Ma Hudsonian Orogeny and is here informally named the Equus Lake formation.

The lowest unit of the Knob Lake Group present in the Tiphane Lake area (Table 1) is the Denault Formation, which forms an extensive band across the central portion of the map area, and several minor outcrops near Tiphane Lake. The Denault Formation consists mainly of buff- to brown-weathering, quartz-rich dolomite (Figure 2.2) with local thin muscovite-bearing pelitic bands. Well preserved stromatolites were found in several localities near the south side of Tiphane Lake and around Mobey Lake. This is one of the few occurrences of stromatolites found in the Grenville Province, others being in Elzevir terrane (Burke, 1984) and in the Iron Ore Company of Canada mine, Gagnon terrane (T. Rivers, pers. comm.). As the top of the Denault formation is approached, there is an increasing amount of chlorite and actinolite which form thin discontinuous bands. There is a complete gradation between the dolomitic Denault Formation and the overlying actinolite/chlorite schists of the McKay River Formation. In the field the two were distinguished on the basis of the predominant lithology at outcrop scale.

Figure 2.2. Field photograph of stromatolitic Denault Formation dolomite. This photo is atypical in that stromatolites are present, but shows the general nature of the formation

The McKay River Formation outcrops throughout the map area and is the dominant lithology present. No consistent internal stratigraphy for the formation could be worked out for the whole map area, but two major divisions were made based on key outcrops in the south, near Ossokmanuan Lake (see map in back pocket). One unit consists of a lower dark brown to black graphitic, chlorite-biotite semipelitic schist (Figure 2.3a) containing numerous quartz veins and, locally, carbonate concretions. South of Mobey Lake and near Dragon Lake this unit contains mildly to intensely deformed mafic flows and pillow lavas. Adjacent to the larger gabbro intrusions this unit has been metamorphosed to a garnet-biotite-epidote hornfels.

An upper unit, which is quite variable throughout the area, ranges from a light- to dark-green, medium grained chlorite-actinolite-rich volcaniclastic schist (Figure 2.3b) to a boulder conglomerate with a chlorite-actinolite matrix and, locally, thin discontinuous semipelitic interlayers. Clasts are angular to subrounded, and composed of tuffaceous material and pillow fragments. One outcrop north of Mobey Lake contains boulder-sized clasts of gabbro. Small occurrences of tuffaceous olivine melilitites near the top of this unit have been described by Noel (1981). East

A

Figure 2.3. Field photographs of McKay Formation schists. A. Mildly deformed pillow lava in chlorite-biotite schist matrix. B. Volcaniclastic conglomerate with a chlorite-actinolite matrix.

B

Figure 2.3. continued.

of Tiphane Lake, the McKay River Formation abruptly changes from volcaniclastic conglomerate to a matrix supported tuffaceous siltstone breccia. The matrix becomes increasingly cherty up stratigraphic section, grading over a distance of 20 meters into chloritic cherty iron formation.

The Sokoman Formation is a banded iron formation outcropping throughout much of the area. Near Tiphane Lake, the Sokoman Formation can be divided into four units based on the dominant lithology in outcrop. Here, the lowest unit in the Sokoman Formation is a massive chert containing discontinuous tuffaceous layers and nearly spherical lapilli (Figure 2.4). Overlying this unit is a grunerite-bearing silicate-carbonate unit that also contains discontinuous tuffaceous layers and lapilli. The next unit is a dark grey and strongly magnetic silicate-oxide iron formation consisting predominantly of quartz and magnetite. Tuffaceous material and lapilli are absent. Overlying this and topping the Sokoman Formation is a grunerite-rich silicate-carbonate unit. This latter unit is distinguished from the lower silicate-carbonate unit by the complete absence of tuffaceous material and lapilli. Near the contact with the overlying Menihek Formation the upper silicate-carbonate unit contains thin discontinuous

Figure 2.4. Field photograph of Sokoman Formation quartzite.

semipelitic layers and millimetre-sized clasts of quartz and feldspar.

The uppermost formation of the Knob Lake Group present in the study area is the Menihek Formation which is restricted to several small occurrences around Tiphane Lake and north of Dave Lake. The Menihek Formation is typically a fine to medium grained chlorite-biotite semipelite with rare millimetre-sized clasts of quartz and feldspar. Millimetre- to centimetre-scale layering in the Menihek Formation is interpreted to be primary laminations or bedding (Figure 2.5).

A previously unrecorded occurrence of a unit, informally named the Equus Lake formation, outcrops immediately east of Equus Lake. The Equus Lake formation is a polymictic boulder conglomerate at its base (Figure 2.6) and fines upward to a medium grained greywacke topped by a well-laminated siltstone. The basal conglomerate contains large well-rounded to angular clasts of the Denault, Sokoman, and Menihek formations, as well as clasts of feldspar, blue quartz, and gabbro of unknown origin. Primary sedimentary features such as graded bedding and cross bedding are locally preserved in the greywacke and siltstone. No stratigraphic position could be determined for this unit because the contacts

Figure 2.5. Field photograph of tightly folded Menihek Formation. Despite the deformation, it is possible to see primary layering in this unit.

Figure 2.6. Field photograph of the Equus Lake formation. Photo shows clasts of Denault Formation (buff colored) and Menihek Formation (grey colored).

with other units, where observed, are tectonic. However, the formation is intruded by the Shabogamo gabbro and must, therefore, be pre-Grenvillian in age. This unit is interpreted to be a Hudsonian molase unit, and may be correlative with the Tamarack Formation further to the northwest, which also contains clasts of Knob Lake Group rocks (Ware and Wardle, 1979).

All cover rocks in the area, including the Equus Lake formation, are intruded by Middle Proterozoic gabbro of the Shabogamo Intrusive Suite. Shabogamo gabbros are generally medium to coarse-grained ophitic to subophitic gabbro to leucogabbro, with, locally, well developed layering (Figure 2.7). These rocks are typically partially retrogressed to chlorite-actinolite and albite-epidote assemblages, though a relict igneous texture is generally preserved and, in the centre of several large bodies, primary igneous assemblages containing pyroxene and plagioclase are found. The Shabogamo gabbros typically outcrop as elongate bodies that follow the trend of lithologic boundaries. These relationship indicate that the gabbro was intruded predominantly as sills.

The presence of gabbro clasts appear in rocks of the McKay River Formation and the Equus Lake formation

Figure 2.7. Field photograph of the Shabogamo Intrusive Suite. This photo shows atypical layering in the gabbro.

indicates the existence of gabbro bodies that predate the Shabogamo Intrusive Suite. However, gabbro bodies in the field area are intrusive into all shelf rocks, and, locally, are seen to cut an older fabric. These intrusive relationships (see Chapter 3) suggest that the gabbro bodies belong to the Shabogamo Intrusive Suite.

CHAPTER 3

Structure

3.1 Introduction

The study area (see attached map in back pocket) is located at the southern end of the Labrador Trough (recently renamed the New Quebec Orogen by Hoffman, 1988) at the junction of the Churchill and Grenville Provinces. The first mapping in the area was carried out in the late 1940's and early 1950's by Labrador Mining and Exploration Company, and Iron Ore Company of Canada (Beland, 1949; Baird, 1950; Tiphane, 1951) in search of mineral deposits, principally iron ore. Geophysical studies were conducted by the Iron Ore Company of Canada and Labrador Mining and Exploration during the late 1950's (Breau, 1957) and by the Geological Survey of Canada during the early 1970's (McKay River, map 6062G, 1972). Regional mapping and compilations of the geology of the area were done by Wynne-Edwards (1961), Noel and Rivers (1980), Rivers (1982, 1983a), and Rivers and Wardle (1985). An honours thesis by Noel (1981) examined the structure and metamorphism of the area, and in particular the geochemistry of the McKay River Formation.

The Grenville Front in this area is poorly exposed, but was interpreted by Rivers (1982), and Rivers and

Wardle (1985) to be located approximately 5km north of Tiphane Lake. The Grenville Front was interpreted by the latter authors to be a thrust fault that places rocks of the Menihek Formation on top of the older Attikamagen Formation, reversing an earlier overturned stratigraphic sequence of the Hudsonian Front zone. The geology of the map area, as presented by Rivers (1982) and Rivers and Wardle (1985), has a rough east-west structural grain that is offset by northwest striking high-angle faults. Rivers (1982) interpreted the regional structure to be dominated by macroscopic north- to northwest-verging, northeast-plunging inclined isoclinal folds that reorient lithological contacts into an east-west orientation, subparallel to the regional foliation. The regional foliation (S_1) dips southeast subparallel to fold axial planes. Rivers (1982) noted that S_1 was locally folded, indicating the presence of F_2 folds, though no description of the F_2 fold style was given. Open, north-trending F_3 folds with east-dipping axial surfaces fold earlier structures. The map area is bound to the south by a thrust fault, largely inferred, that places higher grade metagabbro and metasediments of the Molson Lake terrane (Connelly et al., 1989) structurally on top of rocks in the study area.

Remapping of this part of Gagnon terrane was done

during the summers of 1988 and 1989. Outcrop in the map area is patchy, and varies consideraly from area to area, so particular attention is be paid to structurally homogeneous sub-areas where the local structure can be defined. The structural style of these key areas will form the basis upon which the structural geometry of the map area is interpreted. It should be noted that lithological and structural boundaries are interpreted over large distances and are drawn based on the authors field interpretations.

Based on this mapping and on reinterpretation of some of the data collected by Rivers and Noel during the 1979 field season, it is seen that the structural complexity of the map area makes it difficult, if not impossible, to correlate structural elements over any great distance. Therefore, the area has been divided into four structural domains; the Tiphane Lake domain, the Mobey Lake domain, the Equus Lake domain, and the Dave Lake domain (Figure 3.1).

The macroscopic and mesoscopic structure of the domains and domain boundaries is described in this chapter, followed by a short discussion of each. For each domain, sequences of generations of structural elements are rigorously adhered to. Domain boundaries are

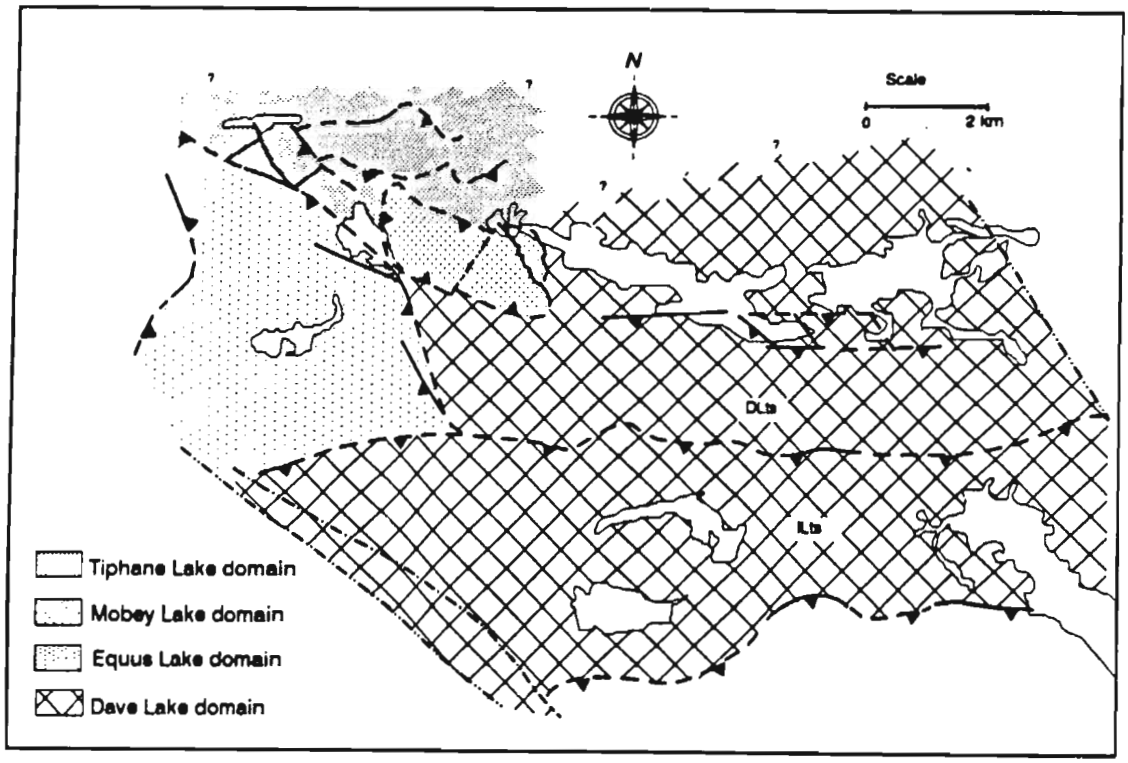

Figure 3.1. Schematic geological map of the study area showing the location of the structural domains. See individual domain maps or the attached map in back pocket for local geology. DLts = Dave Lake thrust sheet. ILts = Isa Lake thrust sheet.

everywhere interpreted to be shear zones (although certain domain boundaries are not seen because of the limit of interpretation) with, typically, a unique fabric orientation. For the purpose of this chapter, fabric elements from domain boundaries have been given the subscript b to differentiate them from fabric elements that are internal to domains. Table 3.1 lists the various structural elements in each domain and its correlation with other elements both within that domain and with other domains.

3.2 Tiphane Lake Domain

3.2.1 Introduction

The Tiphane Lake domain is a structurally complex and polydeformed area that records evidence of at least three generations of structures. It is bound to the north by the limit of interpretation, to the southwest by the Mobey Lake domain, to the south by the Equus Lake domain and, to the southeast by the Dave Lake domain. The domain has an overall northeast-southwest structural grain outlined by lithologic contacts and by southeast-dipping faults (Figure 3.2).

Rocks in the Tiphane Lake domain consist

Table 3.1. Structural elements from each domain in the map area.

Structural Element	Tiphane Lake Domain	Mobey Lake Domain	Equus Lake Domain	Dave Lake Domain	
				Dave Lake thrust sheet	Ice Lake thrust sheet
S1	Penetratively developed and folded by F2. Not found in gabbro. Same as S1 in MLd.	Weakly developed, non-penetrative. Form surface trace folded on map scale. Not found in gabbro. S1 in TLd.	Penetratively developed foliation that is axial planar to F1 folds. Found in gabbro.	Penetratively developed, SE-dipping, axial planar to F1 folds. Same as S2 in TLd.	Non-penetrative foliation locally cut by gabbro dyke. Same as S1 in TLd.
S2	Non-penetrative, axis planar to F2 folds. Developed in gabbro. Typically SE-dipping.	Locally developed as weak, non-penetrative foliation axial planar to F2 folds. Locally found in gabbro.	Not developed.	Locally developed in hinge zones of mesoscopic F2 folds.	Non-penetrative, F2 axial planar, SE- to S-dipping foliation. Same as S1 in Dave Lake thrust sheet.
S3	Non-penetrative, associated with SW-dipping D3 thrusts. Found in gabbro. Same as S1b in MLd.	Not developed.	Not developed.	Not developed.	Not developed.
F1	Variably plunging, typically refolded, mesoscopic folds. Commonly only recognized by bedding-cleavage relationship.	Macroscopically developed on domain scale as refolded W-verging fold that is cut by gabbro.	Mesoscopic, neutral folds internal to ELd. Fold gabbro.	Macroscopic, SE-plunging fold nappes. Typically not found on an outcrop scale.	Clear evidence of F1 not found. Implied by development of S1.
F2	NW- to NE-verging, often recliined, non-cylindrical folds. D2 thrusts cut through overturned limbs.	Poorly developed in outcrop. On domain scale, NE-verging folds that fold gabbro.	Not developed.	Rare, SE-plunging, mesoscopic folds. Possibly related to continued F1 folding.	Macroscopic, NE- to SE-plunging fold nappes. Same as F1 in Dave Lake thrust sheet.
F3	Typically only found as a Crenulation of S2. East of Tiphane Lake, NE-verging folds of S2 foliation.	Not developed.	Not developed.	Not developed.	Not developed.
Ls1	Penetratively developed in S1 and folded by F2. Not found in gabbro.	E- to SE-plunging lineation found along W-verging thrust in west of domain.	S-plunging stretching lineation found along High-angle fault.	Stretching lineation found in SE- to S-dipping thrusts.	Stretching lineation found in SE-dipping thrusts. Same as Ls1 in Dave Lake thrust sheet.
Ls2	Typically SE- to S-plunging in D2 thrust surfaces. Found in gabbro.	Locally developed stretching lineation found along D2 faults. Found in gabbro.	Not developed.	Not developed.	Not developed.
Ls3	SW-plunging in D3 thrust surfaces. Found in gabbro. Same as Ls1b in MLd.	Not developed.	Not developed.	Not developed.	Not developed.
Ls1b	Not applicable.	Typically SW-plunging stretching lineation found along boundary thrust. Same as Ls3 in Tiphane Lake domain. Found in gabbro.	Penetrative, typically folded stretching lineation found along domain boundary.	Not developed.	Poorly developed stretching lineation found along Southern Boundary zone fault.
S1b	Not applicable.	SW-dipping foliation found along boundary thrust. Same as S3 in TLd.	Penetrative, folded foliation found along NE boundary of the domain.	Not applicable.	Penetrative, S-dipping foliation found along Southern boundary zone fault.
S2b	Not applicable.	Not developed.	Non-penetrative, F2b axial planar foliation.	Not applicable.	Not developed.
F1b	Not applicable.	Typically rootless folds found along boundary thrust. Plunge SW, parallel to Ls1b.		Not applicable.	E-plunging mesoscopic folds, often parallel to Ls1b.
F2b	Not applicable.	Not developed.	Mesoscopic folds that fold S1b. S-plunging.	Not applicable.	Not developed.

TLd = Tiphane Lake domain

MLd = Mobey Lake domain

DLd = Dave Lake domain

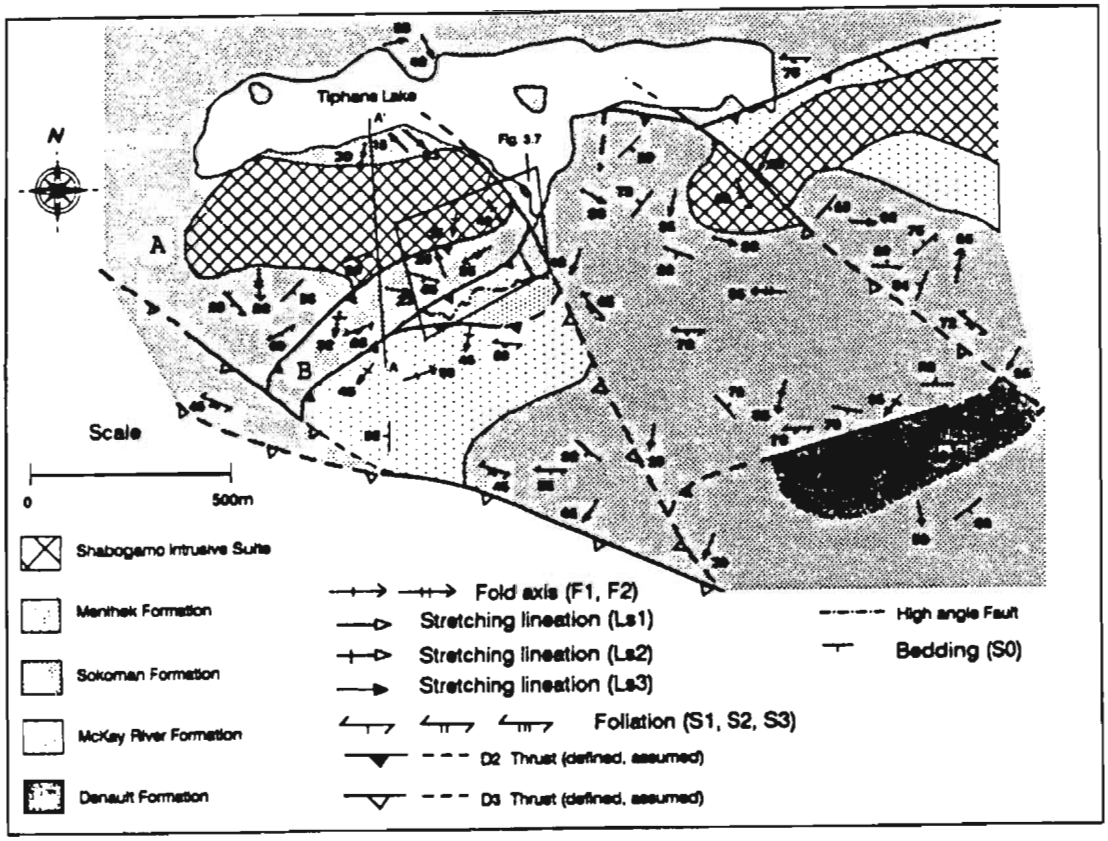

Figure 3.2. Geological map of the Tiphane Lake domain.

predominantly of iron formation (Sokoman Formation), chlorite-actinolite schists (McKay River Formation), and gabbro (Shabogamo Intrusive Suite), with minor pelitic schist and marble (Menihek and Denault Formations, respectively). A well-defined stratigraphic sequence can be worked out for the Sokoman Formation and, based on stratigraphic contacts observed with the McKay River Formation in the southwest-central part of the domain (see map in back) a way-up can be determined. The Sokoman Formation in the Tiphane Lake domain consists of a basal tuffaceous cherty unit, a lower tuffaceous silicate-carbonate unit, a silicate-oxide unit, and an upper silicate-carbonate unit. Mineralogically, all units contain combinations of the minerals grunerite, calcite/dolomite, chlorite, quartz, and magnetite.

The McKay River Formation consists predominantly of thick-bedded, greenish, volcaniclastic, pebble and boulder conglomerate and lesser gray-green, thin-bedded tuffaceous siltstones. Several small outcrops of dark gray to black crystal-lithic flows were also found. The typical assemblage in tuffaceous McKay River Formation is chlorite + actinolite + plagioclase + epidote + sphene +/- biotite. East of Tiphane Lake, the McKay River Formation grades stratigraphically into tuffaceous cherty Sokoman Formation.

Several small outcrops of gray to black laminated schists and slates of the Menihek Formation occur along the southern shore of Tiphane Lake. Here, the Menihek Formation consists of biotite + chlorite + plagioclase + quartz + tourmaline +/- muscovite. These rocks are intensely deformed and any primary sedimentary way-up criteria within the unit have been destroyed.

Rocks of the Denault Formation in the Tiphane Lake area are buff to brown weathering, locally stromatolitic marbles consisting predominantly of dolomite ÷ calcite with minor quartz +/- feldspar. Denault rocks are typically massive, but, locally, stromatolites provide a way-up criteria.

Several large sills of gabbro of Shabogamo Intrusive Suite outcrop in the Tiphane Lake area. The gabbros are typically massive and have relict igneous texture, except along shear zones where they are strongly foliated and lineated. The common assemblage in metamorphosed gabbro is chlorite + actinolite + plagioclase + epidote + quartz +/- biotite +/- garnet +/- muscovite.

3.2.2 Internal Structure

The Tiphane Lake domain has a dominant northeast-

southwest structural grain marked by straight to moderately curved surface traces of lithologic boundaries and by southeast-dipping shear zones (Figure 3.2). Both the lithologic boundaries and the shear zones are truncated by southwest-dipping shear zones. Fabric elements in the domain display complex orientation patterns (Figure 3.2) that suggest the domain has undergone a polydeformational history.

Evidence of the earliest deformation of structures in the domain is preserved as a penetrative foliation (S_1) and a stretching lineation (Ls_1) that have both been folded. Variable angular relationships between bedding and S_1 cleavage indicate the existence of an early phase of mesoscopic to macroscopic F_1 folds that close towards the northwest or southeast. This sense of closure is corroborated in two locations along the southern shore of Tiphane Lake where mesoscopic F_1 folds with Z-asymmetries give a west to northwest sense of vergence despite overprinting by later folding. However, no relation between F_1 folding and spatial distribution of stratigraphy could be worked out. F_2 fold axes have variable plunge directions, with a small concentration plunging towards the south to southwest (Figure 3.3a,b). Orientation of fabric elements vary somewhat between horses in the domain (eg. Figure 3.3a,b). These

differences are discussed below.

The first generation fabrics are a penetrative foliation (S_1) defined by metamorphic chlorite, grunerite, and biotite, and a stretching lineation (Ls_1) defined by stretched quartz and feldspar grains or by the preferred linear alignment of inequidimensional amphiboles and micas.

The macroscopic structure of the Tiphane Lake domain is dominated by two generations of post-D_1 shear zones (Figure 3.2). The earlier generation comprises ductile shear zones that are straight to slightly curved, northeast-striking and dip 30°-60° towards the southeast. These shear zones are one to two meter-wide mylonitic to phyllonitic zones (Figure 3.4a) with a well-developed down-dip stretching lineation, Ls_2. Kinematic indicators such as S-C planes (Figure 3.4b), tailed porphyroclast systems (Passchier and Simpson, 1986), and shear bands indicate that these shear zones have northwest-verging thrust displacement. Locally, they are very strongly lineated and are considered L > S tectonites. Axes of small scale intrafolial rootless folds (Figure 3.4c) in the shear zone fabric plunge southeast, parallel to the elongation lineation. Locally, both S_0 and S_1 are oriented at a high angle to the shear fabrics (Figure

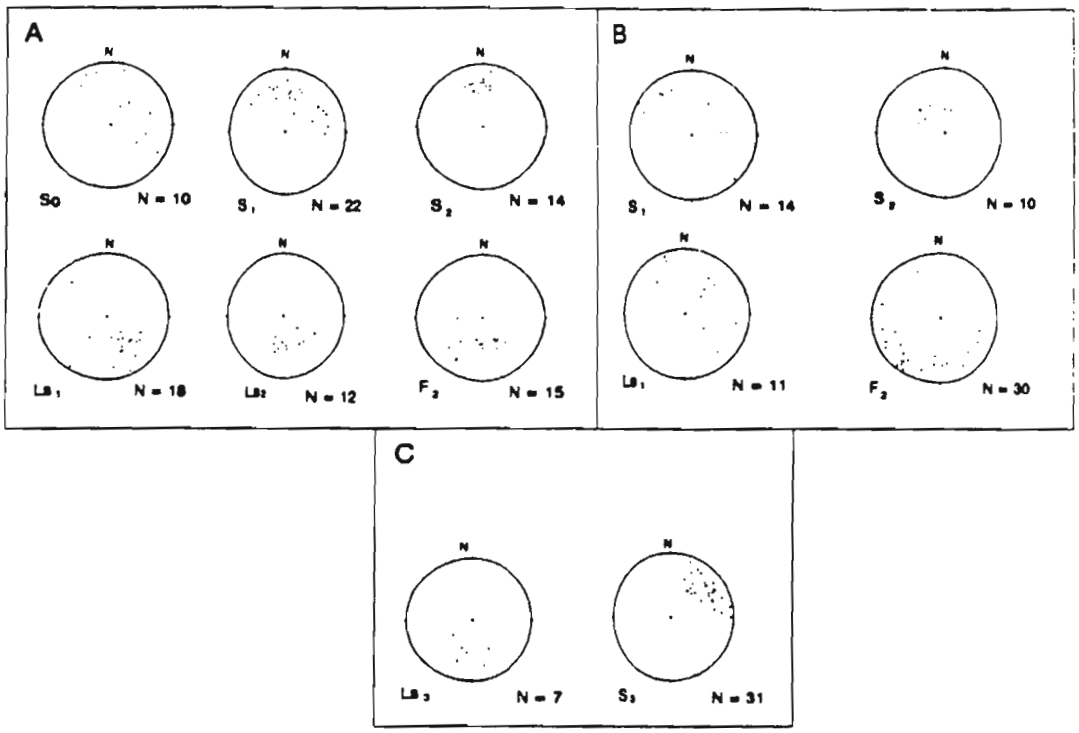

Figure 3.3 Lower hemisphere equal area projections of structural data from the Tiphane Lake domain. Location of A and B are shown on Figure 3.2. C represents southwest-dipping thrusts.

A

B

Figure 3.4. A. Shear zone in Sokoman Formation. Note the high angle between bedding and the shear zone. B. S-C planes in sheared Sokoman Formation (looking SE).

C

Figure 3.4 continued. C. Intrafolial fold in sheared Sokoman Formation.

3.4a) and are truncated by them. These thrusts are referred to as D_2 thrusts, and are themselves truncated by a younger generation of shear zones.

The younger generation of shear zones in the Tiphane Lake domain comprises structures that are one to two meters wide, northwest-striking and moderately southwest-dipping zones of strongly foliated rocks. S-C planes and tailed porphyroclast systems indicate thrust sense movement along these shear zones towards the northeast. These shear zones sharply truncate earlier D_2 shear zones, but in several locations D_2 thrusts are seen to curve into them with a sense of curvature that is compatible with the D_3 movement sense. Foliation development associated with D_3 thrusts (S_3) grades from poorly foliated to mylonitic over a distance of several meters. A stretching lineation, defined by elongate quartz and feldspar grains and by linear alignment of inequant amphiboles and micas, plunges south to southwest in S_3 (Figure 3.3c).

Both D_2 and D_3 fabrics and shear zones occur in, or affect the Shabogamo gabbro.

High-angle fault zones also occur in the Tiphane Lake domain. These features are generally discrete zones

of high strain that place younger rocks on top of older rocks. Southeast of Tiphane Lake, a high-angle fault zone drops rocks of the Sokoman Formation down, juxtaposing them against rocks of the Denault Formation (Figure 3.2). Very few kinematic indicators were found to substantiate this inferred extensional sense of movement, although in one location S-C planes did give an extensional geometry. High-angle fault zones are truncated by both D_2 and D_3 shear zones.

The dominant fold phase in the Tiphane Lake domain pervasively folds the S_1 foliation and Ls_1 lineation, and in several instances can be seen to refold F_1 folds (Figure 3.5). These folds are termed F_2. They occur on both a macroscopic and mesoscopic scale in all stratigraphic units in the domain, and display a variety of fold geometries. Macroscopic F_2 folds in iron formation along the south shore of Tiphane Lake are plane noncylindrical (Figure 3.3a) (fold classification after Turner and Weiss, 1963) with wavelengths of 75 - 100 meters for the highest order of folds. In one instance near the shore of Tiphane Lake, asymmetries of mesoscopic parasitic folds and bedding-S_2 cleavage relationships can be used to infer a south-plunging, west-verging antiform with an overturned limb, and a gentle west-dipping limb and hinge zone of a synform. In another example, F_2 folds

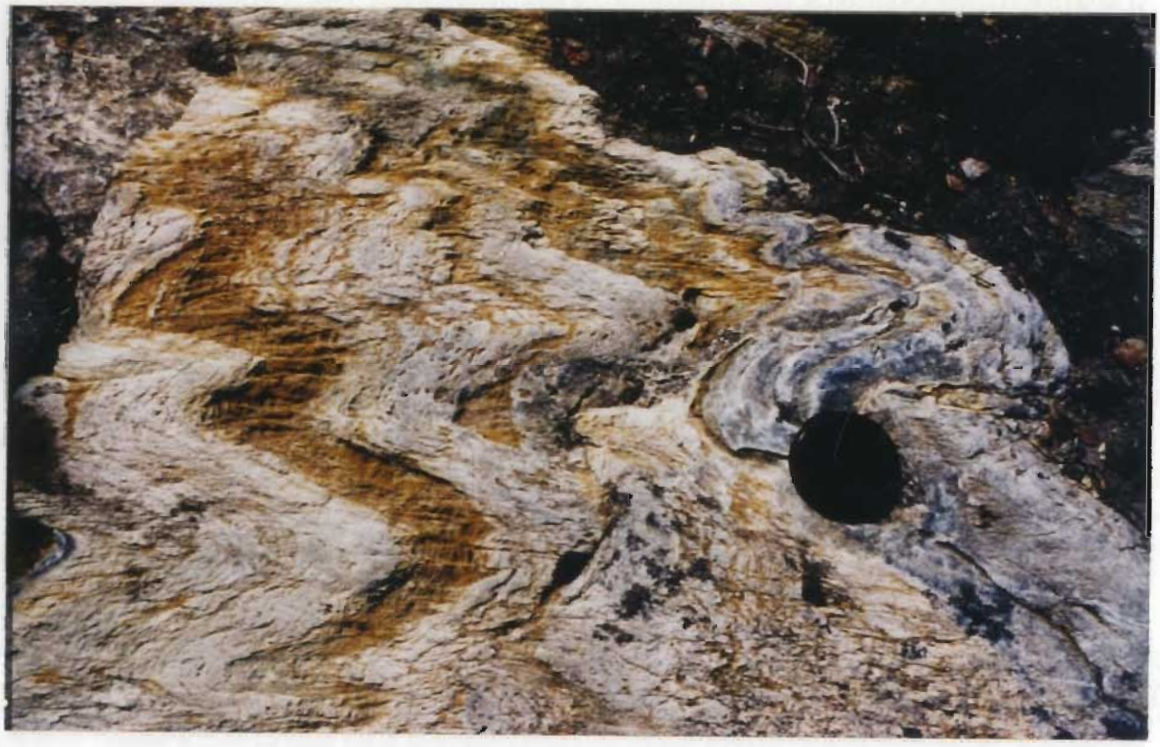

Figure 3.5. A mesoscopic F_2 fold overprinting a F_1 fold in a type 3 interference pattern.

are close to tight, nonplanar noncylindrical folds with a noncylindrical axial surface (Figure 3.3b) and have an overall northwest sense of vergence. Macroscopic F_3 folding is rare in the Tiphane Lake domain. However, macroscopic folding of S_2 and D_2 thrust surface traces east of Tiphane Lake (see attached map in back pocket) may be a result of F_3 folding, although no F_3 related fabric is developed. Mesoscopic F_3 folds are also rare in the Tiphane Lake domain; several mesoscopic were observed immediately south of Tiphane Lake where they overprint both F_1 and F_2 folds. In this area, F_3 crenulation folding with a southeast-plunging crenulation axis may indicate the existence of larger F_3 folds.

Several generations of post-D_1 planar and linear fabrics are found in all metasedimentary rocks and metagabbro in the Tiphane Lake domain (Table 3.1). A second generation foliation, S_2, like S_1, is defined by grunerite, biotite, chlorite or actinolite. S_2 is developed in the hinge areas of F_2 folds where it forms a differentiated axial planar crenulation cleavage (Figure 3.5). The orientation of S_2 varies within the Tiphane Lake domain, but generally dips moderately to steeply south to southeast (Figure 3.3a,b). In high strain zones along D_2 shear zones, an elongation lineation, Ls_2, defined by stretched quartz and feldspars

or preferred orientation of amphiboles and micas plunges south to southeast, typically down-dip or with high pitch angle in S_2.

A third generation fabric in the Tiphane Lake domain occurs along narrow zones associated with the D_3 shear zones discussed above. Peripheral to these shear zones a weakly developed, moderate to steeply southeast dipping foliation, S_3 (Figure 3.3c), defined by aligned platy minerals and (micro)lithons of quartz and feldspar, grades over one to two meters into a D_3 shear zone. An elongation lineation defined by stretched quartz and feldspars, and by preferred alignment of inequant minerals plunges towards the southeast, down-dip in S_3 (Figure 3.3c). Locally, along a D_3 thrust near the southern shore of Tiphane Lake, an earlier fabric (S_2 ?) is partially transposed into S_3 (Figure 3.6).

The structural style recorded by the deformation event responsible for the earliest generation of structural features in the domain is largely obliterated by subsequent penetrative deformation. It is possible, however, to discern some aspects of the D_1 structural style by looking through the effects of D_2. D_1 appears to have caused northwest to west, east to southeast closing macroscopic folding with the development of a penetrative

Figure 3.6. Field photograph showing partial transposition of S_2 into S_3 discussed in text.

axial plane cleavage (S_1) with, locally, an associated lineation (Ls_1). Definitive evidence of D_1 faulting (thrusting or otherwise) has not been found in the Tiphane Lake domain. However, near the south shore of Tiphane Lake a tightly folded fault with an apparent extensional geometry may be a folded and overturned D_1 thrust (this area is discussed in detail below).

The dominant structures in the domain are related to D_2 (Figure 3.2). First order asymmetric F_2 folds verge and face towards the northwest to north and appear to be consistently developed on the normal (upward facing) limbs of presumed macroscopic F_1 folds (for example, see inset in Figure 3.8). The relationship between F_1 and F_2 folding, and D_2 thrusting have typically resulted in an older-over-younger structural sequence, and involve Shabogamo gabbro. For instance, south of Tiphane Lake, D_2 thrusts cut up-section through the forelimb of macroscopic F_2 folds and place older rocks on top of younger (Figure 3.2).

The D_3 structural style of the Tiphane Lake domain is dominated by northeast-verging thrust faults with little associated folding. These thrust faults sharply truncate all structural features related to both D_1 and D_2. Further, as mentioned above, in the east-central part

of the domain (see map in back pocket) D_2 thrust surface-traces and all S_2 foliations appear to be folded, a feature that may be related to folding above a blind D_3 thrust (see Figure 6.2).

The relationships between all three generations of structural features are best exposed in a small area along the south shore of Tiphane Lake Figure 3.7), where several northwest-verging D_2 thrust faults are sharply truncated by a northeast-verging D_3 thrust, and mesoscopic to macroscopic F_1 and F_2 folds, and their associated fabrics are variably overprinted.

In this area, a horse containing rocks of the McKay River, Sokoman, and Menihek formations is bound above and below by south to southeast-dipping D_2 thrusts that place it on top of those of the Sokoman Formation (Figure 3.7, inset). This horse is in turn structurally overlain by rocks of the McKay River Formation, and is truncated to the east by a southwest-dipping D_3 thrust. Within this area, the earliest deformation event is recorded by a penetrative S_1 foliation and a one to two meter-wide phyllonite zone that, in its present orientation, places Menihek Formation on top of McKay River Formation, giving it an extensional geometry. A small block of tuffaceous silicate-carbonate iron formation occurs

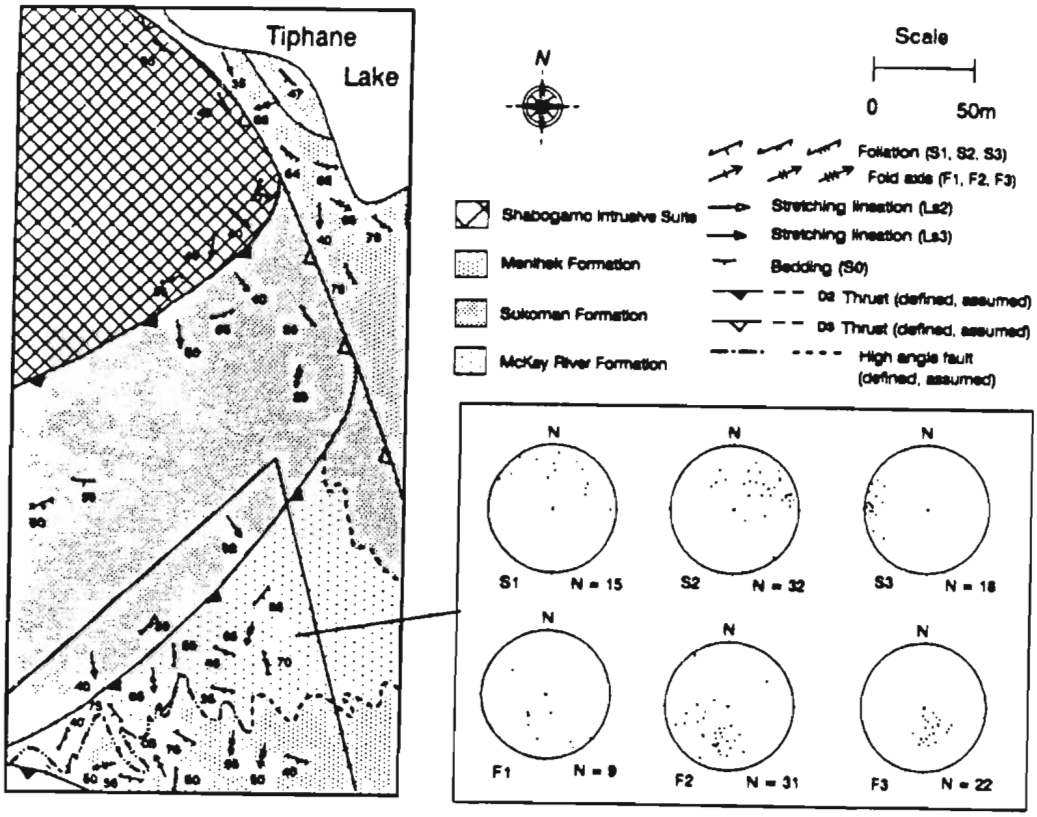

Figure 3.7. Geological map of a small area near the shore of Tiphane Lake (see Fig. 3.2 for location). Structural data presented in lower hemisphere equal area plots.

within the fault zone, in the hinge area of a fold. Sokoman Formation rocks occur in the eastern part of this horse but their exact relationship to the other rocks is unknown. It is assumed that the contact between them is a fault. Tight to isoclinal, southeast to west plunging F_1 folds occur in the Menihek Formation in the hanging wall of the extensional fault. The S_1 foliation dips towards the southeast to west and is axial planar to F_1 folds (Figure 3.7). All D_1 features in this area are either truncated or overprinted by D_2 structures.

The extensional fault is truncated by a D_2 thrust and is folded by tight to isoclinal southwest-plunging, typically reclined, F_2 folds. There is a well developed S_2 foliation in the hinge areas of F_2 folds and, locally, the S_1 foliation is partially transposed into S_2. A third generation of open to close, and south-plunging folds with nearly vertical axial planes are developed locally (Figure 3.7). The scatter in F_2 and S2 orientations are related to folding about F_3 folds.

A southwest-dipping D_3 thrust sharply truncates D_2 thrust. D_2 thrust surfaces bend into the D_3 thrust, reorienting both S_2 and Ls_2 and, in the footwall, S_2 foliations are transposed into a new southwest-dipping S_3 foliation. An elongation lineation, Ls_3, plunges towards

the south, indicating that the D_3 thrust records a component of oblique slip.

3.2.3 Cross-Sections

Because of the highly non-cylindrical nature of structures in the Tiphane Lake domain, and because of the penetrative overprinting of the generations of structures, it is impossible to construct accurate cross-sections, representative of the whole domain. Instead schematic cross-sections were constructed using down-plunge projection methods where possible, and by using field relationships to constrain the local geometry of structures in the plane of the sections (Figure 3.8). Sketches of field relationships are drawn on the cross-sections.

The macroscopic structural geometry of the Tiphane Lake domain is complicated by at least three distinct generations of structures that can be related to separate phases of deformation. The dominant generation of structures in the domain are F_2 folds and D_2 thrusts. South of Tiphane Lake, macroscopic F_2 folds overturn towards the northwest, and, in the Sokoman Formation, D_2

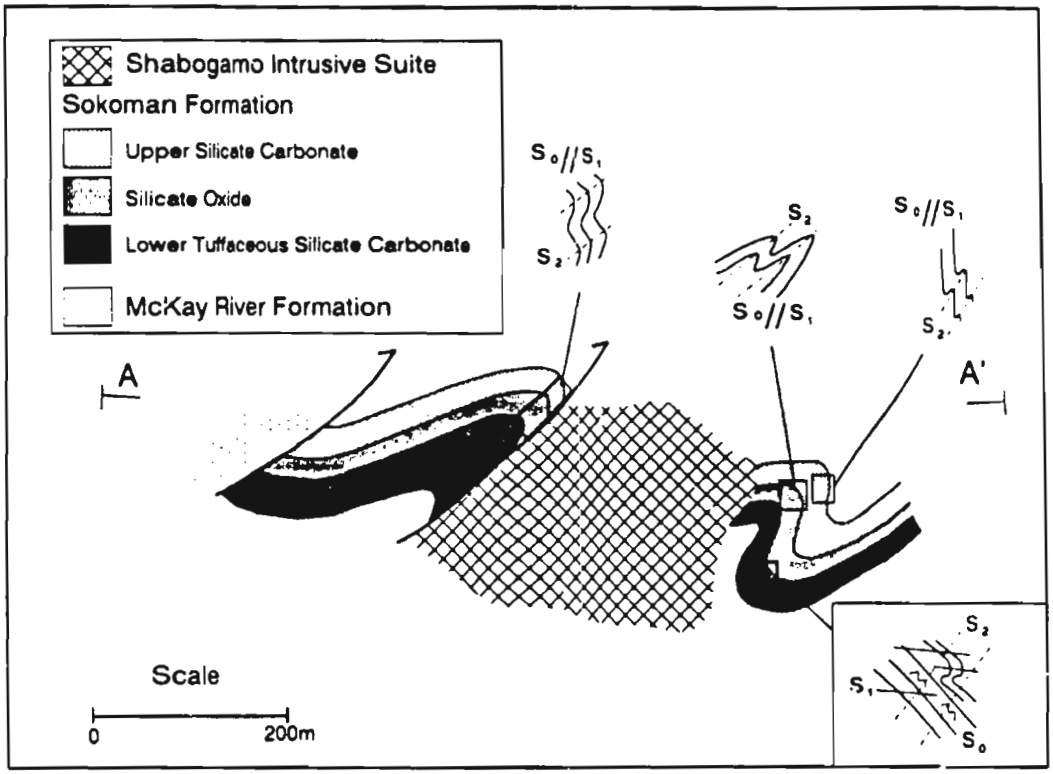

Figure 3.8. Schematic cross-section through the Tiphane Lake domain immediately south of Tiphane Lake. Fabric relationships are shown from field sketches. Inset depicts the relationship between upward-facing F_1 fold and the S_2 foliation in the hinge zone of a F_2 fold.

thrusts can be seen to cut up section through the folds (Figure 3.8). Because of the plane non-cylindrical and non-planar non-cylindrical nature of the F_2 folds, however, thrusts do not always cut through their overturned limbs as shown schematically in Figure 3.8, but also cut the upright, normal fold limbs. The S_2 foliation is everywhere axial planar to F_2 folds, and, in areas where thrusts cut the overturned limbs of folds, commonly curves listrically into parallelism with thrust surfaces.

3.2.4 Discussion

From the structural data presented above it can be seen that the Tiphane Lake domain is a polydeformed area that has undergone at least two phases of penetrative deformation and one phase of non-penetrative deformation. The earliest generation of structures, S_1 and Ls_1, are interpreted to be related to macroscopic D_1 folding. No D_1 generation structures where found in the Shabogamo gabbro, and they are therefore interpreted to be pre-date intrusion of the gabbro. Further, the apparent extensional fault in the D_2 horse discussed above (Figure 3.7) may be interpreted as a pre-F_2 thrust that was subsequently folded and overturned during D_2 (see Chapter 5 for further discussion of Pre-Grenvillian structures).

The second phase of penetrative deformation that is recorded by the rocks in the Tiphane Lake domain, D_2, was caused by northwest- to north-vergent folding and thrusting. This phase of deformation affected all cover rocks in the area including the Shabogamo gabbro. Gabbro bodies in the area are variably deformed but definitely have D2 fabric elements.

The third phase of deformation in the Tiphane Lake domain, D_3, is non-penetrative and is restricted to moderately southwest-dipping one to two meter-wide shear zones that reimbricate earlier structural features. Folding of D_2 thrusts east of Tiphane Lake is thought to be related to folding above a blind D_3 thrust.

3.3 Mobey Lake Domain

3.3.1 Introduction

The Mobey Lake doamin is composed predominantly of rocks of the Denault and McKay River formations and Shabogamo gabbro, with minor Sokoman Formation (Figure 3.9). The Denault Formation in the Mobey Lake doamin is a massive dolomite + calcite + quartz +/- feldspar +/- tremolite +/- talc marble with thin discontinuous

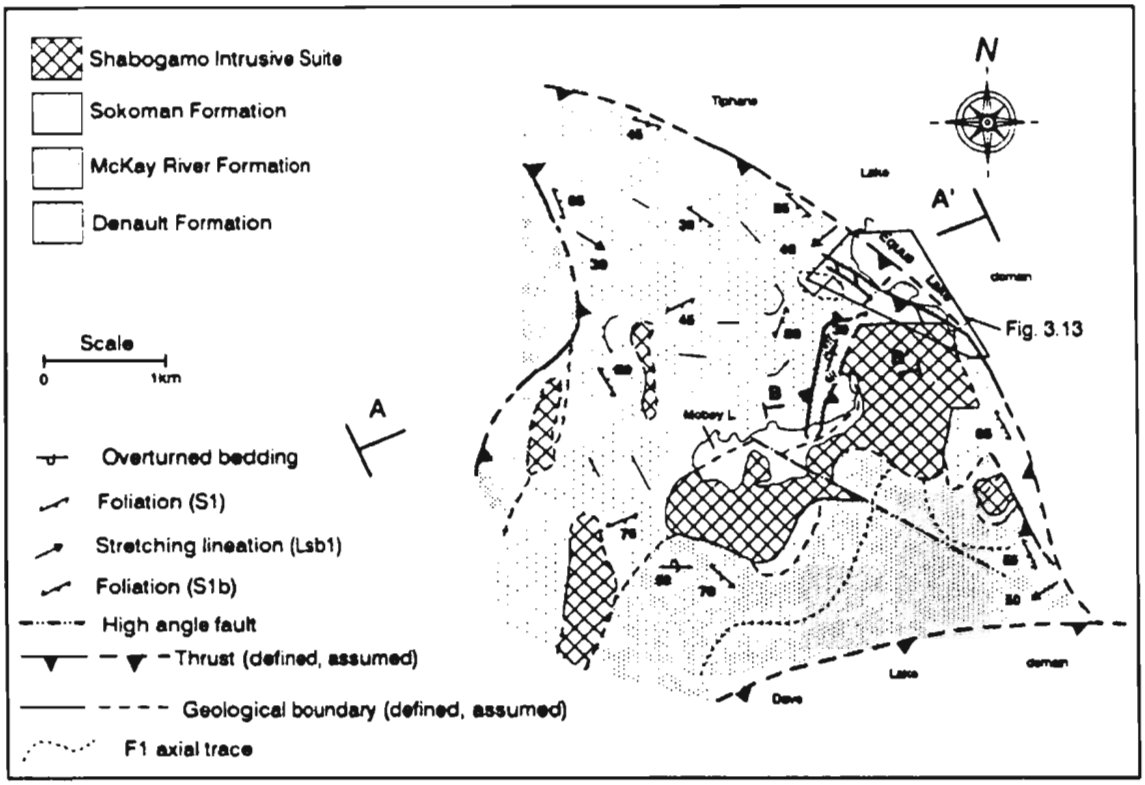

Figure 3.9. Generalized geological map of the Mobey Lake domain.

semipelitic layers of muscovite + quartz +/- biotite. Stromatolites occur locally. The McKay River Formation is typically a massive, matrix-supported pebble to boulder volcaniclastic conglomerate with thin interlayers of siltstone. The conglomerates consist of volcanic derived clasts, pillow breccia, and, in one outcrop, gabbro boulders. The matrix consists of chlorite, actinolite, plagioclase, sphene, and quartz, whereas the siltstone is a fine grained biotite and chlorite-rich rock. The Sokoman Formation in the Mobey Lake domain consists of the upper silicate oxide and silicate carbonate units, composed of quartz, feldspar, magnetite, and grunerite. The Shabogamo Intrusive Suite is a medium to coarse-grained gabbro that typically has a relict igneous texture. The common mineralogy in the metagabbro is chlorite, actinolite, plagioclase, epidote, white mica, biotite, and minor quartz.

Along the shore of Equus Lake the boundary between the Denault Formation and the McKay River Formation is well exposed, dips towards the southwest and grades without interruption from tuffaceous marble upwards into carbonate-rich volcaniclastic conglomerate. Based on this, the contact is interpreted to be stratigraphically normal way-up. South of Mobey Lake, however, the contact relationship between the McKay River Formation and the

Denault Formation is reversed, and southeast-dipping tuffaceous Denault Formation overlies carbonate-rich McKay River Formation implying the sequence is structurally overturned. Confirming this interpretation, stromatolites in the Denault Formation near this contact are upside-down.

The contact between the Sokoman Formation and the McKay River Formation west of Mobey Lake is not exposed, but can be located to within one to two meters in one outcrop where bedding, defined by tuffaceous layers in the Sokoman Formation, dips towards the west, beneath the McKay River Formation. Both rock types have only a weak foliation. This contact is therefore also interpreted to be stratigraphic, and overturned.

Contacts between the Shabogamo gabbro and cover rocks are generally undeformed and interpreted to be intrusive, though locally it can be shown to be tectonic (see below).

3.3.2 Internal Structure

There is no direct evidence in outcrop of macroscopic or mesoscopic F_1 folding in the Mobey Lake

domain. However, indirect evidence, in the form of S_1 foliation development does suggest the presence of a F_1 fold phase. Furthermore, the map pattern defined by the lithological boundaries is compatible with an early fold phase. However, this is somewhat obscured by intrusion of the gabbro and by structural overprinting in a subsequent folding event (Figure 3.9).

No penetrative fabric is developed internally in the Mobey Lake domain. However, the earliest fabric that can be distinguished, S_1 (Table 3.1), is quite widespread throughout the domain, though it is non-penetrative. The S_1 foliation is defined by aligned chlorite and actinolite +/- biotite in the McKay River Formation, and by flattened and elongate carbonate and quartz grains with muscovite and biotite in the Denault Formation. The orientation of S_1 is quite variable, dipping moderately to steeply towards the east-southeast to west (Figure 3.10). This foliation is not seen in the Shabogamo gabbro.

Macroscopic F_2 folds in the Mobey Lake domain are inferred from the pattern outlined by lithological boundaries and the variable orientation of S_1 form surface traces both locally and on the scale of the domain (see map in back pocket). However, macroscopic F_2

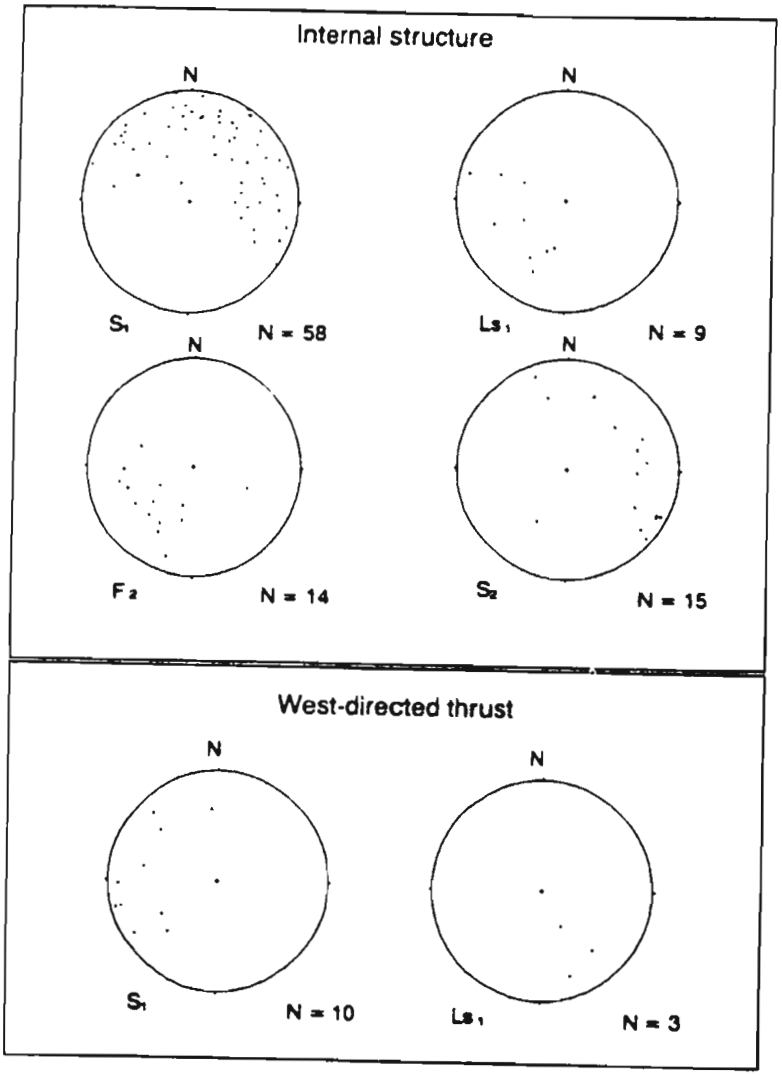

Figure 3.10. Lower hemisphere equal area projections of internal fabric elements from the Mobey Lake domain.

folds are rare, and are restricted to mesoscopic folds in biotite schist of the McKay River Formation in the southeastern part of the domain. These F_2 folds are tight to isoclinal, southwest-plunging and nearly reclined (Figure 3.10). A fine-grained mafic dyke that is possibly related to the Shabogamo gabbro is folded by F_2. A steeply northwest to north-dipping S_2 crenulation cleavage defined by aligned biotite is parallel to the axial plane of these F_2 folds.

Based on the field notes, samples, and thin-sections of Nath Noel and Toby Rivers, a high-angle fault zone is interpreted to cut the Mobey Lake domain in a poorly exposed area southeast of Mobey Lake (see map in back) where it offsets the contact between Shabogamo gabbro and the Denault Formation. This fault is defined by a strongly developed southwest-dipping cleavage and a southeast-plunging elongation lineation.

West of Mobey Lake, a north-striking fault zone with a curved form surface trace follows the fold pattern outlined by S1 form surface traces. Shear zone foliations dip steeply east, with a southeast-plunging elongation lineation in the shear surface (Figure 3.10). Locally, S-C planes indicate a west to northwest-directed reverse sense of movement (Figure 3.10). This geometry indicates

the fault places (older) McKay River Formation rocks on top of (younger) Sokoman Formation rocks. Sokoman Formation rocks occur in both the hangingwall and footwall of this fault suggesting it cuts up-section towards the south. The nature and significance of this fault is discussed in more detail in Chapter 5.

Immediately northeast of Mobey Lake, a narrow, elongate outcrop belt of Sokoman Formation is in contact with McKay River Formation to the west and, to the east, Denault Formation and Shabogamo gabbro. Bedding in the iron formation dips moderately to steeply towards the southeast and, using the stratigraphy worked out for the Sokoman Formation in the Tiphane Lake domain, the sequence youngs towards the northwest and is, therefore, overturned (Figure 3.11). The contact between the various units is not exposed so its precise nature cannot be determined. However, the fact that the Sokoman Formation youngs towards the contact with the McKay River Formation implies a reversal of the known stratigraphy, and of the stratigraphic sequence interpreted to the west of Mobey Lake. Likewise, stratigraphy is missing between the Sokoman Formation and the Denault Formation. Furthermore, as mentioned above, the contact between the McKay River and Denault Formations several hundred meters to the east, along the south shore of Equus Lake, is interpreted

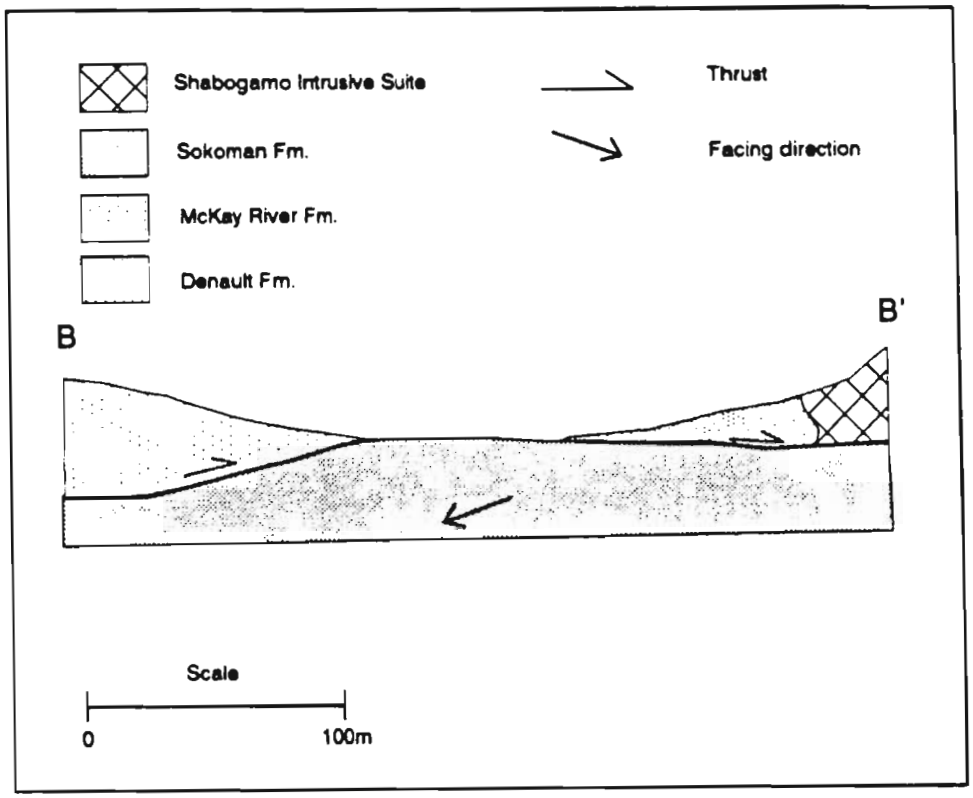

Figure 3.11. Schematic cross-section depicting the relationship of a narrow band of Sokoman Formation with structurally overlying Denault and McKay River formation and Shabogamo Intrusive Suite.

to be stratigraphic and is assumed to be stratigraphic elsewhere throughout the Mobey Lake domain. If stratigraphic continuity is preserved between the McKay River Formation and the Denault Formation, the Sokoman Formation in this area must form a structural slice, either as a klippe or a window. Since the Sokoman Formation appears to dip under the Denault Formation, it is probably a window (Figure 3.11). The fact that the gabbro does not intrude the iron formation may also further support this interpretation.

3.3.3 Boundary Structure

The boundary of the Mobey Lake domain with the southwestern Tiphane Lake domain and the northwestern Dave Lake domain is an arcuate, north- to northwest-striking zone (Mobey Lake domain boundary thrust, Figure 3.9) of intense deformation in which the dominant fabric, S_{1b}, dips moderately to steeply towards the southwest to west (Figure 3.12). An elongation lineation, Ls_{1b}, plunges towards the southwest, typically down-dip or with a high pitch angle in S_{1b}. S_{1b} along the Mobey Lake domain boundary is correlative with S_1 in the Tiphane Lake domain. Isoclinal, intrafolial, and rootless folds are found locally and all plunge southwest, subparallel to

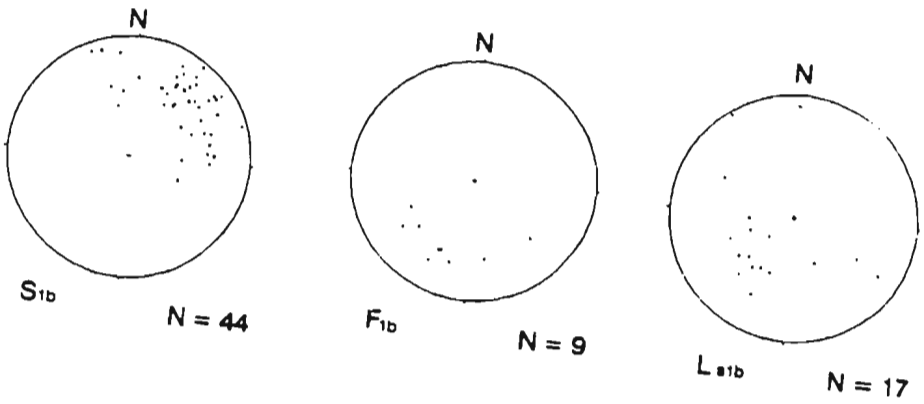

Figure 3.12. Lower hemisphere equal area projections of structural elements from the Mobey Lake domain boundary thrust.

the elongation lineation (Figure 3.12).

The structural style and intensity of deformation within the boundary zone changes along strike. In the northwest, the boundary is a discrete two to three meter-wide zone of mylonitic to phyllonitic volcaniclastic rocks. Locally, S-C planes indicate a northeast-directed thrust sense of movement. Here the boundary thrust places older McKay River Formation rocks of the Mobey Lake domain on top of younger Sokoman Formation rocks of the Tiphane Lake domain. South of Tiphane Lake a number of thrusts splay off the boundary thrust, truncating structures in the Tiphane Lake domain, where they can be correlated with D_3 thrusts in that domain.

The boundary zone is well exposed near the southwest and south sides of Equus Lake, where it was studied in detail (Figure 3.13). Along the southwest shore of Equus Lake the boundary zone shows an overall southwest dip and facing of units, as well as a northwest/southeast structural grain outlined by ductile shear zones that are linked by oblique thrusts. The boundary zone is an intensely imbricated thrust stack consisting of a number of fault-bounded horses of Denault, McKay River, and Sokoman formation rocks. The thrust stack is bound above and below by a roof thrust and a floor thrust,

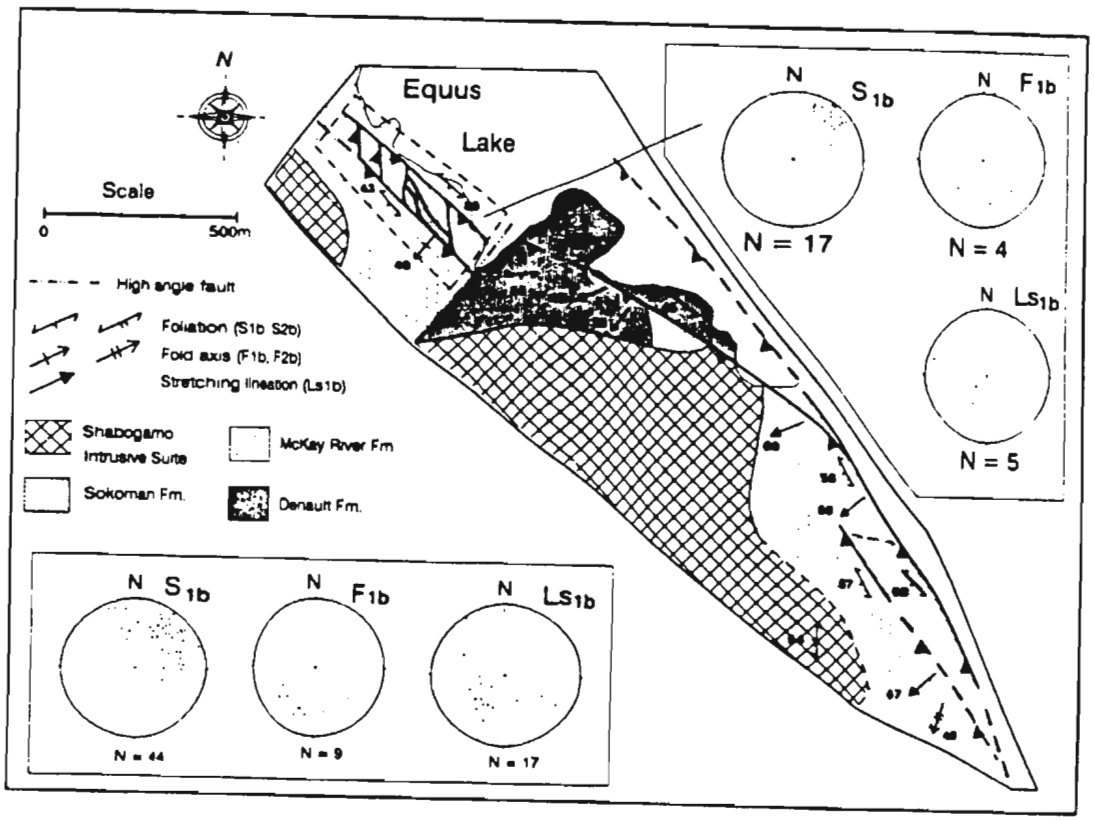

Figure 3.13. Detailed map of a portion of the Mobey Lake domain boundary thrust. See figure 3.9 for location.

respectively, and therefore constitutes part of a duplex. However, because of lack of exposure to the northwest and truncation of the thrust stack by a high-angle fault to the southeast, the floor and roof thrusts are not seen to splay or rejoin. Subsidiary thrusts cut up-section from trailing branch lines along the floor thrust and join the roof thrust along leading branch lines, typical of the geometry of a duplex (Boyer and Elliot, 1982). Kinematic indicators such as C-S planes and tailed porphyroclast systems in the imbricate shear zones indicate that movement occurred by thrusting.

Internally, rocks in the thrust stack are folded and penetratively strained. Open to tight macroscopic F_{1b} folds plunge towards the south to southwest, subparallel to Ls_{1b}. S_{1b} in the thrust stack dips steeply southwest, axial planar to F_{1b} (Figure 3.13).

One horse in the duplex consists of tightly folded and foliated Sokoman Formation rocks. Folds in this horse are typically reclined and plunge southwest, parallel to Ls_{1b}. Lower horses in the thrust stack consist of McKay River Formation schists and, increasingly, Denault Formation marble. In horses that contain rocks of both McKay River and Denault formations in stratigraphic contact, the older Denault Formation is always on top of

the younger McKay River Formation, forming an imbricated overturned fold limb. S_{1b} is penetratively developed in these lower horses and folds are typically open to tight and near reclined. In one horse an axial planar S_{1b} schistosity in a macroscopic fold can be observed to curve listrically into the shear plane of a thrust-through overturned limb. The lowest horse in the thrust stack is less strained and S_{1b} is only developed in the hinge area. However, the relationship between folds and thrusts along the boundary zone as a whole suggest the predominance of fault propagation folding leading to to a forelimb imbricate fan, with local duplexing.

South of Equus Lake, the Mobey Lake domain boundary is a fifty meter wide zone of penetrative shearing in which S_{1b} dips moderately southwest with a down-dip elongation lineation. Intrafolial and rootless folds plunge southwest, parallel to the elongation lineation. C-S planes and tailed porphyroclast systems indicate that movement occurred by northeast-directed thrusting.

3.3.4 Cross-sections

Poor control on orientation of macroscopic structures on the domain scale precludes the construction of accurate cross-sections, or of well-constrained down-

plunge sections. Schematic cross-sections were constructed using local field geometries to constrain the various lithological and structural relationships (Figure 3.14).

The structural geometry of the Mobey Lake domain is dominated by northeast directed folding and thrusting that overprints and truncates an earlier (D_1) phase of folding (Figure 3.14). F_2 folding in the Mobey Lake domain appears to be related to emplacement of the domain, and are interpreted to be fault propagation style folds. Thrusting is restricted to the boundary zone where northeast-verging thrusts emplace Mobey Lake domain rocks on top of the Tiphane Lake domain and the Dave Lake domain. Northeast-verging thrusts in the Tiphane Lake domain (discussed above) are related to the emplacement of the Mobey Lake domain and S_3 foliations are correlative with S_{1b} in the Mobey Lake domain boundary. These thrusts truncate second generation structures in the Tiphane Lake domain (Figure 3.2), with an out-of-sequence geometry.

The amount of tectonic transport incurred by the Mobey Lake domain is impossible to determine with any accuracy. However, if the outcrop of Sokoman Formation rocks along the north shore of Mobey Lake is in a

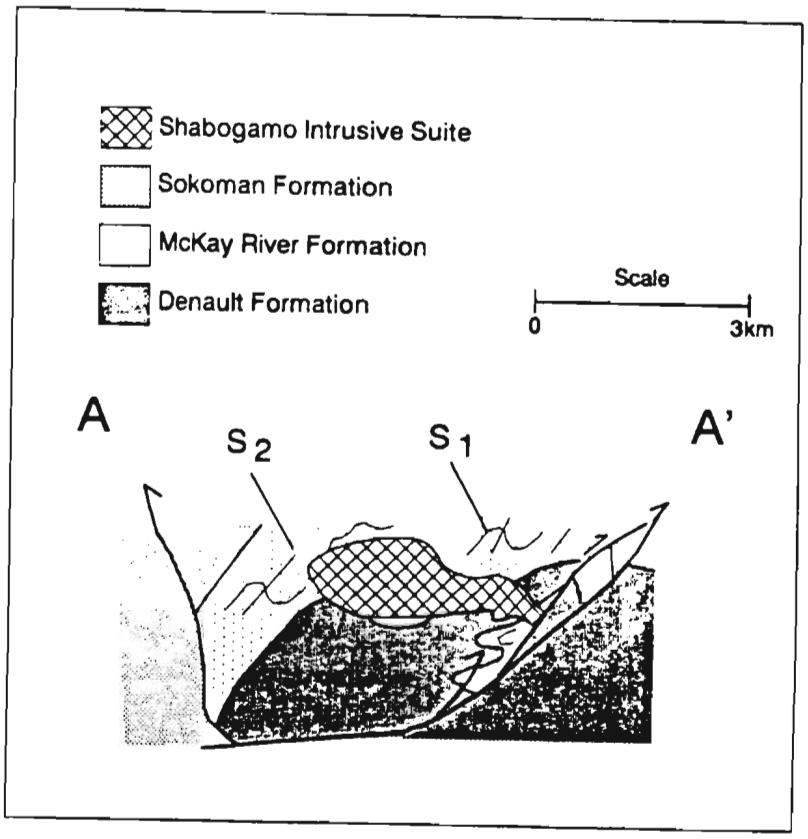

Figure 3.14. Schematic cross-section through the Mobey Lake domain.

structural window, then it is possible to qualitatively determine a minimum distance travelled by the domain. If there is stratigraphic continuity between Sokoman Formation rocks in the Tiphane Lake domain, two to three kilometres to the north to northeast, then the minimum distance travelled by the Mobey Lake domain is of this order. This interpretation may be invalidated if there were any changes in the stratigraphy due to earlier deformation.

3.4 Equus Lake Domain

3.4.1 Introduction

The Equus Lake domain is a northwest-southeast trending elongate structural domain consisting of the Equus Lake formation and Shabogamo gabbro (Figure 3.15). The Equus Lake formation is made up of a basal boulder conglomerate containing clasts of Denault, Sokoman, and Menihek formations that grades stratigraphically upwards to a medium-grained sandstone and greywacke with laminated siltstone at the top. The Shabogamo Intrusive Suite in the Equus Lake domain is a fine to medium-grained gabbro with a relict igneous texture, that locally displays a S_1 schistosity. The common mineralogy

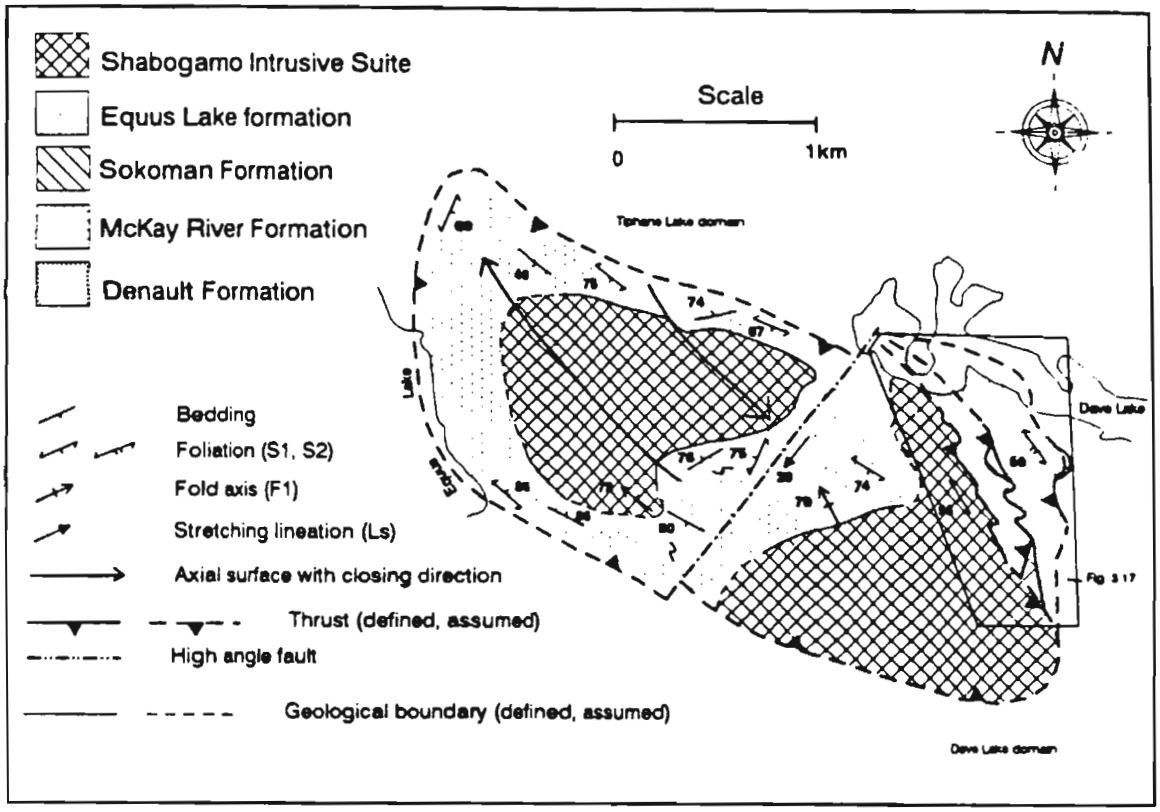

Figure 3.15. Geological map of the Equus Lake domain. The macroscopic fold orientation pattern is neutral and the axial traces of a fold pair are shown.

in the gabbro is chlorite, minor actinolite, plagioclase, epidote, and muscovite. At the contact between the two rock types the Equus Lake formation is a fine-grained hornfels and the gabbro is aphanitic, but locally is deformed. The nature of the contact between the metasediments and the gabbro indicates an intrusive relationship, variably reworked by regional deformation.

3.4.2 Internal Structure

The macroscopic structure of the Equus Lake domain is dominated by a macroscopic, neutral fold pair in both the Equus Lake formation and the Shabogamo gabbro (Figure 3.15). Parasitic Z, M, and S-folds, together with bedding-cleavage relationships, outline the macroscopic fold structure and allow the axial traces of the fold pair to be mapped. Close to tight mesoscopic class 1C to class 2 (Ramsay, 1967) parasitic folds on the limbs and hinges of the macroscopic fold plunge nearly vertically towards the west to northwest, down-dip in their axial surfaces (Figure 3.16). The axial surface traces of the folds are oblique to the northern boundary of the domain and appear to be truncated by it. Graded bedding in the Equus Lake formation indicates the structural facing of the fold structure is towards the northwest. A moderately- to well-developed slaty cleavage in molasse

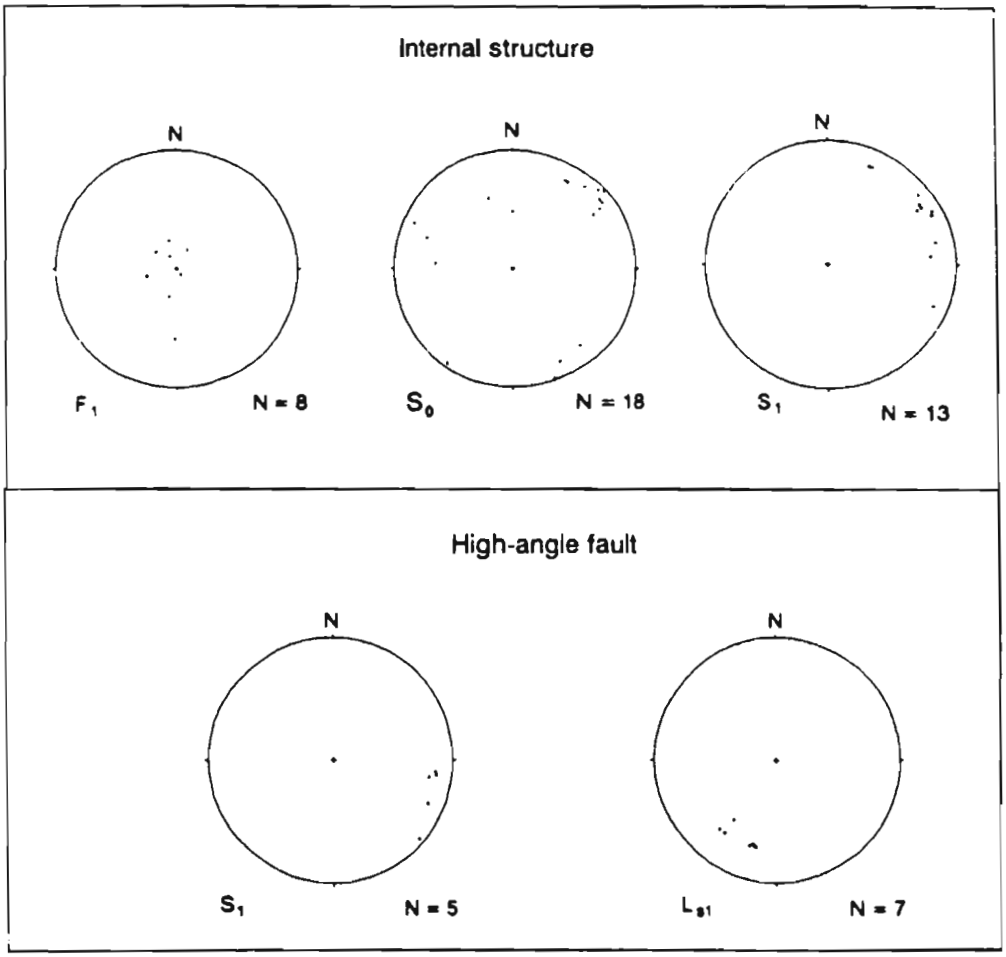

Figure 3.16. Lower hemisphere equal area projections of structural elements from within the Equus Lake domain.

rocks dips steeply southwest, subparallel to the F_1 axial plane.

Evidence of boudinaged and fractured bedding is widespread in metasedimentary rocks throughout the Equus Lake domain. Boudins show no evidence of necking, and the area between individual boudins is typically filled with quartz or calcite. In one outcrop in the southeastern fault block, isolated and variably oriented fold hinges occur in fractured and boundinaged siltstone. Offset on boudinaged layers varies from a few centimetres up to one meter. There is no evidence of boudinaging in the more competent gabbro.

3.4.3 Boundary Structure

The boundary of the Equus Lake domain forms a topographic low that is generally poorly exposed. However, one area near the west end of Dave Lake is well exposed and was studied in some detail (Figure 3.17).

The boundary zone in this area is a 200-300 meter-wide zone with a northwest-southeast structural grain outlined by rocks of the Denault, McKay River, and Sokoman formations that are structurally overlain by, and interleaved with, Shabogamo gabbro (Figure 3.17). The

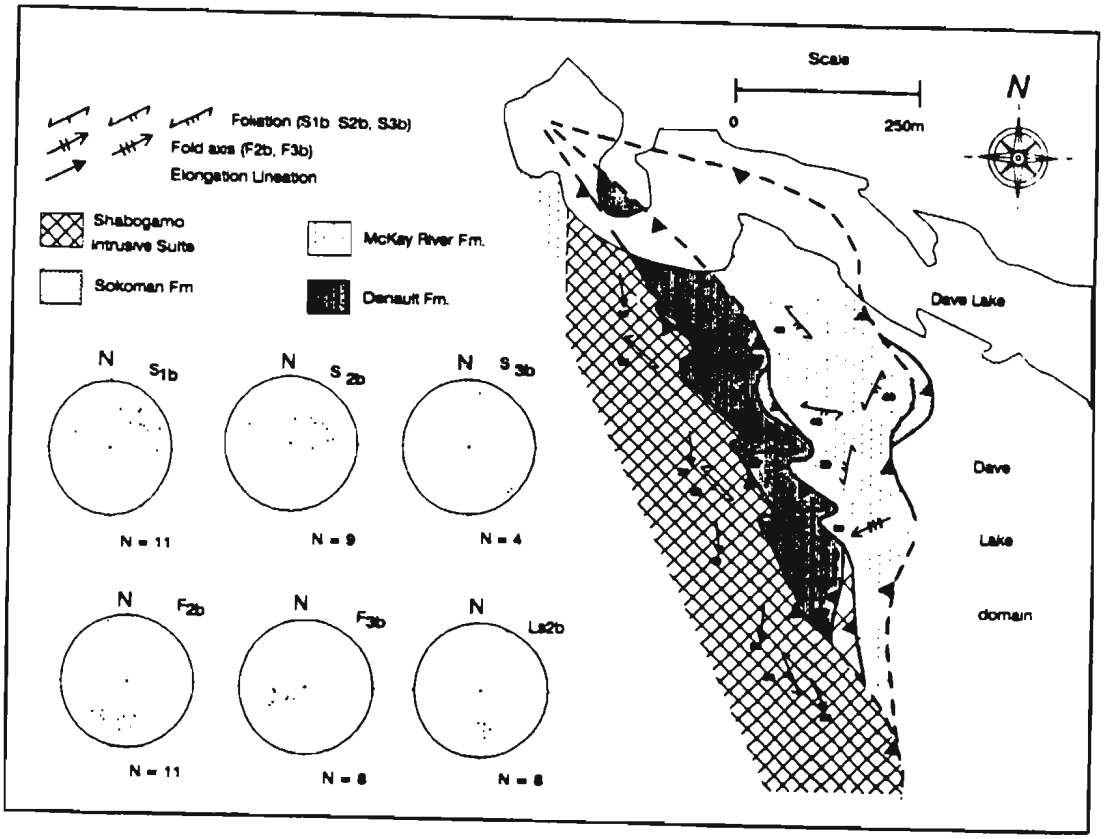

Figure 3.17. Detailed geological map of a portion of the Equus Lake domain boundary (see figure 3.15 for location).

stratigraphic sequence along this part of the boundary is inverted, and Denault Formation rocks overly those of the McKay River Formation. All rocks in this area are penetratively strained, with a folded phyllonitic fabric (S_{1b}) and stretching lineation (Ls_{1b}) developed throughout (Figure 3.17). These fabrics are not related to any structural elements internal to the domain, nor can they be correlated with fabrics in the Tiphane Lake or Dave Lake domains (see map in back pocket).

Blocks of up to 100 meters in size of highly strained gabbro and iron formation decorate the boundary between the Denault and McKay River Formations (Figure 3.17). Sokoman Formation blocks are typically L > S tectonites. The appearance of gabbro and iron formation blocks along boundaries, together with the inversion of stratigraphy and high degree of strain in cover rock, indicates that the contacts between rock types are tectonic, and may be thrusts that place older rocks on top of younger, but also entrain younger rocks.

Along the contact between the Denault Formation and the overlying gabbro, rocks show a southwest-dipping protomylonitic to mylonitic foliation, with an elongation lineation that has a high pitch angle in the shear foliation. These fabrics are also folded and are

interpreted to be S_{2b} and Ls_{2b}, respectively. The strongly lineated and foliated nature of the overlying gabbro along the contact suggests the contact is a heterogeneous shear zone. These shear zones are related to progressive movement along the boundary fault zone (which truncates the internal D_1 neutral folds (Figure 3.15)).

Two phases of mesoscopic folds are developed within the boundary zone and these fold the boundary zone fabrics. The earlier fold generation is close to tight, shallow to moderately south to southwest-plunging, typically reclined folds that fold the S_{1b} and Ls_{1b} (Figure 3.17). These folds are denoted F_{2b}. F_{2b} folds have a well-developed south- to southwest-dipping axial planar cleavage (S_{2b}) in hinge zones that can be correlated with S_{2b} discussed above. In one location, a northeast-verging mesoscopic F_{2b} fold has a thrust-through overturned limb and the axial planar cleavage curves into the shear plane.

Locally, a macroscopic moderately- to steeply-southwest to west-plunging, mesoscopic F_{3b} folds overprint the F_{2b} folds (Figure 3.17). Small-scale F_{3b} folds on the limbs and hinge of the larger F_{3b} fold have a steeply south- to southeast or north- to northwest-dipping axial planar cleavage in fold hinges (S_{3b}).

Overprinting relationships between F_{2b} and F_{3b} folds are typically type three interference patterns (Ramsay, 1967).

Bisecting the Equus Lake domain is a northeast-trending, 4 to 5 meter wide high-angle fault zone that is localized in conglomerate and sandstones of the Equus Lake formation (Figure 3.18). Tailed porphyroclast systems, S-C planes, and Riedel fractures give a sinistral movement sense. A well-developed stretching lineation, defined by quartz rodding and elongation of clasts in the conglomerate, plunges shallowly southwest (Figure 3.16). Cleavage in the metasediments bends into the fault over a distance of some tens of meters and also gives a sinistral shear sense. All kinematic indicators suggest that the fault has a predominantly sinistral strike-slip movement pattern. This fault truncates the Equus Lake domain and domain boundary.

3.4.4 Discussion

The structure of the Equus Lake domain is dominated by a macroscopic neutral fold pair. The steep plunge of the fold structure obviates the necessity of constructing cross-sections since the map pattern itself approximates a down plunge-projection.

Figure 3.18. Field photograph of high-angle fault showing the development of a rodding lineation in a pebble conglomerate of the Equus Lake formation.

The boundary fault of the Equus Lake domain is continuous around the entire domain, and truncates the internal fold structure of the domain. The northeast side of the boundary fault is locally an intense zone of deformation in which phyllonitic metasediments and gabbro have been thrust and folded. The presence of discontinuous slivers of various lithological units in the boundary zone in this area is reminiscent of a tectonic melange containing exotic blocks.

Based on the above, the juxtapositioning of younger Equus Lake formation rocks on top of older Knob Lake Group metasediments is likely tectonic, and the Equus Lake domain is therefore interpreted to be a klippe (Figure 3.19). A possible mechanism for emplacement of the klippe is by gravity sliding. The direction of sliding, as indicated by structural elements along the northern boundary zone, was possibly towards the north to northeast which resulted in thrusting and the development of a tectonic melange along this side of the klippe. The entire domain was later cut by an oblique-slip fault. The distance travelled by the Equus Lake domain cannot be determined because there are no known rocks, either in or outside the map area, that positively correlate with the Equus Lake formation.

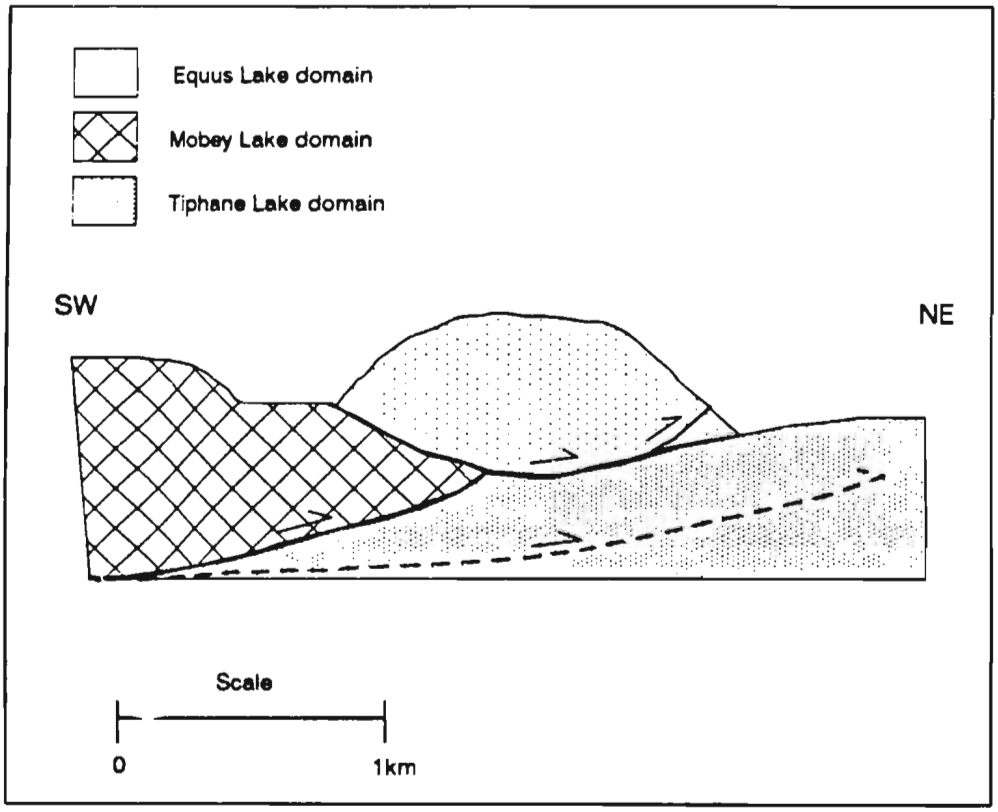

Figure 3.19. Schematic section of the Equus Lake domain showing its structural position as a klippe relative to the Tiphane Lake and Dave Lake domains.

3.5 Dave Lake Domain

3.5.1 Introduction

The Dave Lake domain is the largest domain in the map area, covering approximately 75% of the map (Figure 3.1). It has an overall east-west structural grain outlined by structures and by surface traces of lithological contacts (Figure 3.20). On the basis of structural style and metamorphism, the Dave Lake domain can be divided into two thrust sheets, the Dave Lake thrust sheet to the north, structurally overlain to the south by the Isa Lake thrust sheet (Figure 3.20).

Rocks in the Dave Lake domain consist predominantly of Denault Formation, McKay River Formation, and Shabogamo Intrusive Suite, with minor Sokoman Formation. Marbles of the Denault Formation occur only in the Dave Lake thrust sheet, where they consist of calcite, dolomite, tremolite, quartz, and talc with thin, discontinuous muscovite-rich interlayers. The McKay River Formation outcrops throughout the Dave Lake domain. In the Dave Lake thrust sheet, the McKay River Formation is a volcaniclastic conglomerate to volcaniclastic

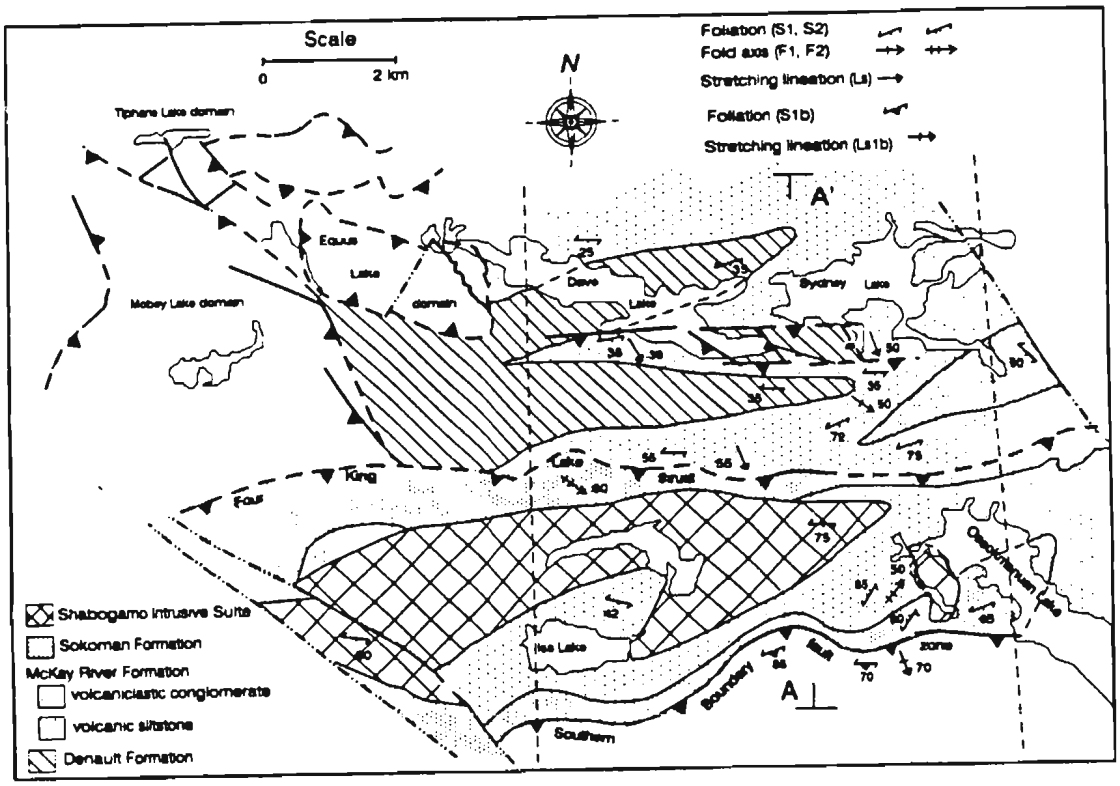

Figure 3.20. Geological map of the Dave Lake domain. DLTS = Dave Lake thrust sheet, ILTS = Isa Lake thrust sheet. Discussion in the text is based on a well exposed corridor marked by the parallel dashed lines.

tuffaceous schist containing typically, chlorite, actinolite, plagioclase, and sphene, with minor quartz and epidote. Late porphyroblasts of actinolite and chlorite are common throughout. The McKay River Formation in the Isa Lake thrust sheet can be subdivided into two lithostratigraphic units consisting of a lower volcaniclastic siltstone and pillow lava unit and an upper volcaniclastic tuffaceous schist unit. The lower unit is a biotite, graphite, plagioclase, and quartz schist, with minor garnet, and amphibole. The Sokoman Formation, which outcrops only in the Dave Lake thrust sheet, consists of grunerite, quartz, feldspar, and magnetite that can be related to the upper silicate-carbonate unit present in the Tiphane Lake domain. Metasedimentary rocks in the Isa Lake thrust sheet are intruded by a large pluton of Shabogamo Intrusive Suite gabbro. In thin-section it can be seen that the gabbro is metamorphosed, but a relict igneous texture is still apparent in the field. The gabbro consists of actinolite, chlorite, plagioclase, epidote, biotite, with minor muscovite and garnet. A metamorphic aureole is developed in schists of the McKay River Formation around the gabbro pluton (see Chapter 4), a number of southeast-trending gabbroic dykes have also been found in the Isa Lake thrust sheet (this is the first time such dykes have been reported anywhere in the map area).

Outcrop in both the Dave Lake thrust sheet and the Isa Lake thrust sheet is sparse and confined to shoreline exposures around the various lakes. The large-scale map pattern (see foldout map in back) is based on extrapolation of lithological and structural relationships from well-exposed areas. The maps of Rivers (1982) and Rivers and Wardle (1985), as well as aeromagnetic maps of the area (Geological Survey of Canada, map 6062G, 1972) were used to constrain the map pattern, which is therefore largely interpretive. The following section will focus on a relatively well-exposed transect through the Dave Lake domain (Figure 3.20).

3.5.2 Internal Structure

3.5.2.1 Dave Lake Thrust Sheet

The following discussion is based on local (scarce) outcrop pattern and the presumed aeromagnetic signatures of the Denault and McKay River formations. South of Dave Lake, mesoscopic close to tight, southeast- to south-plunging non-plane, non-cylindrical (Figure 3.21) M or S-folds are interpreted be parasitic to larger scale folds, and to reflect their geometry. These parasitic folds support the broad map pattern interpretation for the

existence of such macroscopic folds. The macroscopic structure of the Dave Lake thrust sheet is thus interpreted to consist of two macroscopic, tight to isoclinal antiform/synform pairs (see map in back pocket) that transpose lithological boundaries into a east-west striking orientation. A south to southwest-dipping penetrative foliation, S_1, occurs throughout the Dave Lake thrust sheet (Figure 3.21) and is everywhere axial planar to the macroscopic folds which are interpreted to be F_1 folds.

S_1 is defined in McKay River Formation by aligned chlorite and actinolite and (micro)lithons of quartz and plagioclase. Bedding in these rocks is not well defined, but, where present, it is typically subparallel with S_1. There is typically a stretching lineation (Ls_1), defined by the preferred orientation of inequidimensional amphiboles and clasts in the conglomerate, that has a large pitch angle in S_1 (Figure 3.21). In rocks of the Denault Formation, S_1 is generally defined by flattened carbonate and quartz grains, as well as by aligned muscovite in pelite-rich layers. Locally, S_1 is folded by variably-plunging mesoscopic F_2 folds (Figure 3.21).

South- to southwest-dipping shear zones occur along the south shores of Dave Lake and Sydney Lake (Figure

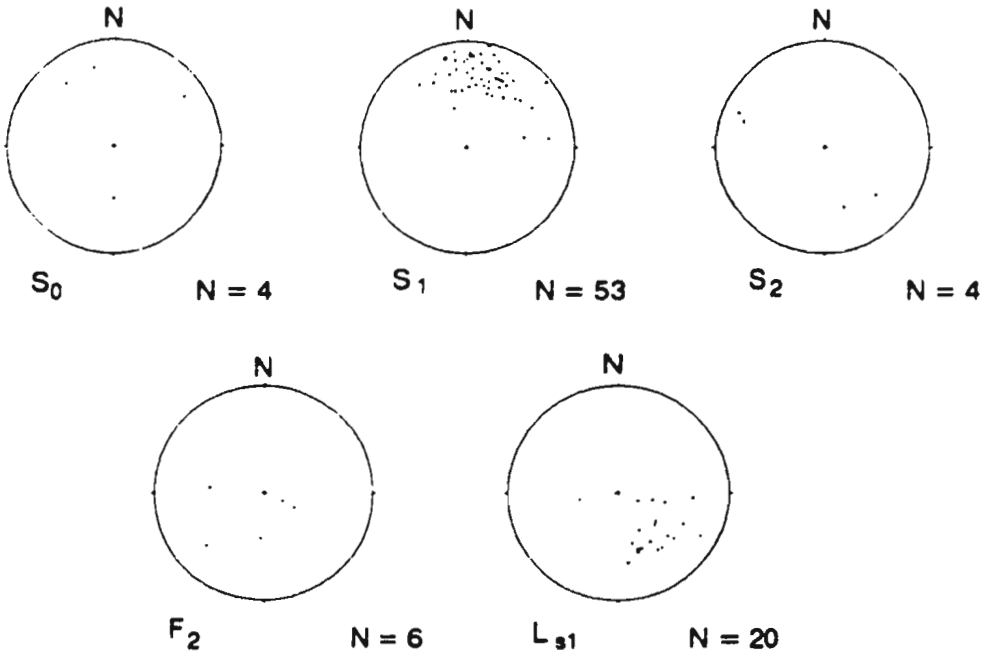

Figure 3.21. Lower hemisphere equal area projections of structural data from the Dave Lake thrust sheet.

3.20). Kinematic indicators (S-C planes and rotated porphyroclast systems), together with a down-dip stretching lineation give north-directed thrust sense of movement. These shear zones are linked by southwest-dipping two to three meter wide subsidiary faults that splay off the lower thrust and rejoin the upper thrust, giving the fault system a duplex geometry. The roof thrust is well exposed in rocks of the Denault Formation along the shoreline of Dave Lake, where it is a four to five meter wide, straight to anastomosing, partially annealed calc-mylonite. The mylonitic fabric wraps around pods of quartz-rich carbonate (Figure 3.22). The duplex is overlain to the south by schistose rocks of the McKay River formation. Along strike to the west, parallel to the shore of Dave Lake, the fault system is a 75 to 100 meter wide phyllonite zone that transposes lithological layering into parallelism with the shear zone fabric which dips southeast to south with a mineral- and clast-defined lineation, Ls_1, that typically plunges down-dip (Figure 3.21).

These shear zones offset lithological boundaries in F_1 limbs and fold hinges and are typically oblique to the S_1 foliation. Shear zones are post-F_1 folding, and possibly formed in a developing fold nappe.

Figure 3.22. Field photograph of calc mylonite with shear zone fabric wrapping around quartz-rich pods.

The Dave Lake thrust sheet is structurally overlain to the south by the Isa Lake thrust sheet (Figure 3.20). The boundary between the two is a ten to fifteen meter-wide southeast-dipping mylonite zone, the Four King Lake thrust. An elongation lineation plunges southeast, down-dip in the mylonitic fabric (Figure 3.23).

3.5.2.2 Isa Lake Thrust Sheet

The earliest structural feature developed in the Isa Lake thrust sheet is a penetrative foliation (S_1) in rocks of the McKay River Formation (Figure 3.20). This foliation is defined by aligned actinolite and to a lesser extent chlorite and biotite in the schistose volcaniclastics, and by biotite and microlithons of quartz and feldspar in the basal metasiltstones. S_1 is typically subparallel to bedding (S_0) in the metasiltstones, but locally their angular relationship indicates the presence of larger north-south-plunging antiformal-synformal closures. S_1 is not seen in the Shabogamo gabbro, and, in one outcrop, a gabbro dyke cuts both the bedding and S_1 in the metasediments, indicating that S_1 pre-dated emplacement of the gabbro. Further, garnet porphyroblasts in McKay River schists in the metamorphic aureole around the gabbro pluton appear to overgrow S_1. These relationships are discussed in more

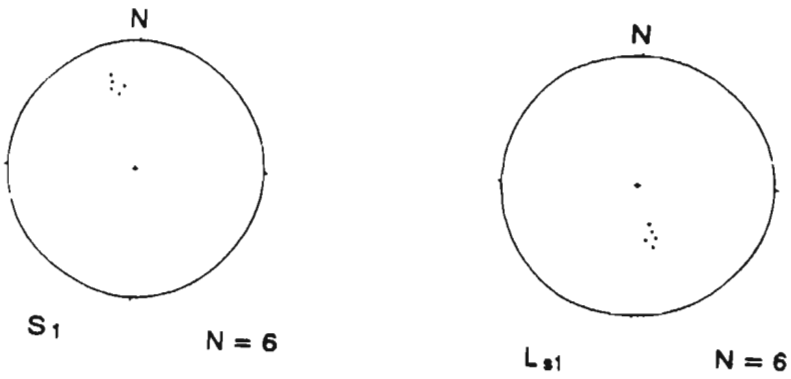

Figure 3.23. Lower hemisphere equal area projections of structural data from the Four King Lake thrust.

detail in Chapters 4 and 5.

The internal structure of the Isa Lake thrust sheet (Figure 3.20) is dominated by macroscopic northeast-southwest-plunging folds (Figure 3.24) that are overturned towards the north. These folds fold the S_1 foliation and are therefore denoted F_2. The F_2 geometry is that of close to tight nonplane noncylindrical folds with a well-developed southwest-northwest-dipping axial plane foliation (S_2) in the hinge zone (Figure 3.24). Locally, S_2 is a pressure solution cleavage. F_2 folds affect the Shabogamo gabbro on both a macroscopic scale (see map in back pocket) and on the outcrop scale where there is an S_2 foliation developed locally. The gabbro dyke described earlier is folded by F_2 and has a S_2 foliation developed at an angle to S_1 in the host rock, which also has a S_2 foliation. The dyke, however, does not contain a S_1 foliation.

3.5.3 Boundary Structure

The northern boundary of the Dave Lake domain is not exposed in the map area. The southern boundary is generally poorly exposed, but can be followed for approximately one kilometre near the shore of Ossokmanuan Lake as a fifty to one hundred meter-wide, sulphide-rich

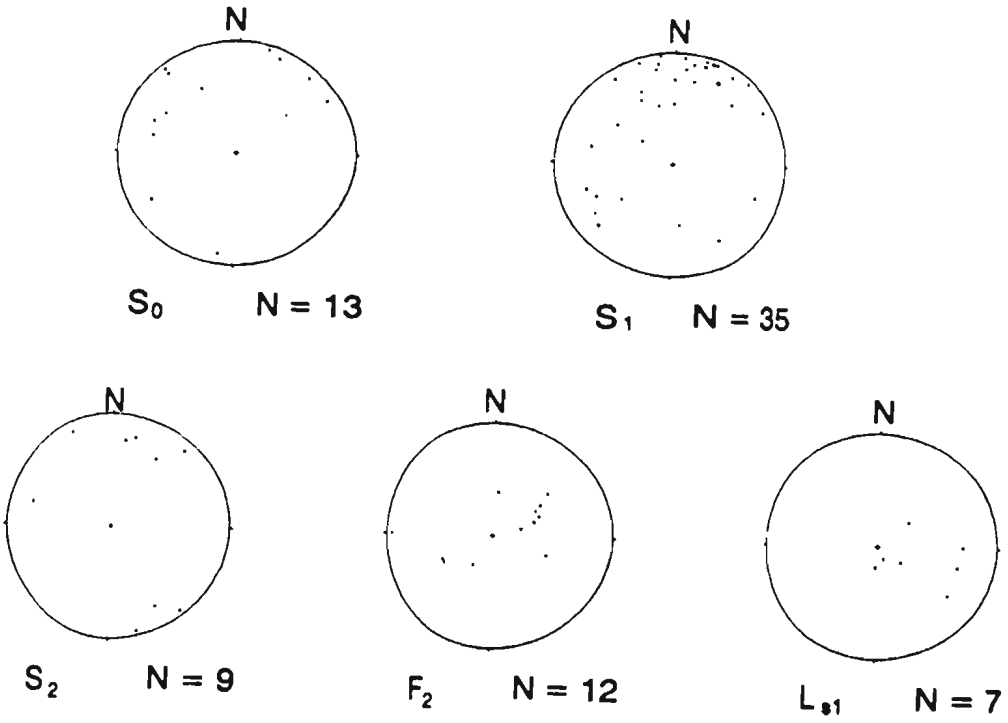

Figure 3.24. Lower hemisphere equal area projections of structural data from the Isa Lake thrust sheet.

shear zone contained in the lower McKay River Formation. This shear zone is named the Southern Boundary zone fault. The Southern Boundary zone fault is marked by a strongly developed, northeast-southwest striking, nearly vertical cleavage (S_{1b}) and a northeast- to east-plunging stretching lineation with a high pitch angle in S_{1b} (Figure 3.25). Rootless, small-scale folds plunge parallel to the stretching lineation. In rocks of the McKay River Formation S_{1b} is a penetrative phyllonitic fabric, whereas in the Shabogamo gabbro it is an inhomogeneous anastomosing zone of deformation that typically grades over a distance of a meter from undeformed gabbro to a several centimetre wide ultramylonite. The Southern Boundary zone fault cuts across F_2 folds in the Isa Lake thrust sheet truncating fold limbs and isolating fold hinges. However, it also has a curved form surface trace (Figure 3.20) that has a fold pattern as F_2 folds within the Isa Lake thrust sheet, and appears to be folded by them. Several small splays branch off the Southern Boundary zone fault, typically cutting across fold limbs and hinges.

Kinematic indicators that give a consistent movement direction were not found along the boundary fault zone. However, the occurrence of garnet coronas around pyroxene porphyroclasts in the overlying gabbro suggest that these

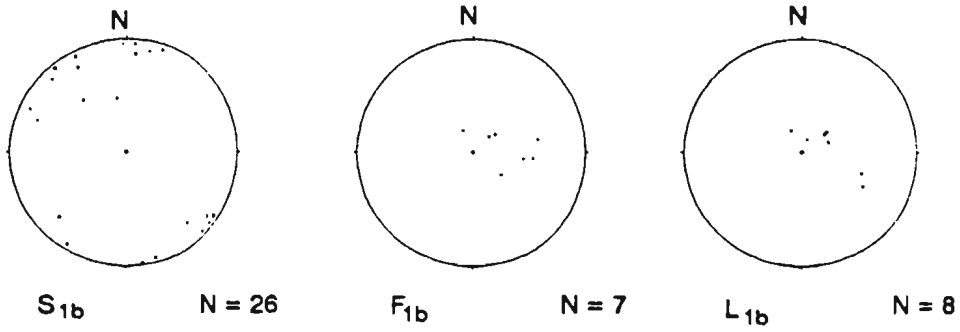

Figure 3.25. Lower hemisphere equal area projection of structural elements from the southern boundary zone.

rocks are of a higher metamorphic grade than those in the Isa Lake thrust (J. Connelly, pers. comm.). The southern boundary fault is therefore interpreted to be a thrust that places a higher grade gabbro-dominated thrust sheet on top of the Dave Lake domain.

The maps of Rivers (1982) and Rivers and Wardle (1985) have a number of interpreted northwest-striking high-angle faults in this area. These interpretations were based on the change in orientation of fabric from the regional southeast to south dip to southwest to west dips along a narrow zone of intense deformation. Lithological boundaries also appear to be offset across these features. Based on this information, the Dave Lake domain is interpreted to be offset to the northeast and the southwest by a series of northwest-striking high angle-faults (see map in back pocket). The map pattern in the southwest suggests that these faults have an apparent sinistral strike-slip offset.

3.5.4 Cross-sections

A schematic cross-section (Figure 3.26) was constructed along a narrow corridor through the Dave Lake domain (Figure 3.20). The structural geometry of the Dave

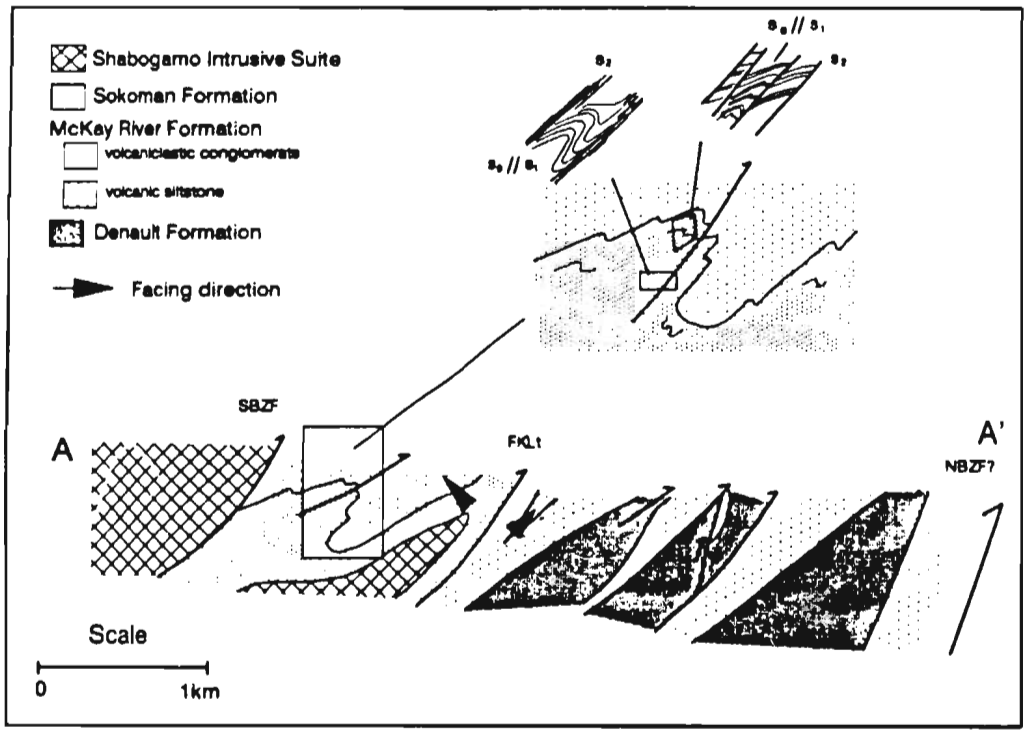

Figure 3.26. Schematic cross-section along a corridor through the Dave Lake (see figure 3.20 for location). SBFZ = southern boundary fault zone. FKLt= Isa Lake thrust sheet northern boundary. NBZF = inferred northern boundary boundary zone fault.

Lake domain is dominated by tight to isoclinal, steeply-plunging to reclined macroscopic D_1 and D_2 folds in the respective thrust sheets. Because of the orientation pattern of the folds in the Dave Lake thrust sheet, fold closures would not show on a vertical cross-section, perpendicular to the regional axial plane trend, if the folds are reclined. Thus Figure 3.26 is interpretative and simplistic, with the thrusts assumed to cut through the forelimbs of the folds, placing older rocks on top of younger.

Deformation in the Isa Lake thrust sheet occurred dominantly by folding, with thrusting restricted to the hinge area of one fold (Figure 3.26, inset). Folds in the thrust sheet plunge northeast-southwest and are typically reclined. The northern boundary thrust of the Isa Lake thrust sheet cuts through the limb of an upward-facing fold, placing older rocks of the Isa Lake thrust sheet on top of younger rocks in a downward-facing fold in the Dave Lake thrust sheet (Figure 3.26). The southern boundary thrust, however, cuts across the limbs of a F_2 fold, isolating the fold hinge in the Isa Lake thrust sheet (Figure 3.20).

3.5.5 Discussion

The Dave Lake domain can be divided into two thrust sheets on the basis of structural style and metamorphic grade (see chapter 4 for discussion of metamorphism). These thrust sheets are the Dave Lake thrust sheet to the north, structurally overlain by the Isa Lake thrust sheet to the south. The dominant structure in the Dave Lake thrust sheet is a penetrative, south-dipping S_1 foliation. S_1 is interpreted to be axial planar to southeast-plunging macroscopic F_1 folds. A duplex occurs along the southeastern shore of Dave Lake, within the thrust sheet. The appearance of Denault Formation in the duplex may reflect the lithologies that occur in the subsurface in the Dave Lake thrust sheet and which have been brought to the surface in the duplex by thrusts that cut through the Denault-cored southeast to south-plunging folds at depth. This geometry places younger rocks of the McKay River Formation on top of older rocks of the Denault Formation, in the direction of thrust movement.

The Isa Lake thrust sheet is dominated by doubly-plunging, northwest-verging F_2 folds that fold a penetrative S_1 foliation that is cut by the Shabogamo gabbro. The Southern Boundary zone fault, which truncates fold structures in the Isa Lake thrust sheet, is itself

folded.

The relationship between folding and thrusting in the Dave Lake domain is not the simple progression of thrust-through overturned folds that place older rocks on top of younger rocks in the direction of thrusting. Instead, there is a complex relationship between the two, in which thrusts truncate earlier folds, as in the Dave Lake thrust sheet, or in which thrusts truncate folds but are themselves folded in a style similar to the folds they cut, as in the Isa Lake thrust sheet. Clearly this would be due to D_2 thrusts cutting through earlier macroscopic F_2 folds, which were possibly refolded by F_2 fault propagation folds to give downward facing folds in the northern part of the Isa Lake thrust sheet.

These relationships suggest that the structural style of the Dave Lake domain is that of a continuously developing D_2 fold nappe in which early formed folds are truncated by synchronous to late thrusts.

CHAPTER 4
Metamorphism

4.1 Introduction

Metamorphic mineral assemblages in the study area were examined briefly by Noel (1981) and by Rivers (1982), both of whom noted a general increase in metamorphic grade from northwest to southeast. Both authors also noted the presence of three metamorphic events: an early, spatially undefined event which they attributed to the Hudsonian orogeny; a minor contact event associated with intrusion of the Shabogamo gabbro; and a widespread event which they interpreted to be related to the Grenvillian orogeny.

Very little evidence exists in the map area for the regional Hudsonian metamorphism or for contact metamorphism related to intrusion of the Shabogamo gabbro. These two pre-Grenvillian events are briefly discussed below, before a more detailed discussion of the Grenvillian metamorphic signature.

4.2.1 Hudsonian Metamorphism

Evidence for Hudsonian metamorphism is principally

restricted to the Tiphane Lake domain where a penetrative foliation (S_1), not found in the Shabogamo gabbro, is deformed by Grenvillian structures (see Chapter 3). A similar, although non-penetrative, foliation is also found locally in the Mobey Lake domain. Evidence for Hudsonian metamorphism in both the Equus Lake and Dave Lake domains is inconclusive, although a fabric predating emplacement of the Shabogamo gabbro has been seen in the Isa Lake thrust sheet of the Dave Lake domain.

In the McKay River Formation in both the Tiphane Lake and Mobey Lake domains, the Hudsonian fabric (S_1) is defined by actinolite and chlorite with microlithons of elongate plagioclase and minor quartz. The Hudsonian fabric (S_1) is typically transposed into a Grenvillian fabric (S_2), but the primary mineral assemblage is preserved as microlithons in fold hinges. The same is true for the Sokoman Formation in which S_1 is typically defined by grunerite and elongate quartz, and, in tuffaceous interbands, by chlorite. These Hudsonian greenschist facies assemblages appear not to have been significantly, if at all, affected by Grenvillian metamorphism, which is recorded by the same assemblages as those that define S_1. Since Hudsonian assemblages that define S_1 are the same as those that define the Grenvillian fabric, it can be argued that Grenvillian metamorphic conditions were comparable to

those of the Hudsonian orogeny in these domains.

It should be noted here that both structural and metamorphic effects of the ca. 1650 Ma. Labradorian orogeny are found in rocks of the Lac Joseph Allochthon, situated 15km to the south of the map area (Rivers and Nunn, 1985). It is possible, therefore, that some or all deformation and metamorphic effects in the study area that predate the Shabogamo gabbro are related to the Labradorian orogeny and not to the Hudsonian orogeny. However, there is a general absence of documented Labradorian fabrics outside of the Grenvillian allochthons, and so the interpretation of S_1 as a Hudsonian fabric is preferred.

4.2.2 Middle Proterozoic Contact Metamorphism

Contact metamorphism in the map area is related to intrusion of the Shabogamo gabbro and is largely confined to within one to two meters of the contact between the gabbro and the host rock. The host rocks in these cases typically display relict hornfelsic textures despite overprinting by Grenvillian deformation and metamorphism. For example, in the Isa Lake thrust sheet it is possible to recognize in thin-section the remnants of a contact

metamorphic aureole around a relatively large gabbro body.

At this locality, thin-section examination of semipelitic schists of the McKay River Formation reveals a mottled texture indicative of pseudomorphic replacement of a pre-existing mineral phase by muscovite and quartz (see Chapter 5, Figure 5.3). It has not been possible to definitively determine the identity of the phase that was pseudomorphed, but the replacement assemblage of muscovite and quartz suggests that it was an aluminous mineral, possibly cordierite. Furthermore, these pseudomorphs contain aligned inclusions of an Fe-Ti oxide mineral that is interpreted to represent a pre-intrusion fabric that was overgrown by a porphyroblastic phase (Figure 5.3) during the contact metamorphism event. This fabric is interpreted to be an Hudsonian fabric (S_1).

Likewise, garnets in these schists appear to have a two stage growth history that consisted of an inclusion-rich core that was subsequently overgrown by a relatively inclusion-free rim in two distinct stages of growth (Figure 5.3). This is interpreted to be the result of contact metamorphism in which garnet overgrew a Hudsonian fabric, upon which a relatively inclusion-free Grenvillian garnet grew. The garnets were not probed to see if they were chemically zoned, and the zoning discussed above is

based on petrographic observations.

4.2.3 Grenvillian Metamorphism

The prevalent metamorphic event in the map area affects all rock units, including the Shabogamo gabbro, to some degree. The fact that the gabbros are metamorphosed implies this metamorphic event postdated intrusion of the gabbros and it is therefore taken to be associated with the Grenvillian orogeny. For a detailed description of the rock types and mineral assemblages within each domain the reader is referred to the introduction of individual domains in Chapter 3 of this thesis.

Grenvillian metamorphic mineral assemblages in the map area show very little variation from domain to domain. Marble of the Denault Formation typically consists of the assemblage dolomite + quartz + tremolite $\pm$ calcite thrcughout the map area. The spatially dominant rock type in the map area, the McKay River Formation, has a typical mineral assemblage consisting of actinolite + hornblende + chlorite + plagioclase + quartz + sphene. In the Isa Lake thrust sheet biotite is also associated with that assemblage and the amphibole is typically hornblende. A semipelitic unit in the McKay River Formation in the Isa

Lake thrust sheet contains the assemblage garnet + biotite + quartz + plagioclase. The Sokoman Formation consists of grunerite + quartz + magnetite + plagioclase + carbonate throughout the map area. The Menihek Formation outcrops only in the Tiphane Lake domain, where it is a chlorite + muscovite + plagioclase + quartz + minor biotite semipelitic schist. The metamorphic mineralogy of the Shabogamo gabbro consists typically of chlorite + actinolite + plagioclase + epidote + sphene. In the Tiphane Lake domain, gabbros also contain garnet. In the Isa Lake thrust sheet, gabbros also contain the assemblage garnet + biotite + quartz + plagioclase, and hornblende + plagioclase + quartz + epidote + sphene.

The appearance of garnet in gabbros from the Isa Lake thrust sheet, as well as in the semipelitic schists of the McKay River Formation indicate an increase in metamorphic grade in this part of the Dave Lake domain above that in the other domains. The mafic assemblages in the McKay River Formation and the Shabogamo gabbros show little variation across the area, but generally do record an increase in the modal proportions of hornblende with respect to actinolite, suggestive of an increase in metamorphic grade.

The mafic assemblages and the garnet-biotite

assemblage were studied in detail to see if a change in Grenvillian metamorphic grade does indeed occur across the map area.

4.3 Geothermometry

Thin-sections from each of the domains in the map area were petrographically examined and those with appropriate assemblages were analyzed using a Jeol JXA-50A electron microprobe and an Hitachi S-570 scanning electron microscope with semi-quantitative capabilities. The SEM was used because of the fine-grained nature of the samples. These instruments have a nominal analytical accuracy of $\pm$ 1% and $\pm$ 2%, respectively. Microprobe analyses were conducted using a beam of 22 nanoamperes and an accelerating voltage of 15 kV. Temperatures were calculated using published calibrations of geothermometers and geobarometers with a computer program written by F. Mengel. Mineral analyses are given in Appendix 1.

4.3.1 Plagioclase-amphibole thermometry

Plagioclase-amphibole bearing equilibrium assemblages occur in a wide variety of metamorphic rocks and have been

used since as early 1920 (Eskola, 1920) to qualitatively indicate changes in metamorphic grade. Recently, attempts have been made to quantitatively constrain the physical conditions of metamorphism by examining reactions between coexisting plagioclase and amphibole, as well as by component substitutions in amphiboles (eg. Spear, 1980, 1981; Laird and Albee, 1981; Plyusnina, 1982; Graham and Navrotsky, 1985).

Plagioclase-amphibole thermometry is based on the partitioning of Na between coexisting plagioclase and amphibole with changing metamorphic grade. Two types of reaction can be written to describe the partitioning (Spear, 1980, 1981); a NaSi = CaAl exchange reaction;

2 albite + tschermakite = 2 anorthite + glaucophane (1)

that partitions Na into the M4 site of the amphibole with increasing temperature, and a Na, Ca, Mg, Al net transfer reaction;

albite + tremolite = edenite + 4 quartz (2)

that partitions Na into the A-site of the amphibole with increasing temperature. These reactions can also be viewed as component substitutions in the amphibole, and can be

examined qualitatively to evaluate a change in metamorphic grade between samples.

Both plagioclase and amphibole are nonideal and show miscibility gaps. Several miscibility gaps occur in the plagioclase solid solution series at various pressures and temperatures over most of the compositional range (eg. An_{60} - An_{90} (Huttenlocher gap), An_{45} - An_{60} (Boggild gap), An_{40} - An_{90} (Vall gap) and An_{5} - An_{20} (peristerite gap)) (eg. Goldsmith, 1982; Maruyama et al. 1982). Miscibility gaps in amphibole compositional space are not well defined (eg. Grapes and Graham, 1978; Oba, 1980, Plyusnina, 1982, and Spear, 1981), though it is generally accepted that several such gaps exist. The models developed by Spear (1980, 1981), and presented below, assume a miscibility gap occurs between actinolite and hornblende, but that the peak of the solvus is not reached at metamorphic conditions below 600°C and 3.5 kbars.

Spear (1980) empirically calibrated a plagioclase-amphibole thermometer based on reaction 1 for which an equilibrium constant (K_{eq}) can be written as:

$$K_{eq}\ (T,P) = (a_{gl}/a_{ts})_{am} \cdot (a_{ab}/a_{an})^{2}_{pl}$$

where a = activity

gl = glaucophane

ts = tschermakite

am = amphibole

an = anorthite

ab = albite

pl = plagioclase

This reaction involves the glaucophane substitution. Due to nonideality and miscibility gaps in both plagioclase and amphibole, it is possible to evaluate the reaction on empirical basis only, by using the ideal portion of the equilibrium constant (K_{id}, Spear, 1980), which can be written as;

$$K_{id} = (X_{Ca}/X_{Na})_{pl} \cdot (X_{Na}/X_{Ca})_{am}$$

where X=mol fraction of Na and Ca in the M4-site of the amphibole, and in the M-site of the plagioclase. Thermodynamic data for reaction 1, calculated by Spear (1980) are;

$$\ln Kd = -11{,}500/T + 11.14$$

$\triangle H$ = 47,000 cal/mol

$\triangle S$ = 22.1 e.u.

$\triangle V$ = -0.22 cal/bar

Spear (1981) also empirically calibrated a thermometer for the reaction 2, which involves the partitioning of Na between the M-site in plagioclase and the A-site in the amphibole. This reaction involves the edenite substitution. Likewise, an equilibrium constant

can be written for this reaction for which the ideal portion is;

$$K_{id} = (X_{Na,M4}/X_{0,A}X_{pl})$$

where X_0 = mol fraction of the vacancy in the A-site of the amphibole. Thermodynamic values calculated by Spear (1981) for reaction 2 are;

$$\ln Kd = 3.45 - 2{,}914\ (1/T)$$

$$\triangle H = 7{,}075 \text{ cal/mol}$$

$$\triangle S = 6.86 \text{ e.u.}$$

$$\triangle V = -0.257 \text{ cal/bar}$$

Spear (1980, 1981) further presented a qualitative graphical method to schematically show the partitioning of Na between plagioclase and coexisting amphibole for reactions 1 and 2 by plotting the mol percent albite in plagioclase against the mol percent Na in either the M4-site or the A-site of the coexisting amphibole. With an increase in temperature both reactions 1 and 2 move progressively to the right, partitioning Ca into plagioclase, making it more anorthite-rich, and Na into the amphibole, making it hornblende-rich. These reactions are represented on the diagram by a change in tie line slope and topology.

Another way to qualitatively show the progression of

reactions 1 and 2 is to compare the edenite substitution [$(Na^{A} + K)$, $Al^{IV} = \square$, Si], glaucophane substitution [Na^{M4}, $(Al^{VI} + Fe^{3+} + Ti + Cr) = Ca$, $(Fe^{2+} + Mg + Mn)$], and tschermakite substitution [$(Al^{VI} + Fe^{3+} + Ti + Cr)$, $Al^{IV} = (Fe^{2+} + Mg + Mn)$, Si] in amphiboles by plotting them against each other on an XY-graph (eg. Laird and Albee, 1981) designed so that the temperature sensitive component plots on the X-axis and the pressure sensitive component on the Y-axis.

4.3.2 Garnet-biotite thermometry

Garnet-biotite thermometry is based on the partitioning of Fe and Mg between coexisting garnet and biotite in the exchange reaction;

almandine + phlogophite = pyrope + annite (3)

Several authors have empirically calibrated the relationship between the Fe-Mg distribution coefficient and temperature for coexisting garnet and biotite (eg. Saxena 1969, Perchuk 1970, Goldman and Albee 1977, Ferry and Spear 1978). Numerous correction factors have been presented in the literature to accommodate non-ideality in both garnet and biotite (eg. Hodges and Spear 1982, Pigage

and Greenwood 1982, Ganguly and Saxena 1984, Perchuk et al. 1985, Indares and Martignole 1985).

In this study, most garnet and biotite compositions satisfy the compositional limits of the Ferry and Spear calibration (i.e. $(Ca + Mn)/(Ca + Mn + Fe + Mg) \leq 0.2$ in garnet, and $(Al_6 + Ti)/(Al_6 + Ti + Fe + Mg) \leq 0.15$ in biotite), the use of which results in realistic temperature estimates. All other calibrations produce unrealistically high temperatures.

The expression calculated by Ferry and Spear (1978) is:

$$T = (2089 + 9.56P)/(\ln K = 0.782)$$

where $K = (Fe/Mg)^{grt}/(Fe/Mg)^{bio}$, and T and P are in °K and bars, respectively.

4.3.3 Petrography of mafic samples

Mafic rocks of the McKay River Formation and the Shabogamo Intrusive Suite throughout the map area were found to contain the 'common assemblage' of Laird and Albee (1982) required for plagioclase-amphibole

thermometry, which consists of; amphibole + plagioclase + chlorite + epidote + Ti-phase ± quartz ± K-mica ± Fe-oxide ± carbonate. An attempt was made to select samples for this study from the Shabogamo gabbro to avoid any pre-Grenvillian metamorphism and to maintain internal consistency in analysis from across the belt. However, deformed and or metamorphosed gabbro does not appear in all domains, so McKay River schists were substituted for the Dave Lake domain, and a tuffaceous interband in the Sokoman Formation was used from the Mobey Lake domain.

One representative sample was analyzed from each domain for plagioclase-amphibole thermometry. Modal abundances of minerals for each sample are given in Table 4.1.

Sample TC-1, from the Tiphane Lake domain, is a protomylonitic gabbro with a well-defined S_2 fabric that is overprinted by a crenulation cleavage. Intergrowths of acicular amphibole + chlorite ± biotite, and subidioblastic, grains of epidote and sphene, along with very fine grained quartz and recrystallized plagioclase define S_2, which anastomoses around relict porphyroclasts of inclusion-rich plagioclase. Non-matrix plagioclase and quartz commonly have undulose extinction, suggestive of subgrain formation. Rare, idioblastic garnet and equant

Table 4.1. Modal abundances of minerals from analyzed samples.

Sample	Amp	Chl	Plag	Epi	Bio	Gnt	Mus	Qtz	Sp	Op
TC-1	30	10	30	10	<1	<2	5	5	3	<5
DB-53	50	<2	15	<2	<2	-	-	15	5	10
DB-117	20	25	35	7	<5	-	5	5	1	<2
DB-163	45	15	10	5	<1	-	-	5	10	5
89-13	20	10	30	5	10	<2	5	10	5	<2

amphiboles cross-cut S_2 locally. An Fe-Ti phase, possibly ilmenite, is rimmed by sphene. Inclusions in plagioclase include epidote group minerals, chlorite, and muscovite.

Sample DB-117, from the Equus Lake domain, is an undeformed, but metamorphosed gabbro consisting of randomly oriented intergrowths of acicular chlorite and amphibole, with very fine-grained epidote and sphene, typically associated with, and commonly pseudomorphically replacing (clino?)pyroxene. Relict pyroxene grains are strongly altered and appear only as xenoblastic cores surrounded by amphibole and chlorite. Remenants of idioblastic plagioclase porphyroclasts are extensively replaced by epidote, muscovite, and quartz, leaving only skeletons of relict grains.

Sample DB-163 comes from schists of the McKay River Formation in the Dave Lake thrust sheet. In this sample, acicular grains of amphibole and chlorite define the dominant foliation (S_2), although microlithons of amphibole and chlorite indicate the presence of an earlier fabric that has been transposed into S_2. Idioblastic sphene occurs throughout the thin-section. Extremely fine-grained plagioclase and quartz, typically with undulose extinction, comprise the matrix of this sample. Several grains of subidioblastic plagioclase porphyroclasts,

around which the fabric anastomoses, are also present. Idioblastic, chlorite porphyroblasts crosscut the fabric.

Sample 89-13 is a schistose metagabbro from within the Isa Lake thrust sheet. This sample consists predominantly of acicular, but commonly prismatic, amphibole, chlorite, and biotite, that define a strong S_2 foliation. Xenoblastic, strongly deformed and altered, inclusion-rich plagioclase porphyroclasts are typically rimmed by equant plagioclase and quartz grains, commonly with 120° triple junctions. Inclusions in plagioclase porphyroclasts include epidote, muscovite, quartz, and rarely amphibole. Sphene is common as very fine-grained aggregates.

Sample DB-54 is a medium-grained tuffaceous interband from within Sokoman iron formation near Mobey Lake. Amphiboles in this sample are typically prismatic, idioblastic grains with local patches of randomly oriented, acicular grains. Plagioclase typically forms subidioblastic grains, with rare 120° triple junctions. Idioblastic quartz grains are common. Sphene typically forms fine-grained clusters. An idioblastic opaque mineral (magnetite ?) is common throughout the sample. There is no tectonic fabric in this sample.

4.3.4 Petrography of pelitic samples

Pelitic assemblages that can be used to quantitatively constrain Grenvillian metamorphism in the area are rare. However, garnet-biotite assemblages occurring in semi-pelitic schists of the McKay River Formation in the Isa Lake thrust sheet have been used to estimate temperature in this part of the map area. Assemblages that could be used for reliable pressure estimates where not found.

Sample 89-23 in a medium-grained biotite + garnet + plagioclase + quartz + chlorite + muscovite + ilmenite schist. The dominant fabric, S_2, is defined by acicular to blocky biotite, and aligned ilmenite. Garnet typically forms idioblastic grains with numerous aligned inclusions, but commonly with inclusion-free rims. S_2 generally wraps around or abuts the garnet. Locally, chlorite rims garnet grains. Quartz and rare plagioclase typically form idioblastic grains in the matrix, with 120° triple junction grain contacts.

Sample NN-311 is a fine to medium grained biotite + garnet + quartz + plagioclase + ilmenite semipelite with no tectonic fabric. Idioblastic biotite and garnet occur throughout the sample and commonly have well defined grain

contacts. Quartz and lesser plagioclase occur as idioblastic grains with no grain shape preferred orientation. Ilmenite is randomly distributed throughout the sample.

4.4 Results

Plagioclase and amphibole formulae were constructed using analyses obtained from both the electron microprobe and the scanning electron microscope. Only those analysis that did not exceed the crystal chemical limit by Robinson et al. (1982) for amphiboles were used to calculate temperatures, and to examine component substitutions. Fe^{3+} was calculated by the 13eCNK method. Analyses obtained by electron microprobe are presented in amphibole composition space in Figure 4.1.

4.4.1 Graphical analysis

The following discussion is based on the graphical analysis of coexisting plagioclase-amphibole pairs and component substitutions in amphiboles outlined above. Semi-quantitative values obtained from the SEM are plotted alongside those from the electron microprobe. However,

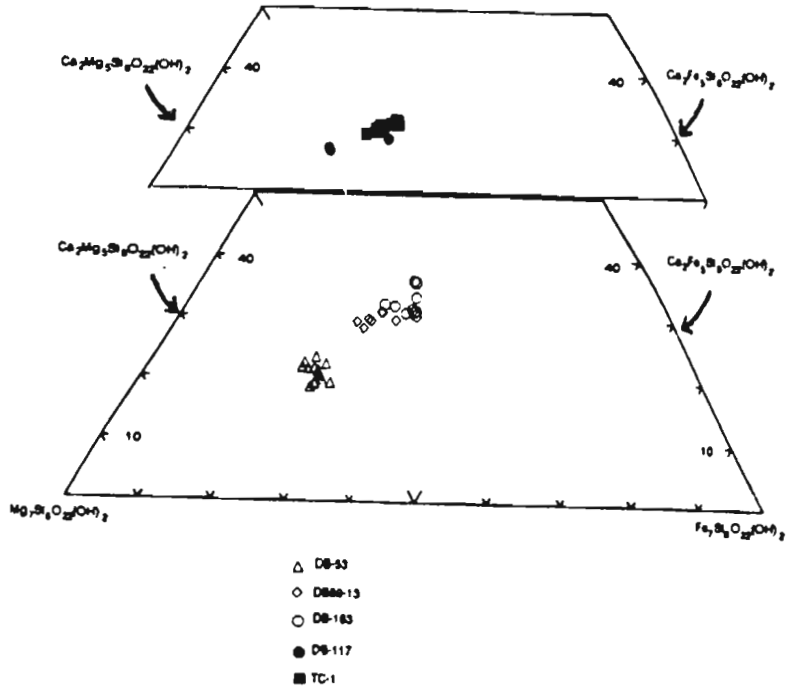

Figure 4.1. Amphibole quadrilateral with all samples plotted in terms of mol percent CaO, MgO, and FeO.

emphasis in the discussion is placed on the microprobe analyses.

Figure 4.2 shows phase diagrams for coexisting plagioclase-amphibole pairs (Table 4.2) from the four domains in the map area, plotted in the manner suggested by Spear (1980, 1981). In the Tiphane Lake domain, albite coexists with a range of amphiboles compositions, suggesting that there are two amphiboles (hornblende and actinolite) coexisting with albite.

In the Mobey Lake domain, albite coexists with a hornblende-rich amphibole. Note that all Na in amphiboles from the Mobey Lake domain occurs in the M4-site (Table 4.2), which is in contrast to amphiboles from the other domains, and likely reflects the different bulk composition of sample DB-53 relative to the other samples.

In the Equus Lake domain, both labradorite and andesine coexist with hornblende. Labradorite is typically associated with amphiboles that have low X_{Na}, whereas andesine coexists with amphiboles with higher X_{Na}.

Within the Dave Lake domain, plagioclase in the Dave Lake thrust sheet consists of albite coexisting with hornblende. In contrast, in the Isa Lake thrust sheet, the

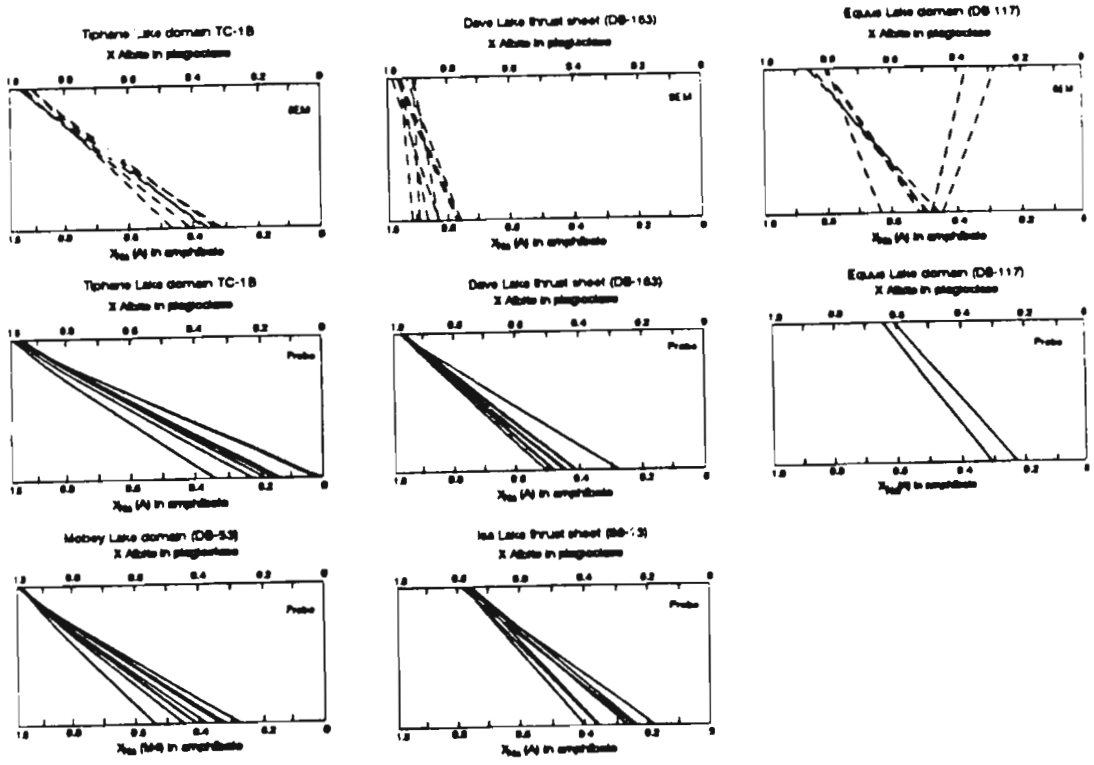

Figure 4.2. Phase diagrams showing the tie lines between coexisting plagioclase and amphibole from each domain for both SEM and probe analyses.

Table 4.2. Compositions of coexisting plagioclase and amphibole.

Sample	Probe		SEM	
	$X_{Na,A}$	X_{Ab}	$X_{Na,A}$	X_{Ab}
	0.195	0.979	0.681	0.956
	0.159	0.960	0.312	0.945
	0.239	0.985	0.312	0.920
TC-1	0.334	0.993	0.351	0.961
	0.099	0.988	0.412	0.946
	0.028	0.984	0.335	0.920
	0.139	0.967	0.465	0.913
		0.534	0.478	0.371
		0.525	0.514	0.802
		0.483	0.447	0.280
DB-117		0.338	0.456	0.857
		0.344	0.635	0.793
		0.398	0.496	0.800
		0.609	0.490	0.844
	0.308	0.641		
	0.231	0.605		
	0.374	0.984	0.828	0.985
	0.450	0.984	0.869	0.959
	0.486	0.982	0.891	0.915
DB-163	0.414	0.984	0.459	0.951
	0.503	0.985	0.832	0.911
	0.443	0.984	0.766	0.954
	0.409	0.981	0.914	0.958
			0.774	0.968
			0.763	0.935
	0.183	0.782		
	0.243	0.776		
	0.355	0.782		
DB89-13	0.256	0.789		
	0.279	0.762		
	0.397	0.781		
	0.360	0.762		
	$X_{Na,M4}$	X_{Ab}		
	0.326	0.997		
	0.448	0.996		
	0.281	1.000		
*DB-53	0.406	0.996		
	0.544	0.994		
	0.377	0.997		
	0.330	0.993		
	0.316	0.997		
	0.407	0.996		
	0.407	0.993		

* All Na in amphiboles from this sample occurs in the M4-site

only plagioclase present is oligoclase which coexists with hornblende.

The phase diagrams in Figure 4.2 show that the X_{Ab} component in plagioclase remains constant in the Tiphane Lake domain, Mobey Lake domain, and Dave Lake thrust sheet, although there is an increase in X_{Na} in amphiboles from the Tiphane Lake domain to Mobey Lake domain. There are differences within the Dave Lake domain, however. In the Dave Lake thrust sheet, plagioclase is albite-rich, but there is an increase in $X_{Na,A}$ in the amphiboles, and in the Isa Lake thrust sheet the appearance of oligoclase coexisting with hornblende suggests that the peristerite gap in plagioclase has been crossed. In the Equus Lake domain, two plagioclases, labradorite and andesine, coexist. These are interpreted to be of different generations, an Labradorite occurs as extensively altered porphyroclasts and is likely of primary igneous composition, whereas andesine occurs as recrystallized grains around the rims of labradorite porphyroclasts, and is considered to be metamorphic.

Component substitutions in amphiboles from all four domains are plotted in Figure 4.3a,b,c. Data are given in Table 4.3. Amphiboles in the Tiphane Lake domain show a wide compositional range in both tschermakite (100

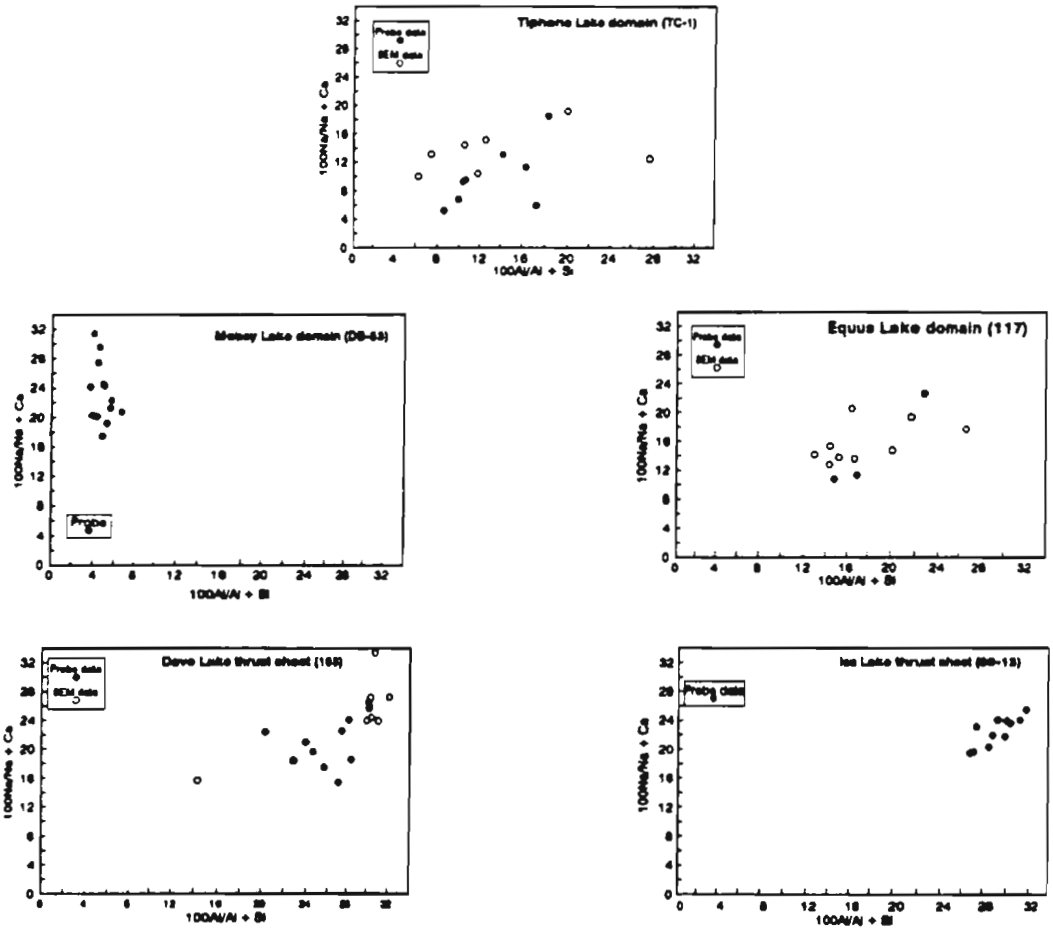

Figure 4.3. Component substitution diagrams for amphiboles from each domain in the map area. (A). Tschermakite vs. glaucophane substitution.

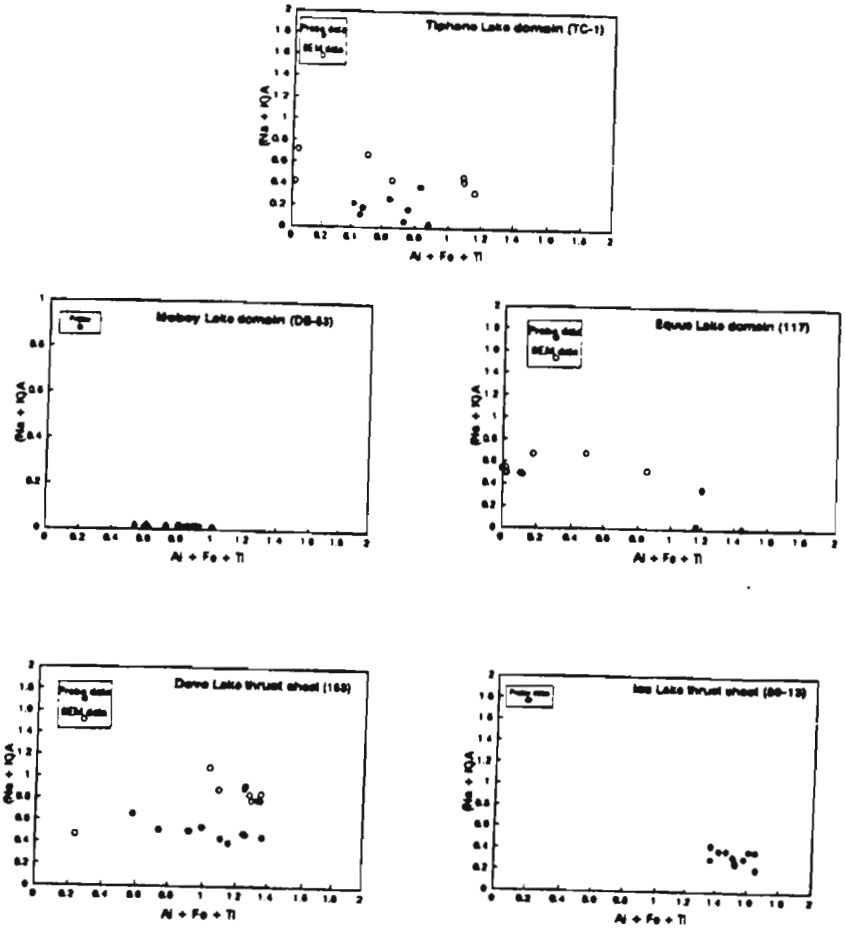

Figure 4.3 (continued). (B). Tschermakite vs. edenite substitution.

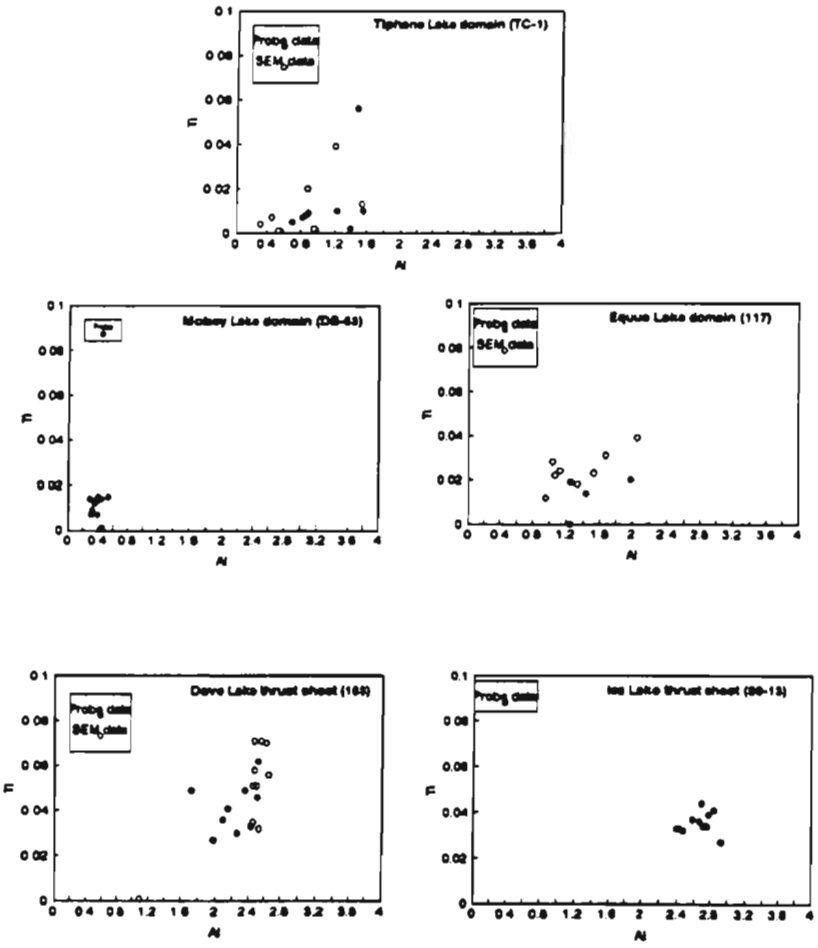

Figure 4.3 (continued). (C). Al vs. Ti substitution.

Table 4.3. Component compositions of analyzed amphiboles.

Sample DB-53

	100Na/Na + Ca	100Al/Al + Si	(Na + K)A	AlB + Fe3 + Ti	Fe2/Fe2 + Mg	Fe3/Fe3 + Fe2	Al	Ti
Probe	19.214	5.259	0.009	0.627	0.202	0.360	0.431	0.090
	24.296	5.034	0.014	0.905	0.126	0.656	0.407	0.015
	17.462	4.867	0.016	0.542	0.243	0.274	0.398	0.007
	21.253	5.587	0.014	0.823	0.154	0.560	0.455	0.014
	31.418	3.998	0.018	0.812	0.176	0.507	0.326	0.009
	20.746	6.698	0.014	0.927	0.156	0.602	0.544	0.015
	20.125	4.359	0.018	0.616	0.222	0.360	0.355	0.013
	20.283	3.912	0.013	0.603	0.214	0.372	0.317	0.007
	24.168	3.685	0.016	0.738	0.191	0.487	0.297	0.014
	29.577	4.523	0.009	0.865	0.195	0.512	0.368	0.013
	24.516	4.888	0.014	0.894	0.102	0.697	0.395	0.013
	27.475	4.412	0.014	0.861	0.154	0.581	0.358	0.012
	22.328	5.694	0.012	0.893	0.109	0.676	0.462	0.001
	36.384	4.369	0.011	1.005	0.116	0.685	0.356	0.013

Sample TC-1

	100Na/Na + Ca	100Al/Al + Si	(Na + K)A	AlB + Fe3 + Ti	Fe2/Fe2 + Mg	Fe3/Fe3 + Fe2	Al	Ti
Probe	9.533	10.662	0.220	0.421	0.370	0.089	0.883	0.009
	9.304	10.390	0.183	0.480	0.386	0.130	0.860	0.008
	11.311	16.393	0.264	0.648	0.401	0.078	1.398	0.012
	13.056	14.256	0.033	0.882	0.353	0.177	1.230	0.010
	18.521	18.323	0.376	0.833	0.401	0.187	1.560	0.010
	5.210	8.651	0.117	0.464	0.320	0.187	0.708	0.005
	6.831	9.972	0.055	0.735	0.296	0.326	0.821	0.007
	5.970	17.352	0.167	0.760	0.440	0.107	1.480	0.056
SEM	12.475	27.580	0.715	0.036	0.139	0.843	1.204	0.039
	10.030	6.318	0.327	1.160	0.145	0.826	0.481	0.007
	19.179	19.987	0.669	0.505	0.500	0.296	0.319	0.004
	10.387	11.816	0.417	0.020	0.586	0.072	1.542	0.013
	15.113	12.564	0.439	0.661	0.374	0.442	0.873	0.020
	13.189	7.433	0.424	1.093	0.442	0.133	0.956	0.002
	14.435	10.523	0.471	1.090	0.416	0.218	0.546	0.001

Table 4.3 (continued)

Sample DB-163

	100Na/Na + Ca	100Al/Al + Si	(Na + K)A	Alt + Fe3 + Ti	Fe2/Fe2 + Mg	Fe3/Fe3 + Fe2	Al	Ti
Probe	17.558	25.708	0.400	1.152	0.431	0.199	2.260	0.030
	22.590	27.488	0.484	1.246	0.430	0.216	2.435	0.033
	18.458	22.862	0.515	0.742	0.436	0.043	1.977	0.027
	24.115	28.223	0.453	1.366	0.423	0.250	2.514	0.046
	22.392	20.385	0.661	0.579	0.498	0.045	1.722	0.049
	21.013	23.920	0.508	0.918	0.469	0.092	2.087	0.036
	18.565	28.507	0.541	0.991	0.481	0.047	2.524	0.062
	19.667	24.629	0.438	1.102	0.412	0.215	2.144	0.041
	15.473	27.182	0.472	1.258	0.387	0.335	2.357	0.049
SEM	25.968	30.316	0.844	1.283	0.452	0.432	2.481	0.058
	26.498	30.196	0.885	1.088	0.536	0.277	2.537	0.032
	27.156	30.379	0.903	1.248	0.449	0.429	2.475	0.071
	15.705	14.283	0.472	0.240	0.366	0.284	1.095	0.001
	25.658	30.245	0.852	1.355	0.440	0.474	2.462	0.035
	24.001	30.038	0.795	1.338	0.457	0.446	2.459	0.051
	27.241	32.184	0.925	1.256	0.480	0.389	2.659	0.056
	24.419	30.459	0.789	1.295	0.465	0.418	2.508	0.051
	33.343	30.794	1.088	1.030	0.573	0.191	2.626	0.070
	23.941	31.139	0.791	1.351	0.450	0.439	2.563	0.071

Sample DB89-13

	100Na/Na + Ca	100Al/Al + Si	(Na + K)A	Alt + Fe3 + Ti	Fe2/Fe2 + Mg	Fe3/Fe3 + Fe2	Al	Ti
Probe	20.384	28.527	0.213	1.657	0.284	0.434	2.579	0.037
	19.707	27.191	0.262	1.527	0.265	0.444	2.422	0.033
	23.953	30.073	0.333	1.510	0.373	0.218	2.764	0.034
	23.612	30.353	0.387	1.469	0.366	0.217	2.776	0.039
	23.140	27.433	0.286	1.524	0.261	0.411	2.465	0.032
	19.550	26.826	0.308	1.366	0.313	0.303	2.397	0.033
	21.819	29.918	0.431	1.366	0.384	0.191	2.713	0.034
	21.936	28.679	0.315	1.579	0.278	0.426	2.691	0.044
	25.439	31.830	0.374	1.653	0.359	0.303	2.932	0.027
	24.079	31.213	0.382	1.912	0.328	0.341	2.845	0.041
	24.094	29.317	0.387	1.419	0.343	0.228	2.666	0.036

Table 4.3 (continued).

Sample DB-117

	100Na/Na + Ca	100Al/Al + Si	(Na + K)A	Alt + Fe3 + Ti	Fe2/Fe2 + Mg	Fe3/Fe3 + Fe2	Al	Ti
Probe	10.782	14.830	0.027	1.185	0.140	0.615	1.253	0.019
	22.707	22.758	0.359	1.199	0.339	0.305	1.985	0.020
	11.385	17.003	0.012	1.449	0.059	0.854	1.434	0.014
SEM	15.390	14.410	0.495	0.111	0.399	0.286	1.072	0.022
	14.830	20.151	0.546	0.022	0.501	0.128	1.525	0.023
	14.197	12.967	0.484	0.123	0.361	0.322	0.961	0.012
	12.790	14.341	0.497	0.028	4.530	0.069	1.046	0.028
	17.752	26.673	0.677	0.488	0.507	0.273	2.065	0.039
	20.620	16.430	0.523	0.849	0.382	0.370	1.332	0.018
	13.652	16.733	0.537	0.000	0.480	0.071	1.250	0.000
	13.820	15.249	0.501	0.023	0.453	0.095	1.130	0.024
	19.448	21.701	0.670	0.182	0.482	0.188	1.672	0.031

Al/Al + Si) and glaucophane (100Na/Na + Ca) components (Figure 4.3a). The tschermakite component forms two loose clusters of points that have variable glaucophane components. Likewise, a plot of the edenite ((Na + K)A) against tschermakite (Al + Fe + Ti) components (Figure 4.3b) shows a scattering of points with, again, two loose clusters of points. Most amphiboles from the Tiphane Lake domain are relatively low in Ti, which when plotted against Al shows two clusters of Al points (Figure 4.3c).

Amphiboles from the Mobey Lake domain have a narrow range in tschermakite compositions, with a much larger range in glaucophane components (Figure 4.3a). These amphiboles have a very low edenite component in the A-site, but with a relatively wide range of tschermakite compositions (Figure 4.3b). Ti values form a tight cluster of points when plotted against Al (Figure 4.3c).

Amphiboles from the Equus Lake domain are very fine-grained and reliable microprobe analysis were difficult to get. However, a number of SEM analysis were obtained and are shown along with microprobe analysis in the following diagrams. Amphiboles from the Equus Lake domain also have a wide range of values for the tschermakite and glaucophane components (Figure 4.3a). The edenite component in these amphiboles (Figure 4.3b) is low, but

they have a high tschermakite component compared to those from the Tiphane Lake domain. Ti is rather constant (Figure 4.3c), with a narrow range in values, and when plotted against Al, the tschermakite component again shows a relatively wide range of values.

Within the Dave Lake domain, amphiboles from the Dave Lake thrust sheet have a range of tschermakite compositions, with relatively little range in glaucophane composition (Figure 4.3a). Likewise, they show a relatively narrow range of edenite component verses a wide range of tschermakite component (Figure 4.3b). Ti in this sample also has a wide range of values relative to Al (Figure 4.3c). Amphiboles from the Isa Lake thrust sheet have little variation in tschermakite composition and glaucophane composition (Figure 4.3a). Likewise, the edenite verses tschermakite components form a tight cluster of points (Figure 4.3b). Also, Ti content has a narrow range of values, and likewise with Al.

From Figures 4.2 and 4.3a,b,c it is apparent that there is a wide range in composition of amphiboles within each sample analyzed, especially in the tschermakite component, but compositions are distinct between domains in many cases. This has been interpreted to be the result of miscibility gaps in the amphiboles, a factor that might

reflect the complete range of amphibole compositions shown in Figure 4.2. A second point that needs to be mentioned is that variability in plagioclase and amphibole compositions between samples may reflect the different bulk compositions of the rock types used, but should not be significant because of the presence of the 'common assemblage'.

The component substitution plots shown in Figure 4.3a,b,c show that there is an general decrease in the tschermakite component (X-axis), but a significant increase in the glaucophane component (Y-axis) from the Tiphane Lake domain to the Mobey Lake domain. There is also a relative decrease in the edenite and the Ti components from the Tiphane Lake domain to the Mobey Lake domain. There is an increase in component substitutions in amphiboles in the Dave Lake domain (with an increase also occurring from the Dave Lake thrust sheet to the Isa Lake thrust sheet). Values for amphiboles from the Equus Lake domain show a relative increase in which component substitutions over amphiboles from the Tiphane Lake domain, but lower than those from Mobey Lake domain and Dave Lake domain.

Amphibole compositions calculated using semiquantitative analyses from SEM are somewhat different

from those obtained using the electron probe (Figures 4.2 and 4.3a,b,c). Despite the fact that the actual values differ, it is apparent from the topology of the above diagrams that the compositional trends described by both sets of data are similar, and show an increase in the tschermakite, glaucophane, edenite, and Ti components in amphiboles between domains. As well, they show a decrease in X_{ab} in plagioclase accompanied by an increase in X_{Na} in the A-site in coexisting amphibole.

4.4.2 Plagioclase-amphibole thermometry

Calculated temperatures for reaction 2 using the thermodynamic data of Spear (1981) were performed only on sample DB-53 from the Mobey Lake domain because all Na in amphiboles from the other domains was situated in the A-site. Amphiboles in DB-53 are hornblende-rich ($X_{Na,M4}$ = 0.316-0.544) and plagioclase is typically very albite-rich (Ca_{plag} = 0.06-0.11). The calculated temperatures range from 367 to 420 °C (Table 4.4)

Calculated temperatures using reaction 1 give unrealistically high values for the Dave Lake domain (DB-163 and DB 89-13) and for the Equus Lake domain (DB-117) (Table 4.4). However, temperatures calculated for the

Table 4.4. Plagioclase-amphibole data and calculated temperatures from each sample.

	Na(A)	K(A)	Ca(plag)	Na(plag)	Kd	T
DB 89-13	0.177	0.036	4.59	9.27	0.349	517
	0.338	0.039	4.53	9.05	0.847	711
	0.295	0.038	4.16	8.72	0.530	598
	0.268	0.040	4.99	8.88	0.630	636
	0.376	0.055	4.52	8.93	1.053	774
TC-1	0.189	0.031	0.39	11.37	0.259	468
	0.155	0.027	0.79	11.53	0.208	436
	0.155	0.027	0.26	11.42	0.031	241
	0.135	0.032	0.36	11.19	0.173	411
DB-163	0.360	0.039	0.34	12.60	0.640	640
	0.424	0.059	0.35	11.89	0.897	727
	0.459	0.056	0.34	11.52	1.032	768
	0.424	0.059	0.32	12.50	0.894	726
	0.459	0.056	0.35	11.89	1.032	768
DB-117	0.096	0.005	13.04	3.72	0.484	579
	0.228	0.013	6.80	7.90	0.566	612
	0.286	0.073	6.86	7.26	0.936	739

	Ca(M4)	Na(M4)	Ca(plag)	Na(plag)	Kd	T
DB-53	1.372	0.326	0.09	12.01	0.002	404
	1.394	0.448	0.07	13.80	0.002	401
	1.503	0.406	0.03	12.54	0.001	367
	1.188	0.544	0.07	12.75	0.003	418
	1.439	0.377	0.04	12.71	0.001	375
	1.311	0.330	0.09	13.16	0.002	403
	1.243	0.316	0.06	12.41	0.001	390
	1.277	0.407	0.11	13.05	0.003	420

Tiphane Lake domain (Table 4.4) range from 411 to 468 °C, and are considered to be geologically reasonable.

4.4.3 Garnet-biotite thermometry

Mineral assemblages that could be used to estimate a pressure were not found in rocks from the Isa Lake thrust sheet. For the purposes of this discussion a pressure of 4 kbars was used as a reasonable estimate for the given mineral assemblages in both the semipelites and in the mafic schists used in the plagioclase-amphibole work above.

Temperatures calculated from sample 89-23 (Table 4.5) range from 484 °C to 560 °C at a pressure of 4 kbars. Those calculated using sample NN 311 (Table 4.5) range from 446 °C to 507 °C at a pressure of 4 kbars. These temperatures are interpreted to be geologically reasonable for the mineral assemblages present.

4.5 Discussion

Following the interpretations of Spear (1981) and

Table 4.5. Mol fractions of garnet-biotite compositions and calculated temperatures.

	Garnet				biotite				
	Xgro	Xpyr	Xalm	Xspe	XMg	XAl	XTi	Kd	T
Sample 89-23	0.2006	0.0576	0.7008	0.0410	0.3708	0.1253	0.0346	0.1396	500
	0.2129	0.0596	0.6802	0.0472	0.3698	0.1021	0.0342	0.1494	520
	0.2006	0.0576	0.7008	0.0410	0.3708	0.1253	0.0346	0.1396	500
	0.2379	0.0663	0.6603	0.0356	0.3708	0.1253	0.0346	0.1703	560
	0.2311	0.0540	0.6761	0.0388	0.3775	0.1452	0.0333	0.1317	484
	0.2006	0.0576	0.7008	0.0410	0.3698	0.1021	0.0342	0.1402	501
	0.2006	0.0576	0.7008	0.0410	0.3775	0.1452	0.0333	0.1357	492
Sample NN-311	0.2247	0.0632	0.6058	0.1062	0.4498	0.1149	0.0375	0.1276	476
	0.2317	0.0671	0.5933	0.1080	0.4498	0.1149	0.0375	0.1383	498
	0.2309	0.0686	0.5964	0.1041	0.4498	0.1149	0.0375	0.1407	503
	0.2381	0.0549	0.5784	0.1286	0.4553	0.1388	0.0363	0.1136	446
	0.2423	0.0627	0.5848	0.1102	0.4625	0.1144	0.0372	0.1246	470
	0.2309	0.0686	0.5964	0.1041	0.4553	0.1388	0.0363	0.1376	496
	0.2309	0.0686	0.5964	0.1041	0.4456	0.1262	0.0346	0.1431	507

gro = grossular

pyr = pyrope

alm = almandine

spe = spessartine

Laird and Albee (1981), a decrease in X_{ab} in plagioclase with a concomitant increase in X_{Na} in the A-site in amphibole, together with the increase in tschermakite, glaucophane, edenite, and Ti components in amphiboles is interpreted to reflect a relative change in temperature and pressure. On the basis of these substitutions, it appears that temperatures in the Tiphane Lake domain were higher than those in the Mobey Lake domain (an interpretation that is confirmed by quantitative plagioclase-amphibole thermometry discussed above), but the graphical analysis suggests a higher pressure in the Mobey Lake domain. Within the Dave Lake domain, there is an apparent increase in both temperature and pressure from the Dave Lake thrust sheet to the Isa Lake thrust sheet. Rocks from the Dave Lake domain qualitatively record higher pressure and temperature conditions than either the Tiphane Lake or the Mobey Lake domains.

The topology of the phase diagram in Figure 4.2 and the component substitution diagrams in Figure 4.3a,b,c for the Equus Lake domain is significantly different from those of either of the other domains. In relative T-P space, rocks from the Equus Lake domain appear to lie between those of the Tiphane Lake domain and the Mobey Lake domain. The difference in topology for the Equus Lake domain diagrams may reflect its significantly different

structural position as a klippe relative to the other domains in the map area (see chapter 3).

Garnet-biotite temperatures calculated for the Isa Lake thrust indicate the temperature of Grenvillian metamorphism in this part of the map area reached upper-greenschist to lower-amphibolite grade (446 °C to 560 °C). These temperatures are significantly lower than those calculated using plagioclase-amphibole assemblages and are interpreted to be geologically more meaningful.

It is apparent from the graphical analysis of plagioclase-amphibole assemblages that there is, qualitatively, an increase in Grenvillian metamorphic grade from northwest to southeast across the map area. Changes in metamorphic grade correspond to domains (increasing in the structurally higher domains) and within the Dave Lake domain, to thrust sheets. The inversion in metamorphic grade is typical of that found in thrust belts, and is a pattern that has been described from Gagnon terrane near Labrador City (Rivers, 1983a; van Gool et al., 1988), implying that thrusting post-dated, or was synchronous with metamorphism.

CHAPTER 5

Summary of Pre-Grenvillian Deformation

5.1 Introduction

Rocks in the map area have undergone several phases of folding and faulting, though no absolute timing can be placed on separate deformation events. Relative ages can, however, be determined in the field using the intrusive relationships between individual structures and gabbro of the Shabogamo Intrusive Suite, and structural overprinting criteria.

Two pre-Grenvillian deformation events have been recognized regionally in this part of the Grenville Province, the Hudsonian orogeny to the north and the Labradorian orogeny to the south. The effects of the Labradorian orogeny on the northern margin of the Grenville Province are unknown and, to date, there is no evidence to suggest that any Labradorian deformation occured within the map area. This chapter presents new macroscopic, mesoscopic, and microscopic evidence for pre-Grenvillian structural features in the Tiphane Lake map area that are here interpreted to be of Hudsonian

age.

5.2 Hudsonian Orogeny

During the 1800-1750 Ma Hudsonian Orogeny, rocks of the Labrador Trough were folded and thrust westward across the Superior Province craton and its miogeoclinal cover (Ware and Wardle, 1979; Wardle et al., 1986). Ware and Wardle (1979), and Rivers (1982, 1983a) placed the Hudsonian deformation front (henceforth the Hudsonian Front) approximately 20 km west of the Tiphane Lake area (Figure 5.1). Rocks within the Hudsonian Front zone include metasedimentary cover rocks of the Knob Lake Group and Archean basement of the Ashuanipi Metamorphic Complex (Ware and Wardle, 1979).

The structural style of the southern part of the Hudsonian Front zone is dominated by macroscopic southwest-verging, northeast-plunging fold nappes and related thrusts (Ware and Wardle, 1979; Rivers, 1982, 1983a). Northwest-trending Hudsonian fabrics are weakly developed in mildly folded cover rocks near the front, but intensity of folding and fabric development increases eastward, where a slaty cleavage is locally developed (Ware and Wardle, 1979). Hudsonian metamorphic grade in cover rocks increases eastward away from the front,

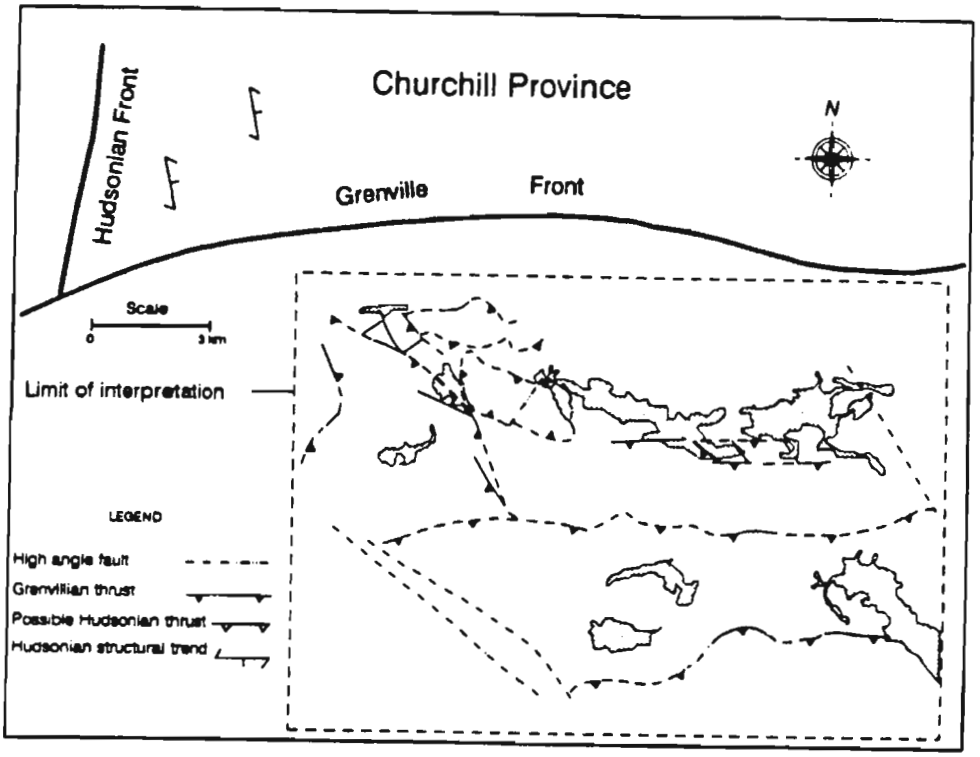

Figure 5.1. Schematic geological map showing the location of the study relative to the Grenville Front and the Hudsonian Front in southwestern Labrador.

from subgreenschist to greenschist facies (Ware and Wardle, 1979; Rivers, 1982).

Prior to this study very little evidence for Hudsonian deformation had been presented from the Tiphane Lake map area. Immediately north of the map area, however, Rivers (1982) described deformation features that were attributed to Hudsonian structures being overprinted by Grenvillian deformation. In one area he described a west-verging fold (assumed to be Hudsonian) whose axial-surface is crosscut at a high angle by a east-west-trending cleavage (assumed to be Grenvillian). Further east, complex thrust relationships were interpreted by Rivers (1982) to be due to reimbrication of a Hudsonian thrust sequence during Grenvillian thrusting.

5.3 Pre-Grenvillian Structural Features

Because of the complex structural nature of the Tiphane Lake area, it is difficult to determine the deformation history based entirely on overprinting relationships in the field. As stated above, the principal criterion used in the field to distinguish between Grenvillian and pre-Grenvillian structures was the intrusive relationship with the Shabogamo gabbro.

Structural features that were cut by the gabbro were assumed to be pre-Grenvillian in view of the age of the gabbro as established elsewhere in the Grenville Province.

Many of the field relationships described below were introduced and described in Chapter 3 and, rather than repeat these entirely, the reader will be referred to the relevant text and figures.

5.3.1 Field relationships

In the Tiphane Lake domain, careful analysis of fabric elements on a variety of scales indicates deformation features that can be attributed to pre-Shabogamo intrusion events. For instance, a penetrative S_1 foliation and, commonly, an associated stretching lineation (Ls_1) are developed in cover rocks throughout the Tiphane Lake domain. Both these fabric elements are pervasively folded by macroscopic, north to northwest-verging F_2 folds and S_1 is locally transposed into the F_2 axial surface orientation (Chapter 3, section 3.1). Nowhere in the Tiphane Lake domain is a planar or linear fabric found in the Shabogamo gabbro that is directly correlative with the regional S_1-L_{s1} fabric found in cover

rocks. The only fabrics in the gabbro are foliations and lineations that occur within shear zones which can be positively interpreted as D_2 and D_3 thrust zones in the regional deformation sequence (Chapter 3, section 3.1). Both S_1 and Ls_1 are, therefore, interpreted to pre-date the intrusion of the Shabogamo gabbro.

Also of note in this context is the occurrence of a fault zone in a D_2 horse along the south shore of Tiphane Lake (Chapter 3, Figures 3.9 and 3.10). In its present orientation, this fault has an extensional geometry, placing Menihek Formation on top of McKay River Formation. The fault itself is a folded, several meter-wide phyllonite zone with a penetrative fabric that can be correlated to the folded S_1 foliation in the horse. The S_1 fabric in this horse is interpreted to be the same as S_1 elsewhere in the Tiphane Lake domain. Thus a possible interpretation for this fault is that it is a pre-Grenvillian thrust that was subsequently overturned and folded during Grenvillian deformation. However, this interpretation is difficult, if not impossible, to substantiate.

The existence of an intrusive relationship between the gabbro and cover rocks has been clearly demonstrated throughout the Mobey Lake domain (Chapter 3, section

3.2). In the vicinity of Mobey Lake, the map pattern outlined by lithologic boundaries suggests that the Denault and McKay River formations were folded by a major F_1 fold (Chapter 3, pp. 20-21; Figures 3.12 and 3.13). Shabogamo gabbro cuts across the lithologic boundaries, truncating both limbs and the hinge zone of the fold. The geometry of this relationship suggests a west-verging, pre-Shabogamo intrusion fold that was subsequently refolded during the Grenvillian deformation event.

West of Mobey Lake, a northeast to southeast-dipping fault places McKay River Formation on top of Sokoman Formation. Locally, kinematic indicators suggest this fault has a west-directed thrust sense of movement (Chapter 3, section 3.2). Its form surface trace is folded in what appears to be an F_2 style fold similar to that found elsewhere in the Mobey Lake domain (Figure 3.13). Both the orientation and kinematics of this fault indicate it may be a pre-Grenvillian, west-directed thrust that was subsequently folded during Grenvillian deformation. Further, the form surface traces of the S_1 foliation (not found in the gabbros in the Mobey Lake domain) are also folded on a map scale (Figure 3.13) in an F_2 style fold. The S_1 foliation is also interpreted to be related to pre-Grenvillian folding and thrusting.

In the southern part of the Dave Lake domain, near the shore of Ossokmanuan Lake, schists of the McKay River Formation are cut by a dyke of Shabogamo gabbro. A moderate to well-developed slaty cleavage (S1), parallel to bedding (S_0) is found in the schist, but not in the gabbro dyke which is discordant to S_1 (Figure 5.2). Both the schist and the dyke are folded by a mesoscopic F_2 fold whose axial planar cleavage (S2) is weakly to moderately developed in both the schist and the gabbro dyke (Figure 5.2). S2 is at an angle of 25 to 30 degrees to S1.

5.3.2 Microstructural relationships

Contact metamorphic aureoles around Shabogamo gabbro bodies have been documented and discussed in chapter 4 of this study. Within McKay River Formation schists in the contact aureole of a large gabbro body in the Isa Lake thrust sheet of the Dave Lake Domain, two microstructural types of garnet porphyroblasts occur on the scale of a thin section (Figure 5.3a). Type 1 garnets are subidioblastic to idioblastic and have randomly oriented inclusions. The foliation, interpreted as S_2, typically wraps around the rim of the porphyroblast, though garnets cross-cut the fabric locally. There is also local

Figure 5.2. Field photograph showing the relationship between a gabbro dyke and foliated schists. An early fabric (S_1) parallels bedding (S_0) in the schists, both of which are truncated by the gabbro dyke. An S_2 foliation is present in both the dyke and the schists.

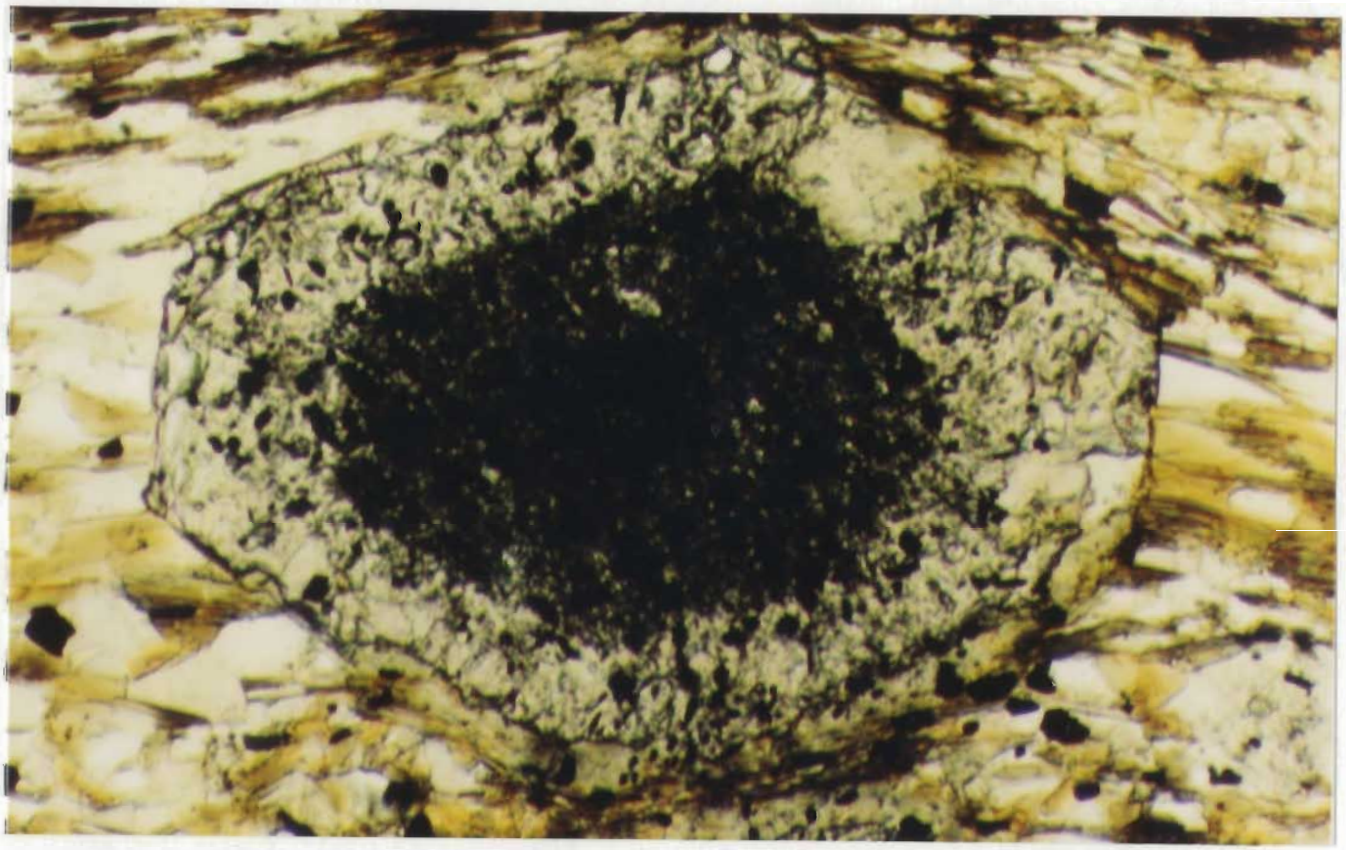

Figure 5.3. A. Thin-section photograph of type 2 garnet. Note the presence of an idioblastic, inclusion-rich core. Base of photograph is 2.5mm.

Figure 5.3 (continued). B. Pseudomorphic replacement of an earlier porphyroblast (cordierite?) by quartz and muscovite. Note the aligned opaque minerals forming an angle with the external S_2 foliation. Base of photograph is 2.5mm.

dissolution of the garnet rim against the S_2 fabric. Type 2 garnets are subidioblastic to idioblastic and have a spherical, inclusion-rich core (Figure 5.3a). Type 2 garnets have typically inclusion-free rims that display the same relationship with S_2 as type 1 garnets.

The cores of type 2 garnets have straight to slightly curved inclusion patterns made up of fine-grained graphite, quartz, and ilmenite (?). Cores with a poorly defined inclusion pattern have a dusty appearance typical of a slaty cleavage microstructure. The inclusion pattern in type 2 garnets occurs only in the core and does not extend into the rim area, and in places where the rim is weakly developed, inclusions are not continuous with the external S_2 fabric. The orientation of inclusion patterns correlates well between porphyroblasts within a single thin section. Nowhere can the inclusion pattern in the cores of type 2 garnets be correlated with the present external fabric in the schists.

Furthermore, these schists have a mottled appearance in thin section indicating possible pseudomorphic replacement of pre-existing minerals (Chapter 4). In several localities Fe-Ti/graphite inclusions in the pseudomorphs have a preferred orientation that, like the type 2 garnet cores, which cannot be related to the

external S_2 fabric (Figure 5.3b). The orientation of the inclusion pattern in pseudomorphs may, however, be correlated with that in the cores of type 2 garnet porphyroblasts.

Another line of reasoning comes for the relative age of S_1 from a thin section in which F_2 folded (in outcrop) garnetiferous McKay River schists have a well-developed axial plane foliation defined by the preferred orientation of elongate quartz grains and dustings of graphite. In this thin section, S_1 has been completely transposed into S_2. Graphite layers show a weak F_3 crenulation. A pre- to syn-kinematic idioblastic garnet, with S_2 wrapping around and abutting it, has overgrown a millimetre-sized fold hinge defined by fine grained graphite inclusions (Figure 5.3c). The axial surface of this fold hinge is at a high angle to both S1 and the crenulation axial plane and appears unrelated to either.

The relationship between type 1 garnet porphyroblasts and type 2 rims with S_2 indicates these garnets are pre- to syn-D_2-deformational (i.e. Grenvillian). The cores of type 2 garnets are interpreted to be relics of pre-existing garnet related to contact metamorphism associated with intrusion of the Shabogamo gabbro. Type two garnets follow a two stage growth model in which the

Figure 5.3 (continued). C. Folded inclusion pattern in garnet from quartz-rich schists. Base of photograph is 2.5mm.

core grew during contact metamorphism and the rims grew during regional metamorphism related to Grenvillian deformation and metamorphism. Pseudomorphs with inclusion patterns also likely represent a contact metamorphic event in which porphyroblasts overgrew a preexisting fabric. Evidence of an early folding event associated with D_2 is represented by the fold hinge preserved in a garnet porphyroblast.

The microstructural examples discussed above record possible relics of a pre-Shabogamo gabbro slaty cleavage. This slaty cleavage may be preserved in outcrop in the form discussed above in which an S_1 cleavage in a mica schist is truncated by a gabbro dyke that in turn contains an S_2 foliation. Porphyroblasts that grew in the metamorphic aureole around the gabbro pluton in the Ossokmanuan Lake Domain overgrew an existing slaty cleavage and recorded it as inclusion patterns within them.

5.4 Discussion

Brooks et al. (1981) and Zindler et al. (1981) obtained a Rb/Sr and Sm/Nd whole rock age for the Shabogamo gabbro of 1375 +/- 60 Ma, and Dallmeyer (1982)

obtained a $^{40}Ar/^{39}Ar$ biotite age of 1353 +/- 17 Ma. Regional metamorphism in Gagnon terrane has been dated at 1050-950 Ma, using Rb/Sr whole rock and $^{40}Ar/^{39}Ar$ methods (Brooks et al. 1981; Dallmeyer and Rivers, 1983). Metamorphism in Shabogamo gabbro in the southwestern Gagnon terrane has been interpreted to be Grenvillian in age (Rivers and Mengel 1988).

Based on field and microscopic observations all gabbro bodies in the Tiphane Lake map area are interpreted to be part of the Shabogamo Intrusive Suite. Thus it is reasonable to suggest that the macro, meso and microscopic structures outlined above are either intruded by Shabogamo gabbro or are a result of Shabogamo contact metamorphism and must, therefore, be pre-Grenvillian. Hudsonian structures occur immediately north and west of the field area (Ware and Wardle, 1979; Rivers, 1982, 1983a), suggesting that it lies to the east of the Hudsonian Front, within the Hudsonian front zone. Most pre-Grenvillian structures in the area can, therefore, be reasonably attributed to Hudsonian deformation.

CHAPTER 6

The Grenvillian Orogeny

6.1 Introduction

A study of the geometry and kinematics of the front zone of an orogenic belt provides important information on the tectonic evolution of the orogen. Several studies have been conducted in the southern part of Gagnon terrane in southwestern Labrador, that examined the geometry, kinematics, and metamorphism of the Grenville Front zone in this area (Rivers, 1983a, 1983b; van Gool et al., 1987, 1988; Brown et al., in press). These studies have shown that the structural geometry of Gagnon terrane in the Labrador City area is similar to that of foreland fold and thrust belts in Paleozoic and younger orogens, albeit representing contractional deformation at a substantially deeper crustal level. This led Brown et al. (in press) to suggest that this part of Gagnon terrane may provide an analogue for the mid-crustal structural style of the front zones of orogenic belts from higher crustal levels.

This thesis has expanded the study of the Grenville Front zone in southwestern Labrador to include the

northeastern part of Gagnon terrane. It provides further evidence of the complex structural nature of the Grenville Front zone in southwestern Labrador. The preceding chapters have documented the field relationships in the map area and provided some broad conclusions regarding the structural and metamorphic evolution of the domains. The following discussion will briefly outline the interpreted sequence and style of Grenvillian deformation in the map area, apply a tectonic model, and discuss the implications for Grenvillian tectonics in this part of Gagnon terrane.

On the basis of structural style, the study area has been divided into four domains, each of which record a polydeformational history that can be related to the ca. 1800 Ma Hudsonian orogeny, and to the ca. 1000 Ma Grenvillian orogeny.

The structural style of the Hudsonian deformation in the field area is poorly understood due to penetrative overprinting of Hudsonian structural elements by Grenvillian deformation (Figure 6.1). However, it is possible, locally, to define a foliation that predates intrusion of the Shabogamo gabbro, and can therefore be related to Hudsonian deformation. A number of faults have also been described that may be related to west-directed

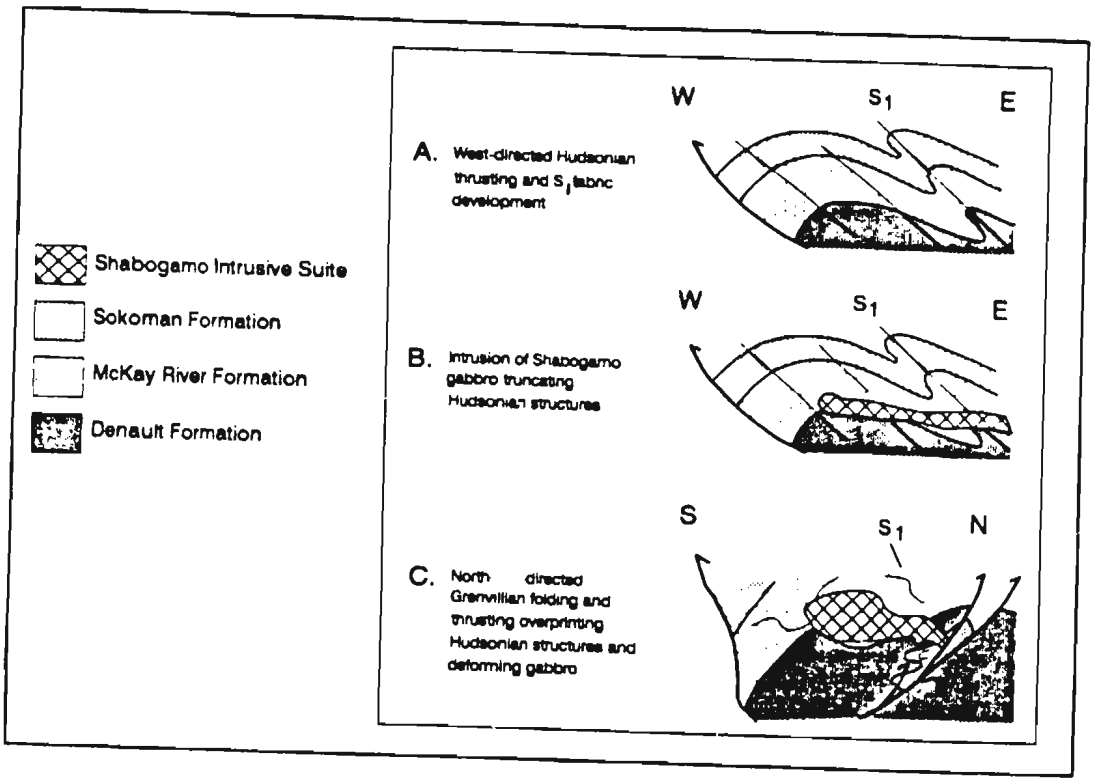

Figure 6.1. Schematic model depicting the tectonic evolution of the study area from the Hudsonian orogeny through to the Grenvillian orogeny.

Hudsonian thrusting. Indirect evidence of the Hudsonian orogeny in the field area appears in the Equus Lake domain where the Equus Lake formation, a conglomeratic to siltstone metasedimentary sequence containing clasts of Knob Lake Group rocks, sits with marked structural unconformity on top of rocks of the Tiphane Lake, Dave Lake, and Mobey Lake domains. Based on the above evidence, and by extrapolating the structural style of the Churchill Province (New Quebec Orogen) to the immediate north, into the field area, the pre-Shabogamo structures are interpreted to have formed as a result of west-directed folding and thrusting during the Hudsonian orogeny.

6.2. Structural synthesis of Grenvillian deformation

From a regional Grenvillian perspective, the map pattern (see map in back pocket) shows a general older-over-younger stacking sequence common to most thrust belts. In detail, the lithostratigraphic relationships within domains, as well as the relationships between domains, and structures related to domain emplacement, indicate a more complex stacking order (Figure 6.2). The Mobey Lake domain boundary fault and thrusts that splay off it truncate D_2 thrusts and F_2 folds in the Tiphane

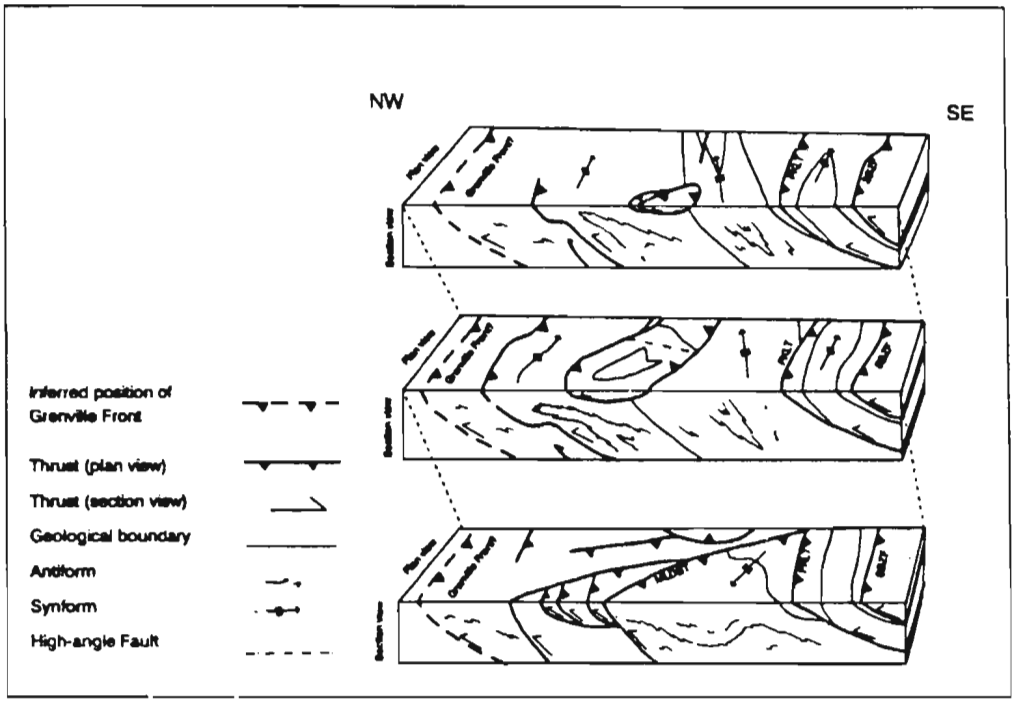

Figure 6.2. Schematic 3-dimensional views of the study area showing the relationships between thrusts and folds. SBZF = Southern Boundary Zone Fault. FKLT = Four King Lake Thrust. MLDBT = Mobey Lake domain Boundary Thrust.

Lake domain, where they are referred to as D_3 thrusts. In another example, from the southeast end of Dave Lake, a macroscopic synform\antiform pair is disrupted by a duplex structure, which places younger rocks on top of older. Furthermore, the southern boundary fault to the Dave Lake domain cuts across the limbs of a macroscopic F_2 fold in its footwall, isolating the hinge zone. Also, the boundary fault itself is folded. Finally, the relatively young rocks within the Equus Lake domain sit with marked structural unconformity on top of older rocks from all other domains in the map area.

Grenvillian deformation in the area started with the development of northwest- to north-directed fold nappes which appear to represent large structures in the southern domains, and with imbricate thrusting taking place in the Tiphane Lake domain. Rocks in the Tiphane Lake domain were folded and thrusted northwestward as thin (200 to 300 meter thick) thrust sheets. Shear zones developed as brittle-ductile, typically S-C mylonites, that cut through the overturned limbs of macroscopic F_2 fold nappes. Southwards, in the Dave Lake domain, fold nappes on a much larger scale were forming simultaneously with those in the Tiphane Lake domain. However, thrusting in the Dave Lake domain postdated the main phase of folding, typically cutting across the

macroscopic folds.

The variation in contractional style between the Tiphane Lake domain and the Dave Lake domain is likely due to the relative positions of the two domains in the developing nappe pile. The Tiphane Lake domain was possibly at the leading edge of the pile, where the basal detachment cut up-section, resulting in the formation of small imbricate thrusts sheets in the more fine scale layered, and more incompetent upper part of the Knob Lake Group sequence. The position of the Dave Lake domain was south of the leading edge of the nappe pile, towards the hinterland where deformation was occurring mostly by buckle folding focused on the more competent lower succession in the Knob Lake Group. A similar structural style is recorded on a much larger scale in the Helvetic Nappes (eg. Milnes and Pfiffner, 1977; Pfiffner, 1981; Ramsay, 1981).

Following the main folding event, rocks in the Mobey Lake domain were thrust northeastward across the Tiphane Lake and Dave Lake domains. The Mobey Lake domain boundary fault and thrusts splaying off it truncate fold nappe related structures in the Tiphane Lake domain. F_2 folding in the Mobey Lake domain appears to be unrelated to the main phase of fold nappe development in the other

domains, and is interpreted to be a result of fault propagation folding during emplacement of the domain.

Rocks in the Isa Lake thrust sheet were thrust northwest across those of the Dave Lake thrust sheet and the Mobey Lake domain. The relationship between the Four King Lake thrust and the Mobey Lake domain boundary thrust was not observed in the field. However, aerial photograph lineaments indicate the two thrusts converge southeast of Mobey Lake and may, in fact, form a branch point. Depending on the interaction between these two thrusts, movement along the Four King Lake thrust can be interpreted to have occurred simultaneously with, or immediately following emplacement of the Mobey Lake domain.

Within the Dave Lake thrust sheet, the duplex near the southeast end of Dave Lake built up, truncating the fold nappes. The occurrence of downward facing folds in the Isa Lake thrust sheet indicated possible refolding of F_1 folds by fault propagation folding above the developing thrusts. However, timing of movement along this duplex relative to other thrusts in the area is difficult to determine, since there were no overprinting relationship observed.

Movement along the southern boundary zone fault is also difficult to date relative to the other thrusts. It does truncate previously formed folds, so is post fold nappe development, but itself is folded. Folding of the southern boundary zone fault may be a result of continued fold nappe development during thrusting, or it may be a result of folding due to emplacement or transport of the overlying thrust sheet.

The features outlined above, and discussed in detail in Chapter 3, suggest that the structural geometry of the map area evolved by fold nappe development concomitant with, and followed by, both foreland and hinterland propagating thrusts, rather than by simple foreland-directed piggyback style folding and thrusting. Most thrusts in the map area can be considered out-of-sequence using the criteria of Morley (1988).

Foreland fold and thrust belts typically form as a critically tapered wedge that accretes new material to its leading edge during development (Davis et al., 1983; Dahlen et al., 1984). The model presented by these authors predicts that the geometry of an orogenic wedge is a function of its internal dynamics, and in order to maintain a critical taper that enables stable sliding of the wedge, it must deform internally. Out-of-sequence

backthrusting and forethrusting to maintain the critical taper of the deforming wedge is common in fold and thrust belts (eg. Platt, 1986; Morley, 1987)

The Grenvillian structure of the area studied in this thesis evolved as a tapered, northwest- to north-directed series of evolving fold nappes above a basal detachment (eg. Pfiffner, 1981). The ductile nature of the structural elements in the area indicates deformation initially occurred at a mid- to upper-crustal levels. Initial, foreland-directed thrusting appears to have been restricted to the leading edge of the deforming wedge, in the Tiphane Lake domain. The tight to isoclinal geometry of most macroscopic folds, and the lack of in-sequence thrusting associated with the macroscopic folding, indicate that shortening within the wedge was accomplished largely by folding in the early stages of deformation. With continued shortening, the deforming wedge was unable to maintain its critical taper by folding alone, resulting in the formation of out-of-sequence thrusts which cut across previously formed fold nappes and stacked the rocks in large thrust sheets that correspond with the domains discussed in Chapter 3.

Strain hardening resulting from locking of the fold system as folds tightened may also account for the

development of out-of-sequence thrusting. This is quite possibly the case with the duplex structure near Dave Lake (DLts) where the macroscopic folds are isoclinal.

The increase in metamorphic grade southeastward across the area is typical of inverted metamorphic gradients in fold and thrust belts (Zwart, 1974; Andreasson and Lagerblad, 1980), and has been noted along the margin of central Gagnon terrane near Labrador City (Rivers, 1983a,b). The preservation of the inverted metamorphic pattern in an out-of-sequence thrust system implies that the structural development of the area was dominated by the formation of fold nappes and in-sequence piggyback stacking. Thus, out-of-sequence thrusts must not have moved much, and rocks of varying (lower) metamorphic grades were not brought up from depth.

CHAPTER 7

Conclusions

The following conclusions, followed in point form, summarize the principal findings of this study.

1. A new rock unit not previously discussed in Gagnon terrne, the Equus Lake formation, was described for the first time. This unit is interpreted to be part of an Hudsonian molasse sequence.

2. The stratigraphy of the the area has been defined, and stratigraphic relationships are refined.

3. A number of structural elements that pre-date intrusion of the Shabogamo gabbro were described for the first time. These features are interpreted to be related to the Hudsonian orogeny.

4. The area described in this study, which lies a few kilometres south of the Grenville Front, developed during the Grenvillian orogeny as a ductile, metamorphic fold and thrust belt that formed at a mid- to upper-crustal level. The geometric development of the belt involved the formation of a series of northwest- to north-directed

fold nappes with minor thrusting along their leading edges, followed by out-of-sequence thrusting. Extensional faulting is interpreted to have occurred to the northeast and southwest of the field area.

5. The metamorphic grade in the area has been qualitatively shown to increase southwards across the belt to form an inverted metamorphic sequence common to many thrust belts.

6. The area described differs somewhat in the details of the geometry and kinematics from that of central Gagnon terrane near Labrador City, but nevertheless is a metamorphic fold and thrust belt that formed as a result of northwest-southeast shortening and emplacement of the overlying Lac Joseph terrane.

7. This study is the first time the intersection of the Grenville Province and the Churchill Province has been described in this area.

REFERENCES

Andreasson, P.G., and Lagerblad, B., 1980. Occurrence and significance of inverted metamorphic gradients in the western Scandinavian Caledonides: J. Geol. Soc. London. v. 137, p.219-230.

Baer, A.J.; 1974. Grenville Geology and Plate Tectonics. Geoscience Canada, v.1, pp.54-61.

Baird, D.M., 1950. Geology of the Evening Lake - south Gabbro Lake area of Labrador. Maps and report, Iron Ore Company of Canada.

Beland, R., 1950. Geology, Gabbro Lake area. Maps and report, Labrador Mining and Exploration Company.

Boyer, S.E., & Elliot, D. 1982. Thrust systems. A.A.P.G. Bull. v.66, pp.1196-1230.

Breau, G., 1957. Geological anomaly investigation, Ossokmanuan Lake area. Maps and report, Labrador Mining and Exploration Company.

Brown, R.L., Chappell, J.F., Moore, J.M., and Thompson, P.H.; 1975. An Ensimatic Island Arc and Ocean Closure in the Grenville Province of southeastern Ontario, Canada. Geoscience Canada, v.2, pp.141-144.

Brown, D.L. 1988. Thin-skinned, basement-involved thrust tectonics in the Emma Lake area, Grenville Front zone, western Labrador. Unpublished BSc. thesis. Memorial University of Newfoundland. 96p.

Brown, D., van Gool, J., Calon, T., and Rivers, T., in press. The geometric and kinematic development of the Emma Lake thrust stack, Grenville Front, southwestern Labrador. Can. J. of Earth Science.

Culotta, R.C., Pratt, T., and Oliver, J., 1990. A tale of two sutures: COCORP's deep seismic surveys of the Grenville Province in eastern U.S. midcontinent. Geology, v.18, pp.646-649.

Connelly, J.N., van Gool, J., & Rivers, T. 1989. Molson Lake terrane, a new terrane in the Parautochthonous

Belt of the Grenville Province in southwestern Labrador. GAC/MAC Program with Abstracts. v.14

Dahlen, F.A., Suppe, J., and Davis, D., 1984, Mechanics of fold- and-thrust belts and accretionary wedges: Cohesive Coulomb theory: J. Geophysical Res., v.89, pp.10087-10101.

Dalhstrom, C.D.A., 1969. Balanced cross-sections. Can. J. of Earth Sci., v.6, pp.743-757.

Davidson,A.; 1986. New Interpretations in the southernmost Grenville Province. In. The Grenville Province. (J.M. Moore, Davidson, A., and Baer, editors). Geog. Ass. Canada Special Paper 31, pp.61-74.

Davis, D., Suppe, J., and Dahlen, F.A., 1983: Mechanics of fold and thrust belts and accretionary wedges: J. Geophysical Res., v.82, pp.1153-1172.

De Paor, D.G., 1988. Balanced section in thrust belts part 1: Construction. A.A.P.G. Bull., v.72, pp.73-90.

Dewey, J.F., and Burke, K.C.A., 1973. Tibetan, Variscan, and Precambrian basement reactivation: products of continental collision. J. of Geology. v.81, pp.683-692.

Eskola, P., 1920. The mineral facies of rocks. Norsk. Geol. Tidsskr., v.6, pp.143-194.

Ferry, J.M., and Spear, F.S., 1977. Experimental calibration of the partitioning of Fe and Mg between biotite and garnet. Contrib. Mineral. Petrol., v.66, pp.113-117

Indares, A., and Martignole, J.,1985. Biotite-garnet geothermometry in the granulite facies: Evaluation of equilibrium criteria. Canad. Mineral., v.23, pp.187-193.

Indares, A., and Martignole, J., 1989. The Grenville Front south of Val d'Or, Quebec. Tectonophysics, v.157, pp. 221-239.

Ganguly, J., and Saxena, S.K., 1984. Mixing properties of aluminosilicate garnets: constraints from natural and experimental data, and applications to geothermo-barometry. Am. Mineral., v.69, pp.88-97.

Goldman, D.S., and Albee, A.L., 1977. Correlation of Mg/Fe-partitioning between garnet and biotite with $^{18}O/^{16}O$ partitioning between quartz and magnetite. Am. J. Sci., v.277, pp.750-767.

Goldsmith, J.R., 1982; Review of the behaviour of plagioclase under metamorphic conditions. Am. Mineral, v.67, p.643-652.

Gower, C.F., Ryan, A.B., Bailey, D.G., and Thomas, A.; 1980. The Position of the Grenville Front in eastern and central Labrador. Can. J. of Earth Sci., v.17, pp.784-788

Gower, C.F., and Loveridge, W.D., 1987. Grenvillian plutonism in the eastern Grenville Province; radiogenic age and isotopic studies. Report 1, Geol. Sur. Paper, Geol. Sur. Canada. 87-2, pp.5-58.

Gower, C.F., and Owen, V., 1984. Pre-Grenvillian and Grenvillian lithotectonic regions of eastern Labrador-Correlation with the Sveconorwegian orogenic belt in Sweden. Can. J. of Earth Sci. v.21, pp.678-693.

Graham, C.M., and Navrotsky, A., 1986; Thermochemistry of the tremolite-edenite amphiboles using fluorine analogues, and applications to amphibole-plagioclase-quartz equilibria. Contrib. Mineral. Petrol., v.93, pp.18-32.

Grapes, R.H., and Graham, C.M., 1978; The actinolite-hornblende series in metabasites and the so-called miscibility gap: a review. Lithos, v.11, pp.85-97.

Green, A.G., Milkereit, B., Davidson, A., Spencer, C., Hutchinson, D.R., Cannon, W.F., Lee, M.W., Agena, W.F., Behrendt, J.C., & Hinze, W.J. 1988. Crustal structure of the Grenville front and adjacent terranes. Geology. v.16, pp.788-792.

Hodges, K.V., and Spear, F.S., 1982. Geothermometry, geobarometry and the Al_2O_3 triple point at Mt. Moosilauke, New Hampshire. AM. Mineral., v.67, pp.1118-1134.

Hoffman, P.F., 1988. United Plates of America, The birth of a craton: Early Proterozoic assembly and growth of Laurentia. Ann. Rev. Earth Planet. Sci., v.16., pp.543-603.

King, J.E., 1986. The metamorphic internal zone of Wopmay Orogen early Proterozoic), Canada: 30 km of structural relief in a composite section based on plunge projection. Tectonics, v.5, pp. 973-994.

Laird, J., and Albee, A.L., 1981; Pressure, temperature, and time indicators in mafic schist: their application to reconstructing the polymetamorphic history of Vermont. Am. J. Sci., v.281, pp.127-175.

Lucas, S.B., 1989. Structural evolution of the Cape Smith thrust belt and the role of out-of-sequence faulting in the thickening of mountain belts. Tectonics, v.8, pp.655-676.

Milnes, A.G., and Pfiffner, O.A., 1977. Structural development of the Infrahelvetic complex, eastern Switzerland. Eclogae geol. Helv., v.70, pp.83-95.

Maruyama, S., Liou, J.G., and Suzuki, K., 1982; The peristerite gap in low-grade metamorphic rocks. Contrib. Mineral. Petrol., v.81, pp.268-276.

Mitra, S., and Namson, J., 1989. Equal-area balancing. Am. J. of Sci., v.289, pp.563-599.

Morley, C.K., 1987. Lateral and vertical changes of deformation style in the Osen-Roa thrust sheet, Oslo Region. J. Struct. Geol., v.9, pp.331-343.

Morley, C.K., 1988. Out-of-sequence thrusts. Tectonics, v.7, pp.539-561.

Noel, N.T., 1981. The geology and geochemistry of the McKay River - Gabbro Lake area. Urpublished BSc. thesis. Memorial University of Newfoundland. 100p.

Noel, N., and Rivers, T., 1980. Geological mapping in the McKay River - Gabbro Lake area, western Labrador. In. Current Research. (O'Driscoll, C.F., and Gibbons, R.V., editors). Newfoundland Department of Mines and Energy, Mineral Development Division, report 80-1, pp.214-221.

Nunn, G.A.G., Thomas, A., and Krogh, T.E., 1985. The Labradorian orogeny: geochronological database. In. Current Research (Brewer, K., Walsh, D., and Gibbons, R.V., editors) Newfoundland Department of Mines and Energy, Mineral Development Division Report 85-1, pp. 43-54.

Oba, T., 1980. Phase relations in the tremolite-

pp.247-256.

Owen, V., Rivers, T., and Gower, C.F., 1986. The Grenville Front on the Labrador coast. In; The Grenville Province. (J.M. Moore, A Davidson, and A.J.Baer, editors). Geol. Ass. of Canada Special Paper 31, p. 95-106.

Passchier, C.W., and Simpson, C., 1986. Porphyroclast systems as kinematic indicators. J. Struct. Geol., v.8, pp.831-843.

Perchuk, L.L., 1970. Equilibrium of biotite with garnet in metamorphic rocks. Geochem. Int., v.1, pp.157-179.

Perchuk, L.L., Aranovich, Ya., L., Podlesskii, K.K., Lavrant'eva, I.V., Gerasimov, V.Yu., Fed'kin, V.V., Kitsul, V.I., Karsanov, L.P., and Berdnikov, N.V., 1985. Kinetics and Equilibrium in mineral reactions. Springer-Verlag, 173-198.

Pfiffner, A.O., 1981. Fold-and-thrust tectonics in the Helvetic Nappes (E Switzerland). In. Thrust and Nappe Tectonics.(McClay, K.R., and Price, N.J., editors). Geol. Soc. London Special Pub. No. 9., pp.319-328.

Pigage, L.C., and Greenwood, H.J., 1982. Internally consistent estimates of pressure and temperature: the staurolite problem. Am. J. Sci., v.282, pp.943-969.

Platt, J.P., 1986. Dynamics of orogenic wedges and the uplift of high-pressure metamorphic rocks. Geol. Soc. Am. Bull., v.97, pp.1037-1043.

Plyusnina, L.P., 1982; Geothermometry and geobarometry of plagioclase-hornblende bearing assemblages. Contrib. Mineral. Petrol., v.80, p.140-146.

Ramsay, J.G., 1967. Folding and Fracturing of Rocks. Springer-Verlag.

Ramsay, J.G., 1981. Tectonics of the Helvetic Nappes. In. Thrust and Nappe Tectonics. (McClay, K.R., and Price, N.J., editors). Geol. Soc. London Special Pub. No. 9., pp.293-310.

Rivers, T.; 1980. Revised Stratigraphic Nomenclature for Aphebian and other rock units, southern Labrador Trough, Grenville Province. Can. J. of Earth Sci.,

v.17, pp.668-670.

Rivers, T. 1982. Preliminary report of the geology of the Gabbro Lake and McKay River map areas (23H/11 and 23H/12), Labrador. Newfoundland Department of Mines and Energy, Mineral Development Division Report 82-2. 27 p.

Rivers, T. 1983a. The northern margin of the Grenville Province in western Labrador - anatomy of an ancient orogenic front. Precambrian Research. v.22, pp.41-73

Rivers, T., 1983b. Progressive metamorphism of pelitic and quartzofeldspathic rocks in the Grenville Province of western Labrador - Tectonic implications of bathozone 6 assemblages. Can. J. of Earth Sci., v.20, pp.1791-1804.

Rivers, T. and Wardle, R.J., 1985. Geology of the Gabbro Lake area, Labrador, 23H(NW). Newfoundland Department of Mines and Energy, Mineral Development Branch. Map 85-26.

Rivers, T., and Nunn, G.A.G., 1985. A reassessment of the Grenvillian orogeny in western Labrador. In. The Deep Proterozoic Crust in the North Atlantic Provinces. (Tobi, A.C., and Touret, J.L.R., editors). NATO Adv. Study Inst., Ser. C, 158, pp. 163-174.

Rivers, T., and Chown, E.H., 1986; The Grenville Orogen in eastern Quebec and western Labrador - definition, identification, and tectonometamorphic relationships of autochthonous, parautochthonous, and allochthonous terranes. In; The Grenville Province. (Moore, J.M., Davidson, A., and Baer, A.J., editors). Geol. Ass. of Canada Special Paper 31, p. 31-51.

Rivers, T., Martignole, J., Gower, C.F., and Davidson, A., 1989; New tectonic divisions of the Grenville Province, southeast Canadian Shield. Tectonics, v.8, p.63-84.

Robinson, P., Spear, F.S., Schumacher, J.C., Laird, J., Klein, C., Evans, B.W., and Doolan, B.L., 1982. Phase relations of metamorphic amphiboles: natural occurrence and theory. In. Amphiboles: Petrology and Experimental Phase Relations. Reviews in Mineralogy, vol. 9B. (Veblen, D.R., and Ribbe, P.H., editors). Mineralogical Society of America.

pp.1-227.

Saxena, S.K., 1969. Distribution of elements in coexisting minerals and the problem of chemical disequilibrium in metamorphosed basic rocks. Contrib. Mineral. Petrol., v.20, pp.177-197.

Silver, L.T., and Lumbers, S.B., 1965. Geochronological studies in the Bancroft-Madoc area of the Grenville Province. Geol. Soc. Am., Spec. Pub. 87, pp. 156.

Simpson, C. & Schmid, S.M. 1983. An evaluation of criteria to deduce the sense of movement in sheared rocks. Geol. Soc. Am. Bull. v.94, pp.1281-1288.

Spear, F.S., 1980; NaSi=CaAl exchange equilibrium between plagioclase and amphibole. Contrib. Mineral. Petrol. v.72, p.33-41.

Spear, F.S., 1981; Amphibole-plagioclase equilibria: an empirical model for the relation albite + tremolite = edenite + 4 quartz. Contrib. Mineral. Petrol., v.77, p.355-364.

Thomas, A., Nunn, G.A.G., and Wardle, J., 1985. A 1650 Ma orogenic belt within the Grenville Province of northeastern Canada. In. The Deep Proterozoic Crust in the North Atlantic Provinces. (Tobi, A.C., and Touret, J.L.R., editors). NATO Adv. Study Inst., Ser. C, 158, pp. 151-161.

Thomas, A., Nunn, G.A.G., and Krogh, T.E., 1986. The Labradorian orogeny: Evidence for a newly identified 1600 to 1700 Ma orogenic event in Grenville Province crystalline rocks from central Labrador. In; The Grenville Province. (J.M. Moore, A Davidson, and A.J.Baer, editors). Geol. Ass. of Canada Special Paper 31, p. 175-190.

Tiphane, M., 1951. Geology of Tiphane Lake area. Map and report, Iron Ore Company of Canada.

Turner, F.J., and Weiss, L.E., 1963. Structural analysis of metamorphic rocks. McGraw-Hill, New York, 545p.

van Gool, J., Calon, T., & Rivers, T. 1987. Preliminary report on the Grenville Front tectonic zone, Bruce Lake area, western Labrador. Current Research, Part A, Geol. Sur. Canada, Paper 87-1A, 435-442.

van Gool, J., Brown, D., Calon, T., & Rivers, T. 1988.

The Grenville Front thrust belt in western Labrador. Current Research, Part C, Geol. Sur. Canada, Paper 88-1C, 245-253.

Wardle, R.J., & Bailey, D.G. 1981. Early Proterozoic sequences in Labrador. In: Proterozoic Basins of Canada. (Campbell, F.H.A., editor). Geological Survey of Canada, paper 81-10, 331-359.

Wardle, R.J., Rivers, T., Gower, C.F., Nunn , G.A.G., and Thomas, A.; 1986. The Northeastern Grenville Province: New Insights. In; The Grenville Province. (J.M. Moore, A Davidson, and A.J.Baer, editors). Geol. Ass. of Canada Special Paper 31, p. 13-29.

Ware, M.J., and Wardle, R.J., 1979. Geology of the Sims - Evening Lake area, western Labrador, with emphasis on the Helikian Sims Group. Newfoundland Department of Mines and Energy, Mineral Development Division, Report 79-5.

Windley, B.F., 1986. Comparative tectonics of the western Grenville Province and the western Himalaya. In; The Grenville Province. (Moore, J.M., Davidson, A., and Baer, .J., editors). Geol. Ass. of Canada Special Paper 31, pp. 341-348.

Windley, B.F., 1989. Anorogenic magmatism and the Grenvillian Orogeny. Can. J. Earth Sci., v.26, pp.479-489.

Wynne-Edwards, H.R., 1961. Ossokmanuan Lake, Labrador, 23H(W1/2). Geol. Sur. Canada, Map 17-1961.

Wynne-Edwards, H.R., 1972, The Grenville Province. In. Variations in Tectonic Styles in Canada (Price, R.A., and Douglas, R.J.W., editors). Geological Association of Canada Special Paper 11, pp. 263-334.

Zwart, H.J., 1970; Structure and metamorphism in the Seve-koli Complex (Scandinavian Caledonides) and its implications concerning the formation of metamorphic nappes. Geologie des Domaines Cristallins, Liege. pp.129-144.

APPENDIX 1

This appendix lists tables of representative mineral analysis used for plagioclase-amphibole thermometry and garnet-biotite thermometry. Analysis were conducted on a JEOL 50A electron microprobe with an accelerating voltage of 22 nanoamperes with a count rate of 60,000 per 30 seconds. Data were corrected using the ZAF correction method.

Amphibole analysis (DB-117)

SiO2	48.91	49.69	46.73	48.91
TiO2	0.13	0.17	0.18	0.13
Al2O3	8.50	7.34	11.68	8.50
FeO	12.34	11.66	15.48	12.34
MnO	0.21	0.14	0.18	0.21
MgO	15.98	15.50	11.77	15.98
CaO	11.69	11.53	11.58	11.69
Na2O	0.83	0.77	1.88	0.83
K2O	0.07	0.15	0.40	0.07
Sum	98.66	96.95	99.88	98.66

Amphibole analysis (DB-163)

SiO2	43.910	43.69	45.82	43.86	39.16	45.48	42.04	42.41
TiO2	0.027	0.30	0.25	0.42	0.07	0.33	0.55	0.44
Al2O3	12.890	14.05	11.52	14.63	23.11	12.13	14.22	13.43
FeO	16.700	16.79	15.89	16.92	13.06	17.28	16.01	16.19
MnO	0.160	0.22	0.17	0.14	0.11	0.12	0.20	0.25
MgO	9.920	9.79	11.03	9.71	9.95	9.97	9.23	9.56
CaO	12.320	12.03	13.03	11.73	11.41	12.38	12.70	14.63
Na2O	1.450	1.94	1.63	2.06	1.93	1.82	1.60	1.48
K2O	0.210	0.32	0.30	0.35	0.47	0.36	0.39	0.27
Sum	97.830	99.13	99.64	99.82	99.27	99.87	96.93	98.66

Amphibole analysis (DB-53)

SiO2	54.79	54.04	54.84	53.79	54.91	52.71	54.58	54.72
TiO2	0.08	0.14	0.07	0.13	0.08	0.14	0.12	0.07
Al2O3	2.58	2.43	2.38	2.70	1.94	3.21	2.11	1.89
FeO	12.10	12.84	13.15	12.28	13.05	13.53	13.41	13.46
MnO	1.55	1.50	1.83	1.32	1.38	1.63	1.59	1.58
MgO	17.15	17.19	16.73	16.61	16.91	16.34	16.89	17.45
CaO	9.13	9.36	8.81	9.99	7.90	9.54	8.69	8.25
Na2O	1.20	1.66	1.03	1.49	2.01	1.38	1.21	1.16
K2O	0.05	0.08	0.09	0.08	0.10	0.08	0.10	0.07
Sum	98.63	99.24	98.93	98.39	98.27	98.56	98.70	98.56

Amphibole analysis (DB89-13)

SiO2	45.01	45.20	44.98	44.17	45.09	44.98	43 91	44.36
TiO2	0.34	0.31	0.32	0.36	0.29	0.30	0.31	0.41
Al2O3	15.24	14.32	16.41	16.33	14.46	13.99	15.90	15.28
FeO	14.09	13.90	13.92	13.73	12.82	13.50	14.24	13.89
MnO	0.21	0.20	0.16	0.14	0.20	0.12	0.22	0.19
MgO	11.28	12.05	10.30	10.45	12.01	11.61	10.37	11.62
CaO	11.45	11.87	11.49	11.65	11.30	11.84	12.06	11.72
Na2O	1.62	1.61	2.01	1.99	1.88	1.59	1.86	1.82
K2O	0.20	0.14	0.21	0.27	0.21	0.22	0.30	0.20
Sum	99.44	99.60	99.79	99.09	98.25	98.15	99.18	99.49

Amphibole analysis (TC-1)

SiO2	51.36	51.34	49.12	47.45	51.41	51.19	48.23
TiO2	0.08	0.07	0.02	0.09	0.05	0.06	0.51
Al2O3	5.20	5.05	8.17	9.03	4.13	4.81	8.59
FeO	15.26	15.60	15.43	16.65	14.51	15.42	16.41
MnO	0.55	0.50	0.53	0.53	0.64	0.62	0.46
MgO	13.30	13.21	11.90	11.34	14.09	13.86	10.46
CaO	12.88	12.70	12.77	12.10	12.84	12.34	13.68
Na2O	0.75	0.72	0.90	1.52	0.39	0.50	0.48
K2O	0.17	0.15	0.17	0.34	0.11	0.15	0.17
Sum	99.55	99.34	99.01	99.05	98.17	98.95	98.99

Plagioclase analysis (DB-117)

SiO2	54.93	56.32	54.65	51.81	52.19	52.78	57.55	57.84
Al2O3	28.88	28.86	29.21	31.45	30.04	29.84	27.21	27.20
FeO	0.36	0.28	0.36	0.57	0.60	0.49	0.48	0.57
MgO	0.05	0.03	0.05	0.03	0.02	0.06	0.36	0.19
CaO	9.84	9.43	10.41	13.04	13.32	12.37	7.98	6.86
Na2O	6.30	5.81	5.43	3.72	3.88	4.55	6.98	7.26
K2O	0.10	0.08	0.10	0.13	0.06	0.08	0.11	0.41
Sum	100.46	100.81	100.21	100.75	100.11	100.17	100.67	100.33

Plagioclase analysis (DB-163)

SiO2	68.31	68.91	67.43	68.84	67.36	68.81	67.46	68.50
Al2O3	19.08	18.83	18.82	19.50	19.34	19.17	19.20	20.22
FeO	0.02	0.07	0.04	0.06	0.15	0.00	0.01	0.03
MgO	0.02	0.00	0.00	0.00	0.04	0.00	0.00	0.01
CaO	0.34	0.35	0.32	0.34	0.44	0.60	0.36	0.34
Na2O	12.60	11.89	12.50	11.52	11.88	11.97	12.58	11.70
K2O	0.02	0.00	0.04	0.03	0.05	0.00	0.02	0.01
Sum	100.39	100.05	99.15	100.29	99.26	100.55	99.63	100.81

Plagioclase analysis (DB-53)

SiO2	68.63	68.55	69.01	68.74	68.68	68.33	68.82	69.05
Al2O3	19.12	18.61	18.50	18.37	18.30	18.43	18.57	18.61
FeO	0.27	0.18	0.25	0.15	0.19	0.00	0.25	0.05
MgO	0.00	0.00	0.00	0.00	0.00	0.00	0.00	0.00
CaO	0.07	0.04	0.03	0.09	0.06	0.11	0.05	0.00
Na2O	12.75	12.71	12.54	13.16	12.41	13.05	13.11	12.15
K2O	0.05	0.03	0.05	0.06	0.01	0.04	0.04	0.00
Sum	100.89	100.12	100.38	100.57	99.73	99.96	100.84	99.86

Plagioclase analysis (DB89-13)

SiO2	62.08	61.64	62.83	61.09	64.01	61.35	60.86	62.96
Al2O3	24.30	24.93	23.97	25.47	23.47	24.94	24.28	24.04
FeO	0.10	0.06	0.17	0.10	0.09	0.65	0.34	0.12
MgO	0.00	0.00	0.00	0.01	0.00	0.02	0.10	0.00
CaO	4.44	4.75	4.59	5.06	4.01	6.32	6.56	4.53
Na2O	9.62	9.18	9.27	9.06	9.35	7.43	7.77	9.05
K2O	0.03	0.03	0.07	0.04	0.04	0.05	0.15	0.02
Sum	100.57	100.59	100.90	100.83	100.97	100.76	100.06	100.72

Plagioclase analysis (TC-1)

SiO2	67.94	67.01	67.94	68.07	67.80	69.11	67.38	68.22
Al2O3	20.56	20.97	20.49	20.67	20.29	20.22	20.71	20.44
FeO	0.19	0.11	0.19	0.11	0.05	0.10	0.60	0.32
MgO	0.02	0.02	0.00	0.00	0.03	0.00	0.12	0.28
CaO	0.39	0.79	0.28	0.09	0.23	0.14	0.26	0.23
Na2O	11.37	11.53	11.66	11.49	11.68	11.09	11.42	11.08
K2O	0.05	0.06	0.04	0.04	0.03	0.10	0.07	0.04
Sum	100.52	100.49	100.60	100.47	100.11	100.75	100.56	100.61

Biotite analysis (DB89-23)

Na2O	0.20	0.08	0.11	0.11	0.19	0.16	0.29	0.22
MgO	8.25	8.08	8.70	8.30	8.02	7.75	7.63	7.93
Al2O3	17.95	17.94	18.55	18.95	18.28	17.69	11.70	18.34
SiO2	35.89	37.13	36.67	37.50	37.21	34.94	35.63	36.71
K2O	9.05	9.20	9.27	9.29	8.82	8.29	7.59	7.51
CaO	0.00	0.00	0.00	0.00	0.00	0.00	0.00	0.01
TiO2	1.75	1.78	1.79	1.64	1.71	1.50	1.61	1.71
Cr2O3	0.03	0.05	0.04	0.01	0.01	0.00	0.05	0.04
MnO	0.01	0.04	0.07	0.04	0.03	0.01	0.06	0.07
FeO	25.05	24.43	25.19	25.03	23.57	24.65	25.51	27.27
Sum	98.18	98.80	100.40	100.88	98.84	94.99	96.07	99.93

Biotite analysis (NN-311)

Na2O	0.17	0.01	0.12	0.06	0.17	0.21	0.00
MgO	9.97	11.40	9.85	10.12	9.98	9.82	10.33
Al2O3	18.19	18.59	18.04	18.01	18.15	18.75	18.23
SiO2	37.35	37.87	38.34	37.51	37.11	36.89	37.25
K2O	8.63	7.80	9.10	9.44	9.39	9.28	9.35
CaO	0.02	0.04	0.02	0.00	0.00	0.02	0.01
TiO2	1.95	1.80	1.89	1.98	2.01	1.80	1.94
Cr2O3	0.06	0.03	0.07	0.07	0.00	0.04	0.05
MnO	0.09	0.00	0.06	0.07	0.13	0.02	0.07
FeO	21.73	22.41	21.01	22.09	21.15	21.77	21.33
Sum	97.96	99.94	98.51	99.33	98.09	98.59	98.55

Garnet analysis (DB89-23)

MgO	1.68	1.69	1.75	1.94	1.57	1.65	1.75	1.62
Al2O3	21.63	21.89	21.30	22.01	21.68	21.80	21.84	21.54
SiO2	36.66	37.43	37.39	37.12	37.26	37.11	37.59	36.82
CaO	7.11	7.23	7.73	7.57	6.97	6.73	7.05	7.10
TiO2	0.10	0.09	0.11	0.04	0.16	0.12	0.09	0.10
MnO	1.94	1.54	1.05	0.63	2.36	2.08	1.55	1.50
FeO	30.21	30.15	30.40	30.85	29.69	29.72	29.99	30.43
Sum	99.34	100.01	99.72	100.16	99.70	99.21	100.87	99.11

Garnet analysis (NN-311)

MgO	1.63	1.78	1.60	1.59	1.64	1.61
Al2O3	21.59	21.48	21.50	21.61	21.79	21.50
SiO2	36.83	37.01	36.65	37.22	37.14	36.65
CaO	8.06	8.33	8.60	8.46	8.07	7.82
TiO2	0.09	0.06	0.15	0.11	0.14	0.08
MnO	4.82	4.75	4.95	5.41	4.96	4.64
FeO	27.84	27.57	26.60	25.60	25.90	26.77
Sum	100.85	100.98	100.04	100.01	99.63	99.07